Quantifying Burn Severity Patterns and Post-Fire Recovery

A Dissertation
Presented in Partial Fulfillment of the Requirements for the
Degree of Doctor of Philosophy
with a
Major in Natural Resources
in the
College of Graduate Studies
University of Idaho
by

Darcy H. Hammond

Major Professor: Eva K. Strand, Ph.D.
Committee Members: Penelope Morgan, Ph.D.; Andrew T. Hudak, Ph.D.;
Beth A. Newingham, Ph.D.
Department Administrator: Charles Goebel, Ph.D.

December 2020

Authorization to Submit Dissertation

This dissertation of Darcy H. Hammond, submitted for the degree of Doctor of Philosophy with a Major in Natural Resources and titled "Quantifying Burn Severity Patterns and Post-Fire Recovery," has been reviewed in final form. Permission, as indicated by the signatures and dates below, is now granted to submit final copies to the College of Graduate Studies for approval.

Major Professor: _____ Date: _____
Eva K. Strand, Ph.D.

Committee Members: _____ Date: _____
Penelope Morgan, Ph.D.

_____ Date: _____
Andrew T. Hudak, Ph.D.

_____ Date: _____
Beth A. Newingham, Ph.D.

Department Administrator: _____ Date: _____
Charles Goebel, Ph.D.

Abstract

Burn severity, the degree of ecological change following a fire, is frequently used in both management and research contexts to estimate how an ecosystem is expected to respond to fire in the long-term. By better understanding how burn severity and spatial patterns of differing severity levels impact post-fire processes, we can improve our understanding of how fires will impact ecosystems and future fires under changing climate and management conditions. The research in this dissertation found that remotely-sensed burn severity, as captured in the first year following fire, influences long-term ecosystem processes including ponderosa pine seedling density and height growth as well as boreal spruce understory species assemblages and downed woody fuels. Spatial patterns of burn severity also related strongly to distance to live tree, which is an important indicator of post-fire tree recovery. This work informs the ability of managers and researchers to use remotely sensed burn severity as an indicator of long-term ecosystem trajectory and presents the first test of how an emerging landscape model captures burn severity patterns.

Acknowledgements

Thank you to my committee members for their time and desire to make me the best researcher I can be. The Joint Fire Science Program funded much of this work. Thank you also to John Byrne and Ben Bright, without whom these projects would not have been possible. Many people helped with fieldwork and data entry, including Jessie Dodge, Jon Bontrager, Eli Berman, Mattie Schmidt, Emily Mangini, and others.

Dedication

This work is dedicated to my parents, who sparked and nurtured a passion for inquiry and exploring that got me to where I am today in more ways than one. This work is also dedicated to my friends for keeping me (mostly) sane on this wild ride! Thank you for the wonderful nerdy discussions that remind me why I chose to do grad school, and for the shenanigans that helped distract me from grad school.

Table of Contents

List of Tables

List of Figures

Chapter 1: Introduction

Fire has acted to shape global ecosystems for millennia, with fire and plants influencing each other and their surroundings through space and time (Bond et al. 2005; Pausas & Keeley 2009; Bond & Scott 2010; Keeley et al. 2011; He et al. 2012). In western North America forested ecosystems developed a wide range of natural fire regimes, from infrequent (fire return interval >300 years) severe crown fires in some temperate coastal and subalpine forests to frequent (1-25 year return interval) low severity surface fires in parts of the ponderosa pine (*Pinus ponderosa*) range (Agee 1993). Prior to European settlement, these fire regimes were driven mainly by climate, topography, and the vegetation and fuels present, with lightning and anthropogenic burning by Native Americans serving as the primary ignition sources (Agee 1993).

Since European settlement many forests in the western United States have experienced shifts in wildland fuels and climate that bring challenges to our current management and understanding of fire behavior and effects. Fire suppression policies of the mid-1900s likely resulted in an accumulation of fuels (Covington & Moore 1994) that have now increased the probability of severe fire above historic levels (Schoennagel et al. 2004), particularly in areas that historically experienced frequent low severity burning. In areas with historically mixed or high severity fire regimes, the influence of warmer temperatures and a lengthened fire season due to earlier spring snowmelt appears to be driving an increase in fire frequency (Westerling et al. 2006).

Burn severity (sometimes used interchangeably with the term fire severity [Keeley 2009]) is defined broadly as a measure of the degree of ecosystem change or the magnitude of negative impacts to an ecosystem following a fire (Simard 1991; Lentile et al. 2006). Though many have highlighted the ambiguity of these definitions and the necessity of ecosystem-specific measures and interpretation (Simard 1991; Keeley 2006; Morgan et al. 2014), burn severity remains an important concept to both researchers and managers due to the need to characterize post-fire effects and resulting ecosystem recovery trajectories following fire (Lentile et al. 2006). With the wider availability of satellite products, as well as growing concern about the increasing size and severity of wildfires, landscape-level analysis of fires

with remote sensing has been increasingly used to characterize burn severity at a fire or multi-fire level (Jakubauskas et al. 1990; Lopez-Garcia & Caselles 1991; Key & Benson 2006). A number of sensors have been evaluated for this purpose, with Landsat Thematic Mapper/Enhanced Thematic Mapper being the primary data source for burn severity products in research and management applications (Key & Benson 2006; Keeley 2009).

Because burn severity in this sense also includes expectations of ecosystem recovery time, where an ecosystem is considered "recovered" when it returns to the same ecosystem type and structure as it was pre-fire, how burn severity affects recovery post-fire has been the topic of much investigation in forested ecosystems (Keeley 2009). Burn severity can have lasting impacts on the post-fire landscape (Turner et al. 1997; Arseneault 2001), though these post-fire effects can be highly spatially variable, even among sites of the same severity level within a single fire (Lentile et al. 2007). With predicted future increases in fire size and severity comes the desire to manage landscapes in a way that best mitigates potential damage to the ecosystem from both an ecological and social viewpoint. Therefore a significant proportion of current research and management has focused on the effects, prevention, and rehabilitation of areas burned specifically at high severity. However, there remains a need for long-term, multi-scale investigations into the patterns and effects of burn severity on natural post-fire vegetation and fuels recovery in order increase our broader understanding of the fire ecology of western forests as well as to help guide and prioritize limited management resources.

We expect that differing post-fire conditions, including burn severity, will impact post-fire recovery. The following chapters were therefore developed to explore aspects of both spatial and temporal impacts of burn severity in ponderosa pine and boreal spruce forests. The first chapter examines two different landscape models for characterizing burn severity spatial patterns and contrasts how the different models relate to post-fire ponderosa pine seedling density and understory richness. The second chapter examines what post-fire factors, including burn severity and climate, impact ponderosa pine seedling height growth vs seedling density. The third examines how a remotely-remotely sensed burn severity index relates to vegetation and woody fuels conditions 12 years after large wildfires in boreal spruce forests. Together these studies will further our understanding of how to characterize

post-fire burn severity patterns to inform post-fire processes and how burn severity may impact post-fire processes and ecosystem services.

Chapter 2: Impacts of scale and landscape model on the relationship between post-fire landscape patterns and processes

Abstract

In post-wildfire environments, understory plant diversity and conifer seedling recruitment are strongly driven by dispersion processes, which often need recolonization from off-site, particularly in areas burned at high severity. Post-burn landscape patterns can impact these recolonization processes and understanding these relationships can potentially aid post-wildfire recovery modeling and management. The dominant model for quantifying landscape patterns is the patch-matrix model, which conceptualizes landscapes as composed of discrete, internally homogenous patches of different classes. One alternative, the gradient model, represents landscapes as a continuous surface; the lack of distinct classes and patches addresses the fundamental criticism of patch-matrix models, which is that the categorization of continuous data hides important landscape variation. In order to examine how a suite of gradient and patch-based metrics related to post-fire processes (ponderosa pine seedling density and understory species richness), we used fine-scale QuickBird imagery to create continuous and categorical burn severity maps for the 2007 Egley Fire (Oregon). We found that the spatial variation across our sites exhibited a consistent range of 8m regardless of the burn severity of the site but that overall variance was markedly lower in high severity sites. Both patch-matrix and gradient model metrics correlated strongly with distance to nearest seed tree; however neither model's metrics relate strongly to seedling density or understory species richness. Our results do not provide evidence that the gradient model allows the inclusion of additional ecologically important variation that would be lost in the patch-matrix model when characterizing recruitment processes in post-fire landscapes.

Introduction

Metrics in landscape ecology

Quantifying landscape pattern and structure and determining the relationship of these patterns to landscape processes are central goals of landscape ecology (Turner 1989, 2005; Frazier and Kedron 2017a). Landscape pattern here refers to the spatial configuration and composition of landscape features or components within an ecosystem (Turner et al. 2001). Spatial heterogeneity in particular is key to the field of landscape ecology, and studying of the impacts of spatial heterogeneity on ecological and environmental processes has been an important part of the field (Pickett and Cadenasso 1995; Wu 2013).

In order to study landscape-scale pattern and structure a number of different models (i.e. ways of conceptualizing a real-world landscape) have been used. The patch-matrix or patch-mosaic model is the foundational and most commonly used model, which conceptualizes landscapes as being composed of discrete, internally homogenous patches of different classes (Cushman et al. 2010). This model has been widely used because of the relative simplicity and intuitiveness of the model, especially when defining habitat for wildlife or plant communities. A multitude of patch metrics have been developed to describe different aspects of landscapes based on the patch matrix model, including the composition, spatial arrangement, and connectedness. Using the patch matrix model to describe landscapes also means that many patch metrics can be calculated, with differing interpretations, at the individual patch, class, or whole landscape level (McGarigal and Marks 1995).

Patch metrics can be generally categorized as measuring either composition or spatial configuration (McGarigal and Marks 1995; Gustafson 1998). Composition metrics measure some aspect of the number and/or abundance of different types of patches on the landscape and include metrics such as proportional abundance of each class, richness, evenness, or diversity. Structural configuration metrics, on the other hand, are explicitly concerned with the arrangement or position of patches with relation to other patches within the class or landscape and include a wide variety of metrics with slightly different focuses. These metrics measure edge, shape complexity, core area, aggregation, and other similar attributes and many can be calculated at the patch, class, or landscape level. Because of the near universal

adoption of this model, significant research has been done on the scaling and behavior of patch metrics. These properties are critical to the interpretation and comparison of metrics between landscapes. Patch metrics, with a few exceptions, have been found to be dependent on the grain, extent, and thematic resolution of the landscape being analyzed and that these relationships are not always predictable as scale changes (Wu 2004; Shen et al. 2004; Buyantuyev and Wu 2007; Kupfer 2012; Lustig et al. 2015).

Despite the ubiquity and success of the patch matrix model and associated patch metrics, there are known flaws within the model. In addition many studies have highlighted that, while patch metrics are related to certain processes within landscapes (Wiens et al. 1993; Uuemaa et al. 2013), it has been difficult to establish scalable, overarching causal relationships between processes and patterns across landscapes (Cushman et al. 2010; Kupfer 2012; Frazier and Kedron 2017a). This may be because the patch matrix model assumes discrete boundaries between homogenous patches of different classes, which may not accurately capture the full scale of thematic variation within a given patch or class that may in turn be important to the processes in question (McGarigal and Cushman 2005; Lausch et al. 2015).

The gradient model approach

These criticisms of the patch matrix model have led some landscape ecologists to propose alternate models to address some of the issues that have been raised with the patch matrix model and associated patch metrics. One of these proposed alternatives is the gradient model, wherein a landscape is represented as a continuous surface of a variable of interest (McGarigal and Cushman 2005; Lausch et al. 2015). These gradient models address one of the fundamental concerns about the patch matrix model, that the categorization of continuous data hides important variation on the landscape, by removing the need to define distinct classes and patches. Although the majority of gradient metrics have been developed to quantify surface structure for mechanical engineering and manufacturing purposes, the use of gradient metrics to quantify landscape surfaces has recently been the topic of increasing interest in landscape ecology (Frazier 2019). However, the origin of gradient metrics in the field of engineering contributes to current difficulties in the calculation and interpretation of

these metrics in a landscape context (Kedron et al. 2018). Throughout this paper we will use "gradient metrics" to refer to surface metrology metrics calculated based on the gradient model continuous surface and "patch metrics" to refer to metrics calculated based on the patch matrix model categorical landscape, while "landscape metrics" refers to both gradient and patch metrics.

Because the application of the gradient model and associated metrics to landscapes is relatively new, much of the scholarship has focused on how gradient metrics might be categorized and how they relate to existing patch metrics (McGarigal et al. 2009; Kedron et al. 2018). Based on an examination of forested landscapes in Turkey, McGarigal et al. (2009) defined four categories of gradient metrics based on the different components of landscape structure that the metrics measure: surface roughness, shape of surface height distribution, angular texture, and radial texture. Surface roughness metrics measure overall variability in surface height as well as local variability in slopes, which means that some metrics are explicitly spatial (e.g. surface area ratio [*Sdr*]) while others are not and simply reflect composition (e.g. average roughness [*Sa*], ten-point height [*S10z*]). Metrics measuring the shape of surface height distribution are also compositional (nonspatial) in nature and measure departures from a Gaussian distribution of surface heights, these metrics include skewness (*Ssk*) and kurtosis (*Sku*). Angular texture metrics such as dominant texture direction (*Std*) and texture direction index (*Stdi*) are spatial metrics that measure the angular orientation or direction of surface texture (anisotropy). Similarly, radial texture metrics such as radial wavelength (*Srw*) or radial wavelength index (*Srwi*) are inherently spatial since they measure repeated patterns of height variation within concentric circles (i.e. radiating) from a location.

Because of the relative newness of using the gradient model for ecological applications, there has been limited work examining the effects of scale on gradient metrics. Frazier (2016) evaluated scaling with grain (pixel) size and found that a number of gradient metrics responded consistently with changing grain and several were able to successfully scale (i.e. accurately predict metric values at finer resolution). Other work looking at effects of extent have focused on extents larger than $1km^2$ (e.g. Wu et al. 2002), likely because the conventional understanding is that you need to have a sufficiently large extent [2-5x larger than the largest patch of interest per O'Neill et al. (1996)] to avoid biases when capturing

landscape patterns. However, these same considerations may not apply to gradient metrics since they do not rely on delineation of patches and certain processes such as seed dispersal may happen on finer scales and could therefore be more influenced by the landscape context at more local scales.

Previous investigations into how gradient metrics behave and relate to patch metrics have used a variety of surface types (tree canopy height, elevation, tree canopy cover, remote sensing indices such as the Normalized Difference Vegetation Index [NDVI], etc.), however no studies to date have focused on post-fire landscapes and their patterns of burn severity. There is significant interest and a long history of seeking to quantify the structure of post-fire landscapes (Turner et al. 1997; Collins and Stephens 2010; Collins et al. 2017) because fire is a significant source of landscape-level change and often impact landscape patterns for decades or centuries. Indicators of burn severity [degree of ecological change following fire (Lentile et al. 2006; Keeley 2009)] can be derived from remotely-sensed indices and mapped as either a continuous surface of the raw index or as categorical maps based on established breakpoints that represent low, moderate, or high severity (Key and Benson 2006). Burn severity has been cited as a process that would likely be modeled well by the patch matrix model (McGarigal et al. 2009) however much of the work done that links patch metrics to post-fire processes was done in mixed conifer, stand-replacing fire regimes (Turner et al. 1997, 1999) where boundaries between burn severity levels may be more naturally discrete. However, in other fire regimes, such as ponderosa pine burn, severity may be less successfully modeled by the patch matrix model due to larger areas that burn the understory without killing or damaging overstory trees.

Objectives

We evaluated how landscape metrics (**Table 2-1**) computed at varying spatial scales relate to post-fire regeneration processes, including ponderosa pine (*Pinus ponderosa*) seedling density, distance to seed source, and understory species richness. Landscape metrics were computed from high resolution (0.6m) Quickbird imagery of immediate post-fire NDVI of the Egley Fire Complex that burned in ponderosa pine forest in Oregon in 2007.

1. We hypothesized that a more heterogeneous landscape with regard to post-fire NDVI would have shorter distances to seed sources and more variation in microsite habitats, both of which should lead to higher seedling densities. Landscape characteristics of NDVI (which reflect remaining green vegetation in the first several weeks following the Egley Fire) are expected to relate to seedling density by impacting distance to seed source on a broad scale and also potentially microsite habitat differences on finer scales.
2. We evaluated whether the gradient model-based metrics more effectively capture patterns related to important ecological processes compared to the traditional patch matrix model-based metrics.
3. We hypothesized that the relationships between our response variables (distance to seed source, seedling density, and understory species richness) and the landscape metrics would vary across six spatial scales: 15m, 30m, 60m, 120m, 240m, and 480m window sizes. We expected that the relationship between landscape patterns and seedling density would be strongest at the 120 m scale because previous research has shown that ponderosa pine has a seed dispersal distance of approximately 60m (where a 120m window captures the landscape 60m from a site in each direction).

Table 2-1 Landscape metrics based on the gradient and patch-matrix models. Patch metric descriptions from McGarigal and Marks 1995, gradient metrics descriptions are drawn from McGarigal et al. 2009 and Kedron et al. 2018.

	Metric	Description
Patch-matrix model	NP	**Number of patches**; based on 8-neighbor rule
	LPI	**Largest patch index**; 0<LPI<100; Equal to the area of the largest patch in the landscape divided by total landscape area, approaches 0 when the largest patch is increasingly small and is 100 when the entire landscape is a single patch
	AREA_MN	**Patch area mean** average area (ha) of all patches on the landscape
	SHAPE_MN	**Patch shape mean**; where shape equals the patch perimeter divided by the minimum perimeter possible for a maximally compact patch, shape is equal to 1 when the patch is maximally compact and increases without limit with increasing irregularity of shape
	CONTIG_MN	**Mean contiguity index**; where contiguity index assesses the spatial connectedness, or contiguity, of cells within a grid-cell patch to provide an index of patch boundary configuration and thus patch shape
	CONTAG	**Contagion index**; 0<CONTAG≤100; Observed contagion over the maximum possible for the given number of patch types, where the index approaches 0 when the patch types are maximally disaggregated and interspersed and is equal to 100 when all patch types are maximally aggregated (i.e. a landscape of a single patch)
	PLADJ	**Percent of like adjacencies,** 0<PLADJ<100; number of like adjacencies involving the focal class divided by the total number of cell adjacencies involving the focal class, equal to 0 when the corresponding patch type is maximally disaggregated.
Gradient model	*Sa*	**Roughness average**
	Sds	**Density of summits**; number of local maximums per area (1/surface units)
	S10z	**Ten point height**; the average height of the five highest local maximums plus the average height of the five lowest local minimums
	Sdq	**Root mean square gradient**; RMS-value of the surface slope within the sample area
	Sdr	**Surfaces area ratio**; increment of the interfacial surface area relative to the area of the projected (flat) x,y plane, for a totally flat surface Sdr=0%
	Ssk	**Surface skewness**; nonspatial shape of the surface height distribution based on departure from a Gaussian distribution, describes the asymmetry of the high distribution histogram where Ssk=0 symmetric, Ssk<0 is a surface with "holes", and Ssk>0 is flat with peaks. Values greater than |1.0| can indicate extreme holes or peaks
	Sku	**Surface kurtosis**; nonspatial shape of the surface height distribution based on departure from a Gaussian distribution, describes the "peakedness" of the surface

Methods and Materials

Field data

The Egley Complex was a lightning-ignited group of three wildfires that burned 56,800 ha of the Malheur National Forest (central Oregon) from July 7-21, 2007. Field sites were stratified on burn severity from the Monitoring Trends in Burn Severity (MTBS; www.mtbs.gov) one-year post-fire delta Normalized Burn Ratio (dNBR) classified burn severity product (unburned, low, moderate, high; **Figure 2-1**), transformed aspect (Roberts and Cooper 1989), and elevation (high or low, based on the elevation spread within the fire). Transformed aspect reflects sites that are cool-wet or warm-dry based on the topographic solar-radiation index (TRASP) transformation (Roberts and Cooper 1989) which varies from 0 (cool, moist) to 1 (warm, dry) [0 = 30º and 1= 210º]. Field data were collected nine years after the fire over the summer of 2016, as described in Dodge et al. (2019). Each site consisted of five plots; at each plot ponderosa pine seedlings (defined as shorter than 1.37m but at least 15cm tall) were tallied within a 5.6m radius, and cover of moss, fungi, and ferns was estimated along with all vascular plants, which were identified to species, within a $1m^2$ quadrat.

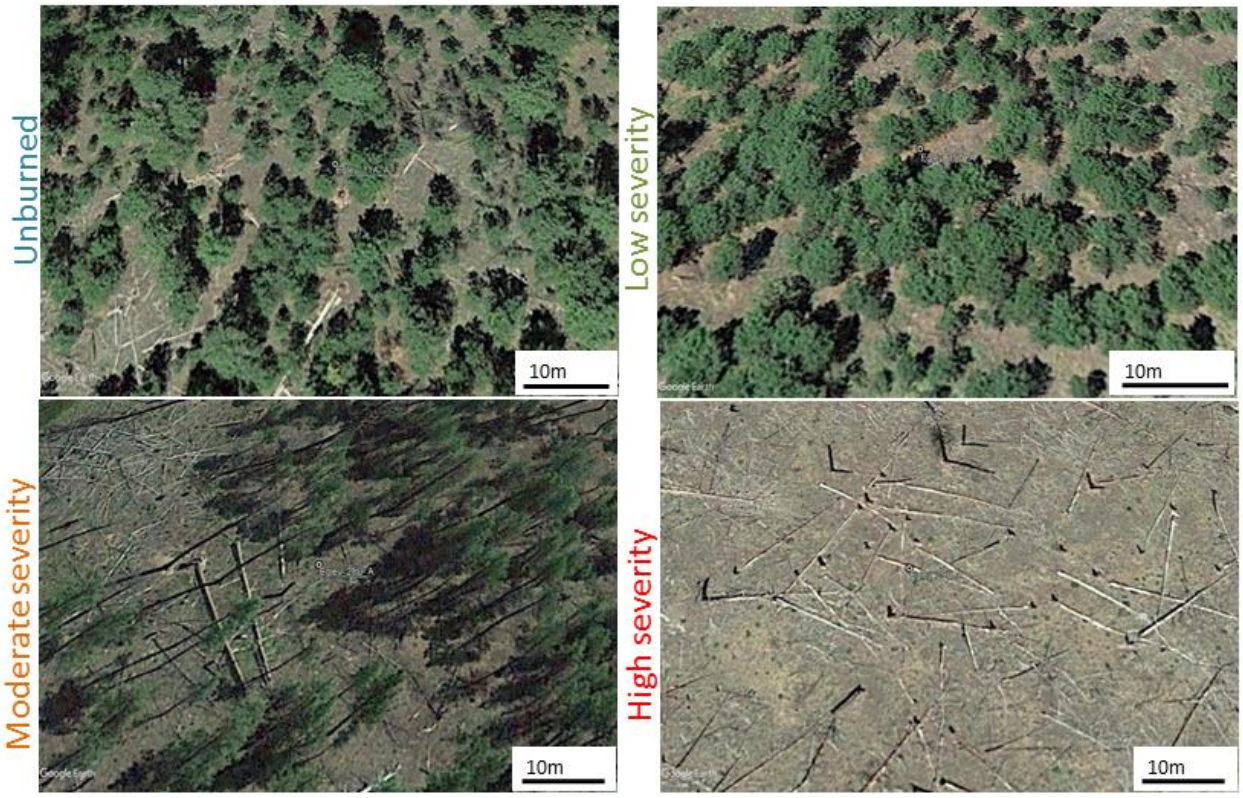

Figure 2-1 Representative GoogleEarth (imagery date 6/18/2016, accessed 8/11/2020) views of sites in unburned (top left), low, moderate, and high (bottom right) severity sites in summer 2016, when field sampling took place.

Image processing

Quickbird imagery was acquired in three passes (July 26, August 8, and August 13, 2007) following the containment of the Egley Complex on July 21, 2007. The pan-fused and orthorectified Quickbird images with a final resolution of 0.6 m were obtained by the Malheur National Forest from Digital Globe, Inc. (Longmont, CO). The Normalized Differenced Vegetation Index (NDVI) was then calculated as using the near-infrared (NIR) and visible red (R) bands as (NIR-R)/(NIR+R). This index ranges in value from +1 to -1 and is highly sensitive to the amount of green vegetation in a pixel (positive numbers). To create a patch-matrix model version of the continuous NDVI we manually determined NDVI cutoff points that best corresponded to the MTBS classified burn severity product (unburned, low, moderate, high) (**Table 2-2**, **Figure 2-2**). The nearest live tree to each plot was also manually

identified in the image and distance to the plot measured in order to estimate nearest potential seed tree.

Table 2-2 NDVI cutoff values for classified burn severity product, based on comparison of aggregated NDVI to MTBS burn severity classes.

MTBS burn severity class	Aggregated QuickBird NDVI
Low/unburn	≥0.28
Low	≥0.16 – 0.28
Moderate	≥0.09 – 0.16
High	<0.09

To avoid issues of within-site pseudoreplication, we used only the field data from a single plot at each site to serve as the center of progressively larger window sizes within with the landscape metrics were calculated. Window sizes were 15m, 30m, 60m, 120m, 240m, and 480m (**Figure 2-3**), which were chosen based on previous research indicating a cutoff of roughly 60m for ponderosa pine seed dispersal distance (Kemp et al. 2016). At each site we calculated the full suite of landscape metrics (**Table 2-1**) at all six window sizes. Patch metrics were calculated in FRAGSTATS using the 8-cell neighbor rule (McGarigal and Marks 1995) and gradient metrics were calculated using the R package *geodiv* (Smith et al. 2019).

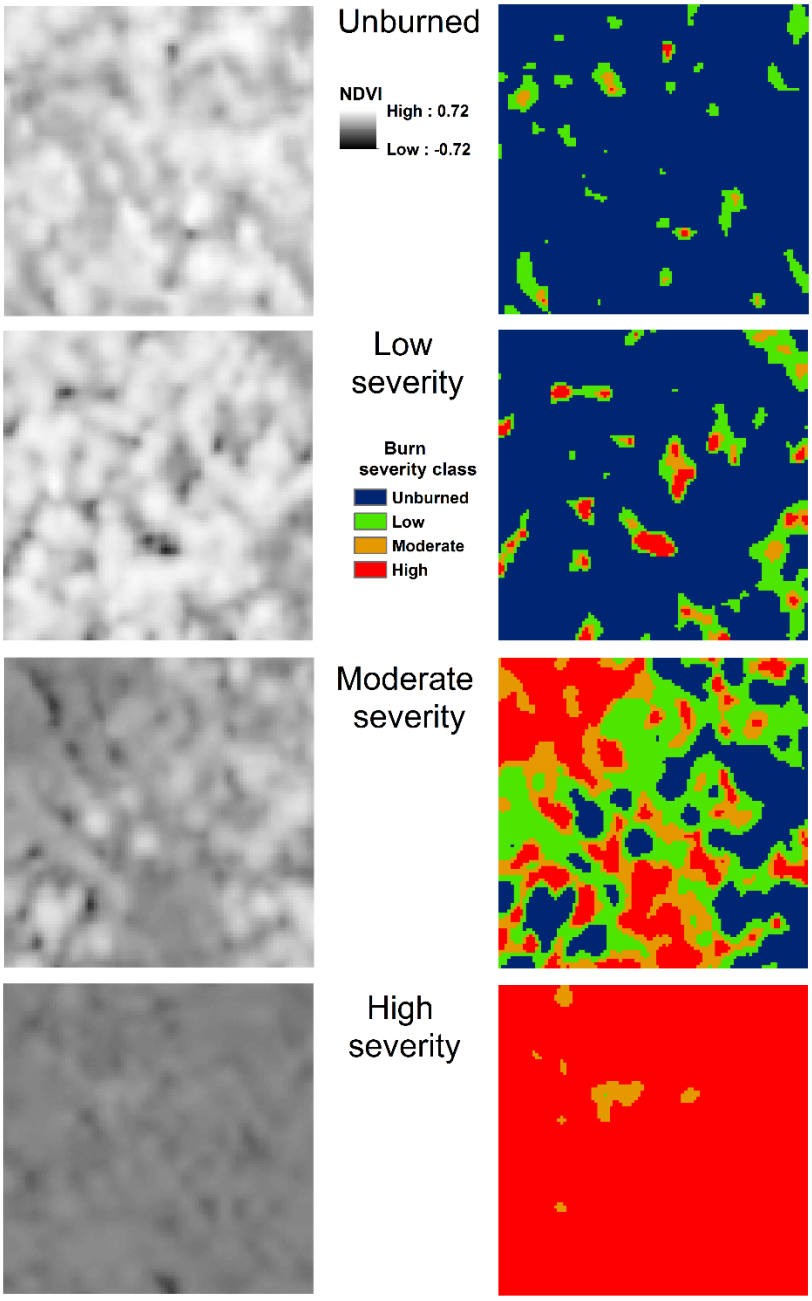

Figure 2-2 Raw NDVI and classified NDVI in 60x60m windows for selected sites at unburned, low, moderate, and high severity.

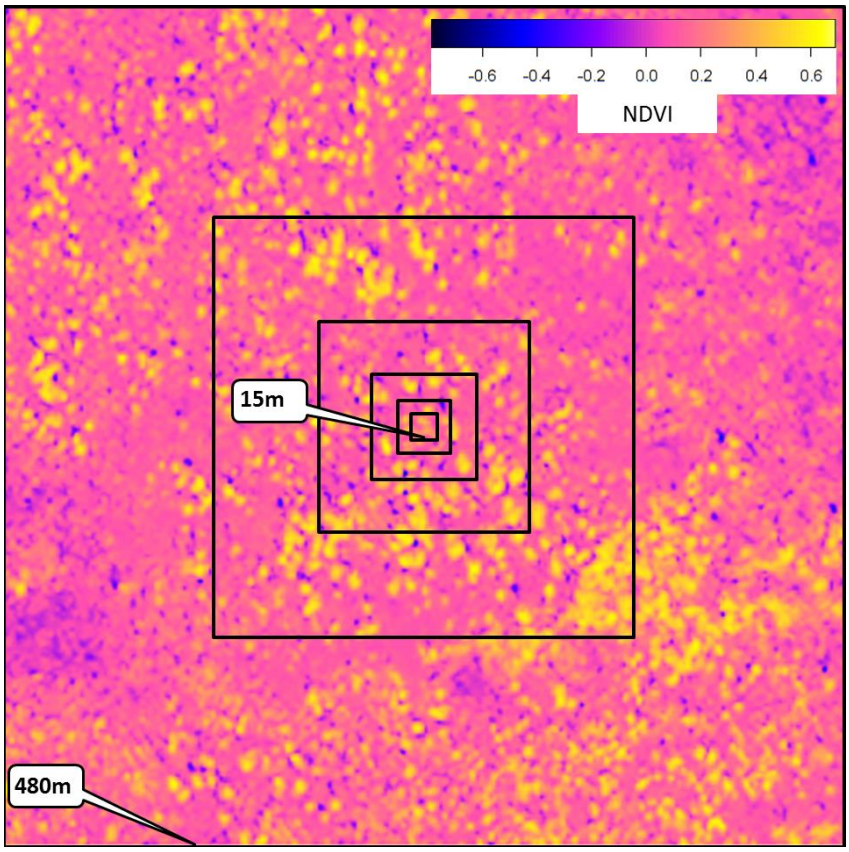

Figure 2-3 Metrics were calculated within windows of varying size (outlined in black) centered around each field site. The smallest window is 15m and window sizes double (30m, 60m, 120m, 240m) to the largest window of 480m. Window sizes are overlayed on a Normalized Differenced Vegetation Index (NDVI) image where values approaching 1 are very green vegetation and values approaching -1 are bare soil, rock, or char.

Statistical analysis

We created semivariograms of each site to examine the overall spatial structure of NDVI. Only the results for the 60m window are presented because examination of preliminary semivariograms revealed that the sill (indicating spatial independence of pixel values within) was under 15m and no secondary sill was found even at the 480m window, indicating that the 60m window was sufficiently large to capture the full range of variation in NDVI for the study area. Spearman rank correlations were obtained from *rcorr()* in the Hmisc R package (Harrell 2020), correlations were run at each window size to examine the individual relationships between each metric and measure of interest (distance to seed tree, seedling

density, and understory richness). This analysis allowed us to evaluate whether the relationship, if it existed, varied depending on the scale at which a metric was calculated as well as the direction and strength of the relationship. A correlation was deemed to be "strong" if rho≥|0.5|. To test for significant differences in correlations between window sizes, p-values were obtained by using Pearson and Filon's *z* calculated with the *cocor()* function in the cocor R package (Diedenhofen and Musch 2015).

Results

Though there was a wide range of variation among sites there was a clear trend of lower sill (maximum semivariance) with increasing burn severity (**Figure 2-4**), as well as a narrowing of the standard deviation, indicating less variation among sites of increasing burn severity level. The sill is reached at a range of approximately 8m regardless of burn severity class, indicating that it takes about 8m for NDVI values at these sites to become spatially independent.

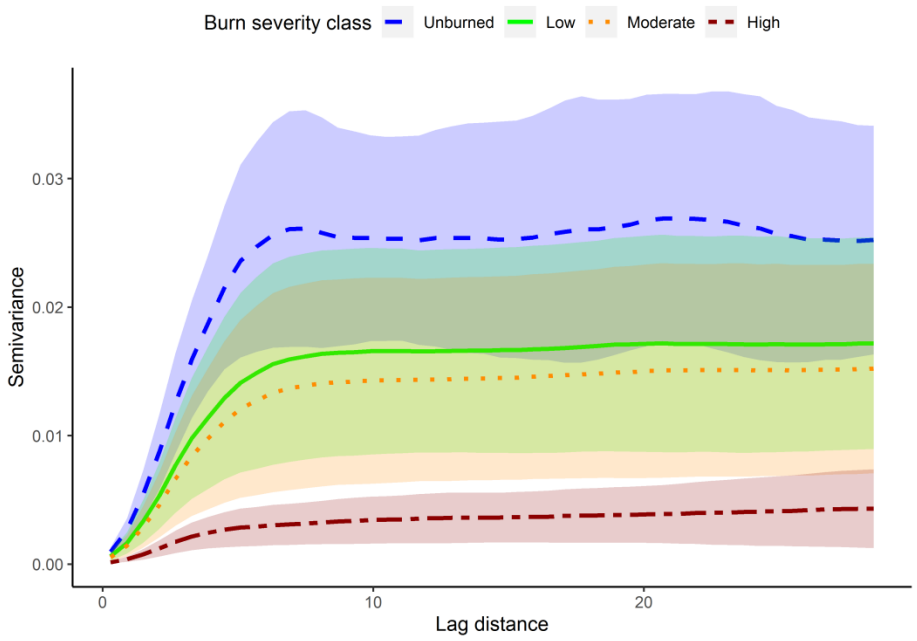

Figure 2-4 Semivariograms of post-fire NDVI within 60m windows of sites on the Egley Fire Complex (OR). Lines represent mean semivariance values while shaded areas are ± standard deviation for sites within each burn severity class.

Distance to live seed source immediately post-fire a had clear relationship to seedling density nine years post-fire, with very few seedlings at sites farther than ~60m from a live tree (**Figure 2-5**). However, there was still considerable variation in seedling density at sites with live trees within that 0-60m range, including multiple sites with zero seedlings, and as a result the correlation between distance to seed source and seedling density was weak (rho= -0.14). More comprehensive spatial data, as provided by the patch or gradient metrics, could provide more information than just distance to single nearest seed source and therefore have a stronger relationship.

All but one (mean contiguity index) of the patch metrics had significant, strong relationships (rho>|0.5|) to distance to live tree (**Figure 2-6A, Table 2-3**). All metrics had a consistent pattern of increasing correlation as window size increases until a peak in correlation at the 120m or 240m window, many metrics had significantly higher correlations at these windows (**Table 2-3**). Closer examination of a representative metric (mean patch area) showed that the

relationship was relatively consistent across window size (**Figure 2-7**). This was consistent with the metrics reflecting the importance of a 60m seed dispersal distance, because the 120m window represented an area 60m in each direction from the site in the center of the window. Only four of the gradient metrics (*S10z, Sa*, *Sdq, Sds*) exhibited significant and strong relationships to distance to live tree (**Figure 2-6B, Table 2-4**), however all four exhibited the same trend of increasing strength of correlation with increasing window size and a peak in correlation at 120m. A representative metric (surface roughness) again demonstrated that while the strongest correlation was at 120m the relationship was generally consistent across all window sizes (**Figure 2-8**).

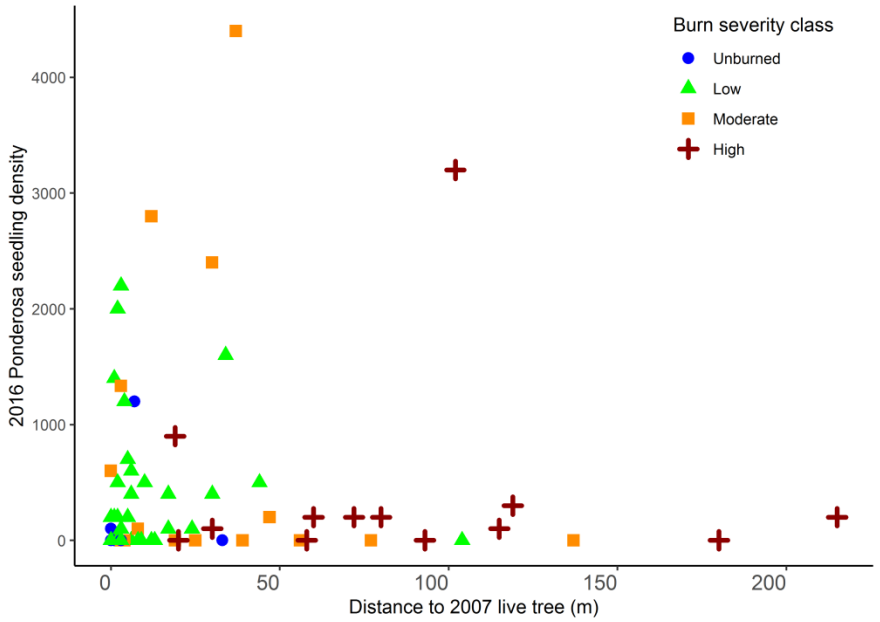

Figure 2-5 Distance to live tree in 2007 (as identified from QuickBird imagery) with density of ponderosa pine seedlings in 2016.

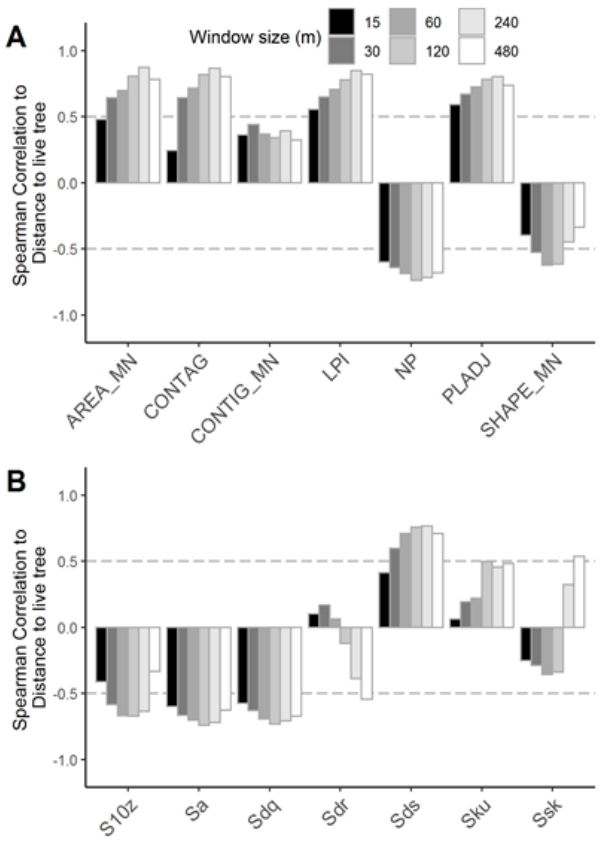

Figure 2-6 Spearman correlation of patch metrics (A) and gradient metrics (B) to distance to nearest ponderosa pine seed tree. Results of all window sizes are shown as separate colors, dashed line at Spearman rho=|0.5| represents the threshold for a strong correlation. See **Table 2-1** for full metric names and definitions and **Table 2-3** and **Table 2-4** for p-values and pairwise significance testing.

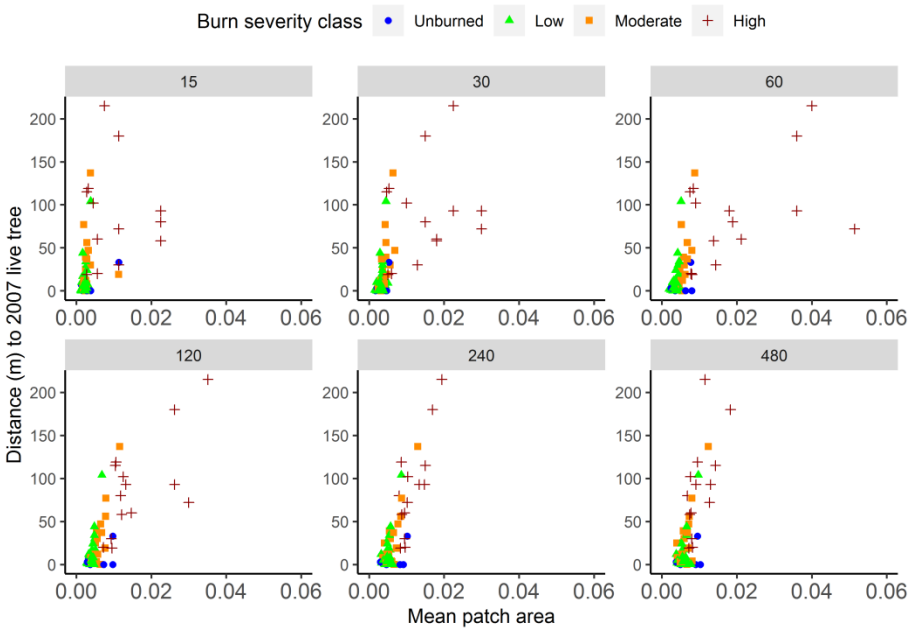

Figure 2-7 Relationship between distance to live seed tree and the patch metric Mean Patch Area (AREA_MN), panels show the metric calculated on the same sites within windows of increasing size (15m to 480m).

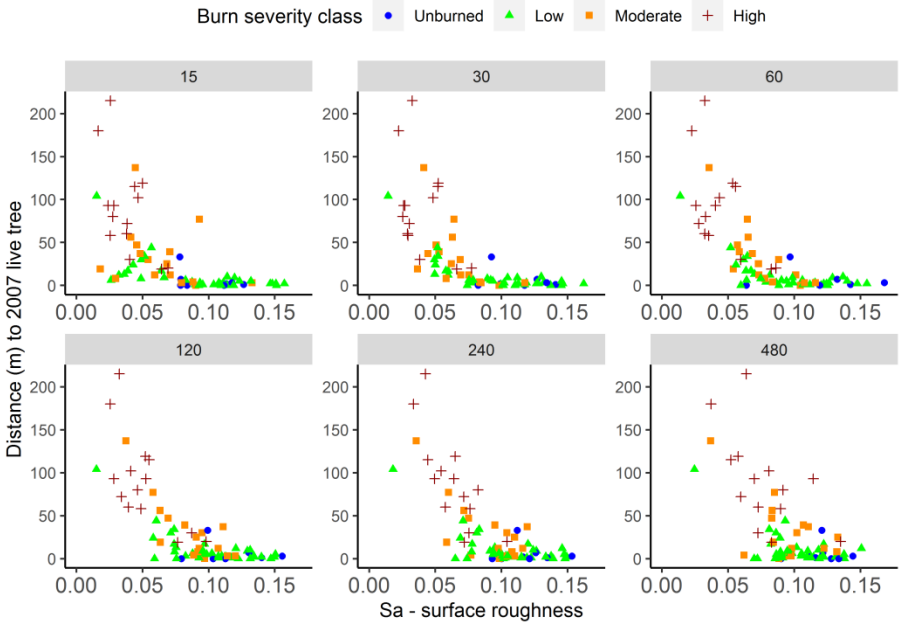

Figure 2-8 Relationship between distance to live seed tree and the gradient metric surface roughness (*Sa*), panels show the metric calculated on the same sites within windows of increasing size (15m to 480m).

Despite their strong relationships to distance to seed source, none of the patch metrics had a strong correlation with seedling density regardless of window size although mean shape index had significant correlations (**Table 2-3**). However, many of the patch metric and seedling density correlations were stronger than the baseline correlation of distance to live tree and seedling density (rho= -0.14) (**Figure 2-9A**). While the correlations between metrics and seedling density were generally less consistent than those between metrics and distance to live source, looking at a representative patch metric (largest patch index [LPI]) showed a consistent relationship that emerged in the 120m window (**Figure 2-10**). Similar to the patch metrics, the gradient metrics did not show any strong relationships to seedling density, and no metrics had significant correlations (**Table 2-4**) but two had correlations stronger than the baseline (**Figure 2-9B**). However, a closer examination of surface ten-point height shows little consistent relationship to seedling density (**Figure 2-11**).

Table 2-3 Correlation values for patch-matrix model metrics as calculated within six different window sizes and field variables (distance to live tree, ponderosa pine seedling density, and understory species richness). Spearmen's *rho* values are given with p-values in brackets, significant differences for *rho* between window sizes are indicated by different letters. Only significant correlations were tested for differences between windows.

Patch metric	**Window**	**Field variable**		
		Distance to live tree	*Seedling density ha^{-1}*	*Species richness*
Patch area mean	15m	0.48 [<0.001]A	-0.15 [0.454]	0.02 [0.109]
	30m	0.64 [<0.001]B	-0.09 [0.697]	-0.10 [0.160]
	60m	0.70 [<0.001]BD	-0.08 [0.282]	-0.15 [0.142]
	120m	0.81 [<0.001]C	-0.06 [0.811]	-0.17 [0.388]
	240m	0.87 [<0.001]E	-0.10 [0.614]	-0.12 [0.903]
	480m	0.78 [<0.001]CD	-0.15 [0.348]	-0.14 [0.596]
Contagion index	15m	0.24 [0.154]	-0.12 [0.361]	-0.17 [0.280]
	30m	0.64 [<0.001]A	-0.13 [0.367]	-0.06 [0.656]
	60m	0.72 [<0.001]B	-0.12 [0.567]	-0.08 [0.562]
	120m	0.82 [<0.001]C	-0.11 [0.331]	-0.08 [0.622]
	240m	0.87 [<0.001]D	-0.12 [0.316]	-0.08 [0.726]
	480m	0.80 [<0.001]BC	-0.19 [0.312]	-0.08 [0.871]

Contiguity index mean	15m	0.36 [<0.001]A	0.04 [0.581]	0.31 [0.001]
	30m	0.44 [<0.001]A	0.08 [0.644]	0.19 [0.114]
	60m	0.37 [<0.001]A	0.13 [0.590]	0.25 [0.022]
	120m	0.34 [<0.001]A	-0.03 [0.717]	0.10 [0.353]
	240m	0.39 [<0.001]A	-0.06 [0.932]	0.02 [0.853]
	480m	0.32 [0.006]A	0.01 [0.411]	-0.12 [0.480]
Largest patch index	15m	0.56 [<0.001]A	-0.21 [0.056]	-0.09 [0.928]
	30m	0.65 [<0.001]B	-0.13 [0.218]	-0.09 [0.852]
	60m	0.71 [<0.001]B	-0.18 [0.225]	-0.08 [0.957]
	120m	0.78 [<0.001]C	-0.19 [0.165]	-0.09 [0.715]
	240m	0.85 [<0.001]D	-0.12 [0.541]	-0.06 [0.888]
	480m	0.82 [<0.001]C	-0.20 [0.188]	-0.04 [0.963]
Number of patches	15m	-0.60 [<0.001]A	0.07 [0.446]	-0.13 [0.110]
	30m	-0.64 [<0.001]A	-0.03 [0.943]	-0.09 [0.153]
	60m	-0.69 [<0.001]AC	-0.10 [0.283]	-0.10 [0.144]
	120m	-0.74 [<0.001]BC	-0.04 [0.808]	-0.03 [0.403]
	240m	-0.72 [<0.001]A	0.03[0.637]	0.03 [0.882]
	480m	-0.68 [<0.001]A	0.10 [0.363]	0.11 [0.573]
Percent like adjacencies	15m	0.59 [<0.001]A	-0.11 [0.311]	-0.05 [0.931]
	30m	0.67 [<0.001]B	-0.07 [0.751]	-0.03 [0.674]
	60m	0.72 [<0.001]C	-0.05 [0.895]	-0.03 [0.505]
	120m	0.78 [<0.001]DE	-0.03[0.902]	-0.05 [0.646]
	240m	0.80 [<0.001]E	-0.07 [0.367]	-0.04 [0.810]
	480m	0.74 [<0.001]BCD	-0.15 [0.293]	-0.07 [0.903]
Mean shape index	15m	-0.40 [0.001]A	0.10 [0.609]	0.15 [0.537]
	30m	-0.53 [<0.001]ABC	0.20 [0.147]	0.06 [0.931]
	60m	-0.62 [0.003]C	0.22 [0.043]	0.19 [0.269]
	120m	-0.61 [0.004]C	0.14 [0.142]	0.13 [0.938]
	240m	-0.45 [0.005]AB	0.18 [0.051]	0.02 [0.662]
	480m	-0.34 [0.07]	0.10 [0.408]	0.02 [0.787]

Table 2-4 Correlation values for gradient model metrics as calculated within six different window sizes and field variables (distance to live tree, ponderosa pine seedling density, and understory species richness). Spearmen's *rho* values are given with p-values in brackets, significant differences for *rho* between window sizes are indicated by different letters. Only significant correlations were tested for differences between windows.

Gradient metric	**Window**	**Field variable**		
		Distance to live tree	*Seedling density ha-1*	*Species richness*
S10z	15m	-0.41 [<0.001]A	-0.05 [0.414]	-0.05 [0.442]

	30m	-0.58 [<0.001]B	-0.04 [0.738]	-0.21 [0.054]
	60m	-0.67 [<0.001]B	0.02 [0.599]	-0.10 [0.202]
	120m	-0.67 [<0.001]B	0.15 [0.404]	-0.02 [0.460]
	240m	-0.64 [<0.001]B	0.16 [0.202]	0.05 [0.743]
	480m	-0.33 [0.045]A	0.14 [0.319]	0.02 [0.977]
Sa	15m	-0.60 [<0.001]AD	-0.03 [0.924]	-0.23 [0.051]
	30m	-0.67 [<0.001]ABD	-0.03 [0.841]	-0.19 [0.061]
	60m	-0.70 [<0.001]BCD	0.03 [0.818]	-0.10 [0.180]
	120m	-0.74 [<0.001]BC	0.10 [0.740]	-0.07 [0.267]
	240m	-0.72 [<0.001]AC	0.11 [0.767]	-0.02 [0.446]
	480m	-0.63 [<0.001]D	0.11 [0.907]	0.10 [0.540]
Sdq	15m	-0.58 [<0.001]A	-0.06 [0.799]	-0.20 [0.048]
	30m	-0.63 [<0.001]A	-0.06 [0.569]	-0.25 [0.013]
	60m	-0.69 [<0.001]BC	-0.03 [0.765]	-0.14 [0.115]
	120m	-0.73 [<0.001]BD	0.02 [0.986]	-0.08 [0.216]
	240m	-0.71 [<0.001]ACD	0.07 [0.678]	-0.01 [0.414]
	480m	-0.67 [<0.001]ACD	0.10 [0.583]	0.08 [0.874]
Sdr	15m	0.10 [0.886]	-0.08 [0.511]	-0.12 [0.285]
	30m	0.17 [0.836]	-0.18 [0.329]	-0.26 [0.085]
	60m	0.06 [0.416]	-0.18 [0.119]	-0.20 [0.530]
	120m	-0.12 [0.017]A	-0.16 [0.178]	-0.17 [0.407]
	240m	-0.39 [<0.001]B	-0.10 [0.737]	-0.10 [0.665]
	480m	-0.54 [<0.001]C	-0.03 [0.967]	0.03 [0.684]
Sds	15m	0.41 [<0.001]A	0.00 [0.634]	0.05 [0.612]
	30m	0.60 [<0.001]B	0.07 [0.621]	0.16 [0.027]
	60m	0.71 [<0.001]CD	-0.01 [0.833]	0.09 [0.117]
	120m	0.76 [<0.001]CD	0.01 [0.933]	0.11 [0.037]
	240m	0.77 [<0.001]CD	-0.03 [0.903]	0.11 [0.034]
	480m	0.71 [<0.001]BD	-0.08 [0.669]	0.03 [0.527]
Sku	15m	0.06 [0.042]A	-0.06 [0.897]	-0.02 [0.159]
	30m	0.19 [0.045]AC	0.04 [0.692]	0.02 [0.708]
	60m	0.22 [0.008]AD	-0.04 [0.742]	0.05 [0.403]
	120m	0.50 [<0.001]B	-0.01 [0.627]	-0.01 [0.244]
	240m	0.45 [<0.001]BCD	-0.07 [0.903]	-0.07 [0.478]
	480m	0.48 [<0.001]BD	-0.12 [0.932]	-0.15 [0.535]
Ssk	15m	-0.25 [0.006]A	-0.06 [0.591]	-0.06 [0.969]
	30m	-0.29 [0.060]	0.05 [0.550]	0.10 [0.534]
	60m	-0.36 [0.072]	0.00 [0.845]	0.10 [0.584]
	120m	-0.34 [0.729]	0.00 [0.661]	0.21 [0.132]
	240m	0.32 [0.010]B	0.00 [0.858]	0.04 [0.610]
	480m	0.54 [<0.001]C	-0.13 [0.161]	-0.17 [0.362]

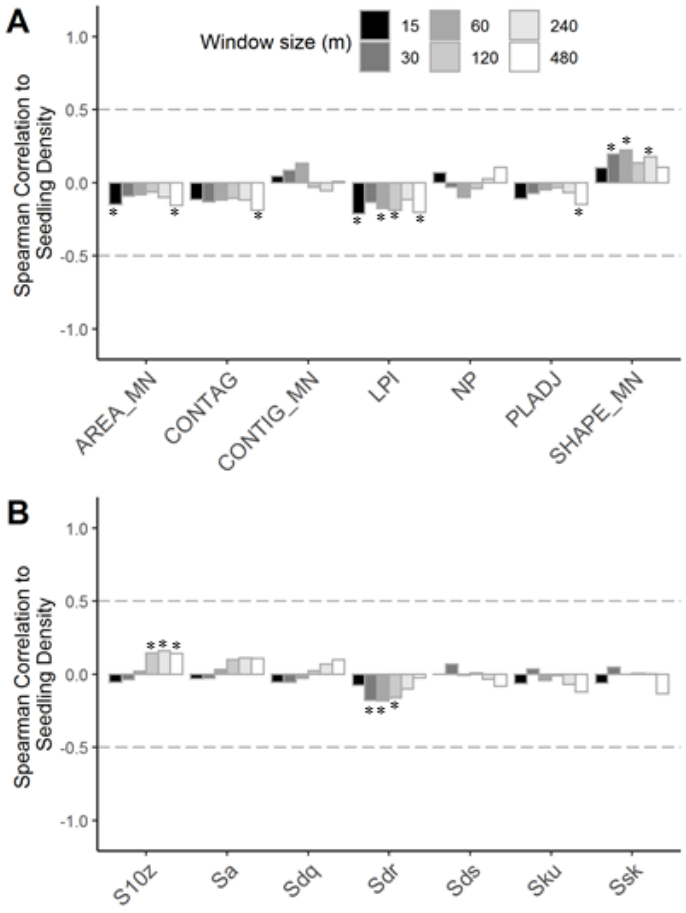

Figure 2-9 Spearman correlation of patch metrics (A) and gradient metrics (B) to ponderosa seedling density. Results of all window sizes are shown as separate colors, dashed line at Spearman rho=|0.5| represents the threshold for a strong correlation. Asterisks indicate correlations at least as strong as the correlation between distance to seed source and seedling density. See **Table 2-1** for full metric names and descriptions and **Table 2-3** and **Table 2-4** for p-values and pairwise significance testing.

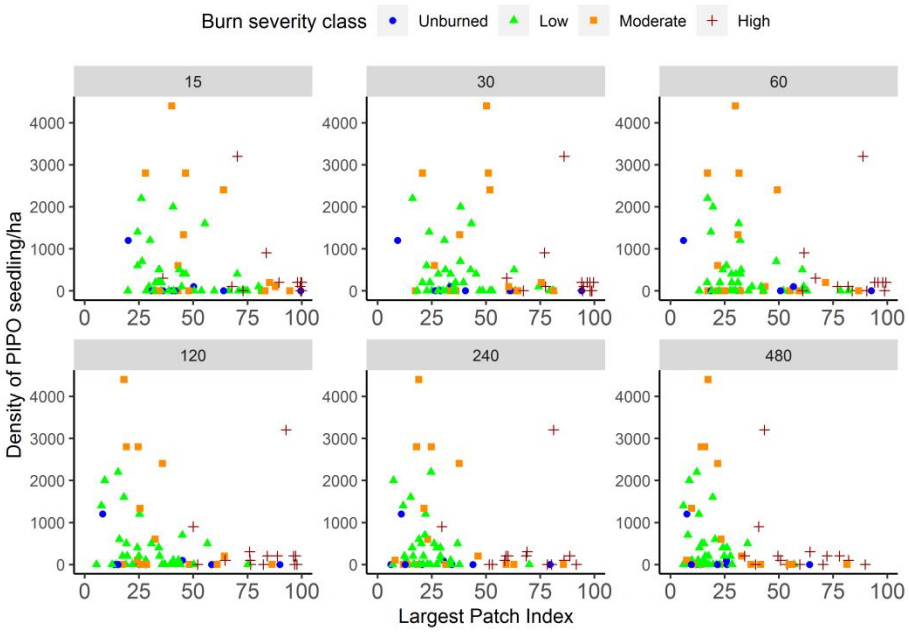

Figure 2-10 Relationship between density of ponderosa seedlings and the patch metric Largest Patch Index (LPI), panels show the metric calculated on the same sites within windows of increasing size (15m to 480m).

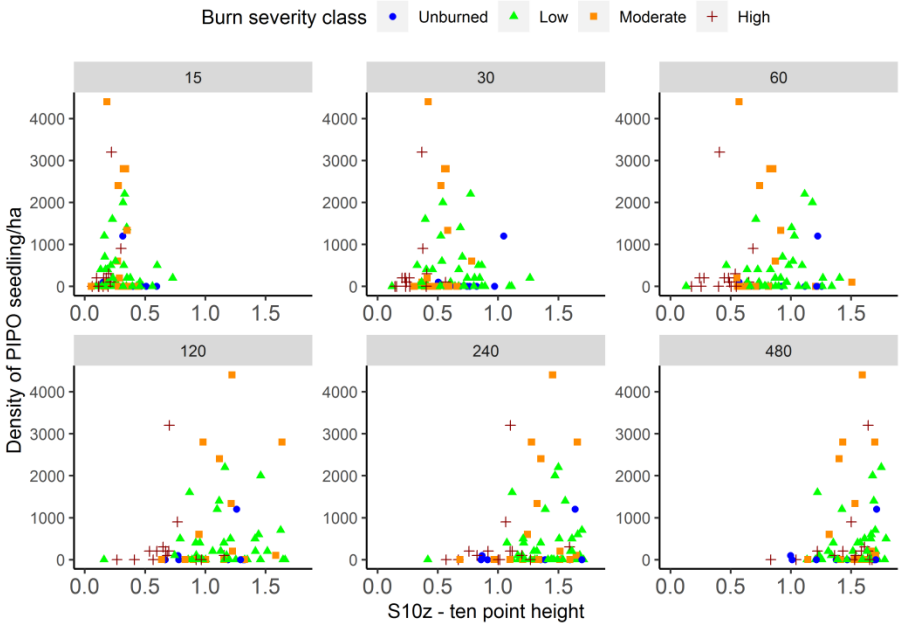

Figure 2-11 Relationship between density of ponderosa seedlings and the gradient metric surface ten point height (*S10z*), panels show the metric calculated on the same sites within windows of increasing size (15m to 480m).

None of the landscape metrics relate strongly to understory species richness (**Figure 2-12**). Among the patch metrics, mean contiguity index is by far the strongest relationship and has significant correlations (**Table 2-3**), particularly at smaller window sizes while no meaningful relationship is shown at larger windows (**Figure 2-13**). Similarly, the gradient metrics (**Table 2-4**) have a generally weaker relationship with increasing window size, which can be seen with surface roughness (**Figure 2-14**).

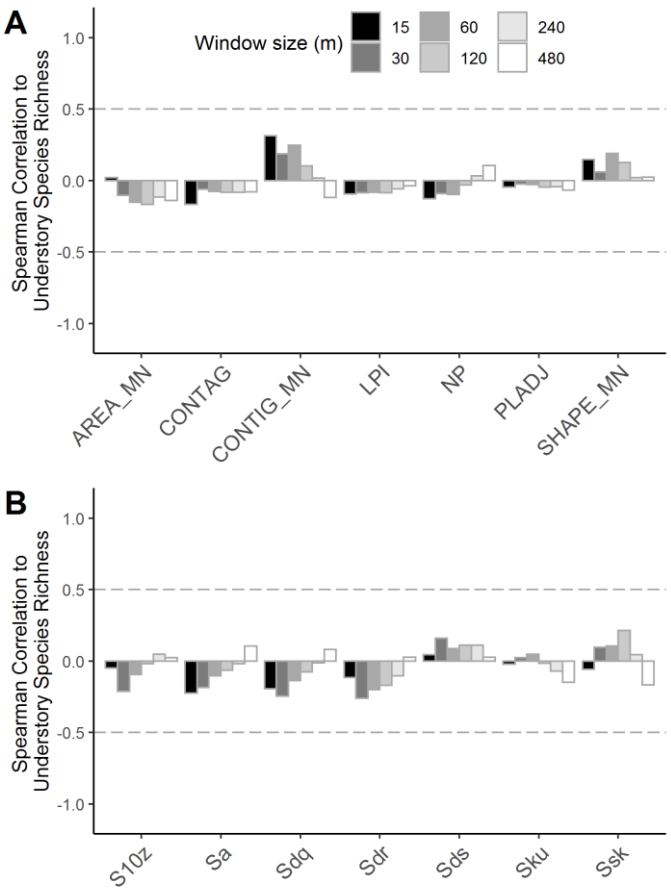

Figure 2-12 Spearman correlation of patch metrics (A) and gradient metrics (B) to understory species richness. Results of all window sizes are shown as separate colors, dashed line at Spearman rho=|0.5| represents the threshold for a strong correlation. See **Table 2-1** for full metric names and descriptions and **Table 2-3** and **Table 2-4** for p-values and pairwise significance testing.

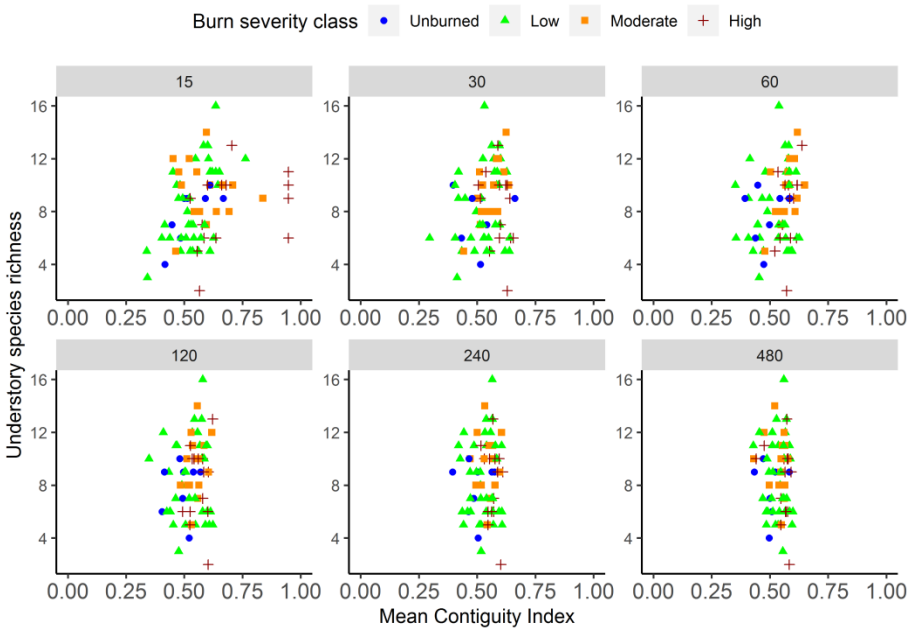

Figure 2-13 Relationship between understory species richness and the patch metric Mean Contiguity Index (CONTIG_MN), panels show the metric calculated on the same sites within windows of increasing size (15m to 480m).

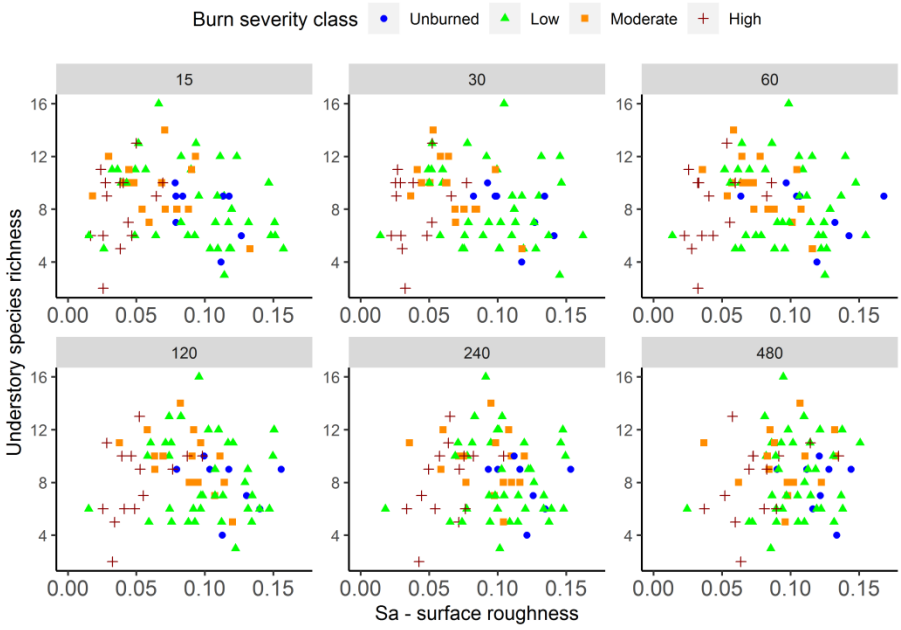

Figure 2-14 Relationship between understory species richness and the gradient metric surface roughness (*Sa*), panels show the metric calculated on the same sites within windows of increasing size (15m to 480m).

Discussion

The objectives of this study were to compare how patch and gradient metrics correlate to post-fire processes and to determine whether these relationships changed depending on the scale at which the metrics were calculated. Gradient metrics have been proposed as a solution to certain issues with the standard patch metrics, namely that gradient metrics do not require a landscape to be categorized into homogenous patches in order to calculate the metrics. This use of homogenous patches in the patch-matrix model means that the model fails to fully capture spatially heterogeneity and often creates artificially hard boundaries between class or patch types (Cushman et al. 2010). However, none of the metrics in our study had a strong relationship to understory species richness, similar to previous research showing relationships between landscape metrics and species richness failed to produce any strong relationships (Gallardo-Cruz et al. 2018). In a tropical, species-rich landscape in Mexico, Gallardo-Cruz et al. (2018) did suggest that metrics based on a continuous landscape model were generally more consistent and recommended that they may perform better in future efforts than patch-based metrics to predict species richness.

In contrast to the results for understory richness, both patch and gradient metrics correlate strongly with distance to live trees in burned areas. Based on visual inspection of the imagery and the consistent range of 8m from our semivaiogram results it appears that tree crowns are driving the landscape patterns being captured in this imagery. The variation in sill height within our results likely reflects the number and density of trees within an image, which explains why the overall variation is clearly impacted by burn severity. Because individual trees and clusters of trees are driving the variation within an image it is unsurprising that many of the landscape metrics we calculated managed to capture distance to live trees so well. Landscape metrics could be investigated as valid replacements for field-measured distance to seed source in future predictive models, which could improve the ability of managers or researchers to apply existing models of seedling density/presence to large areas. One barrier to using landscape metrics for this application is that the ability to detect individual trees would necessitate using fine-scale imagery similar to the QuickBird imagery we used, which is not always widely available.

When trying to relate landscape metrics directly to seedling density, however, our hypothesis of metrics contributing additional information and performing better than distance to seed source was disproven. None of the metrics, at any of the scales calculated, correlated to seedling density demonstrably better than the field-measured distance to live tree did. This is likely because seedling density could be dependent on multiple processes, including the distance to seed source and the suitability for a site to support seedlings (microsite and climate effects). We had hypothesized that landscape metrics would capture some of the microsite effects, in addition to capturing distance to seed source, but that does not appear to be the case based on the low correlation values.

Certain limitations should be considered in interpreting our results, the first being that our data is from a single fire, which limits the ability to generalize findings more broadly as these patterns may be specific to this fire. Additionally, while the satellite imagery used to calculate the metrics was captured shortly following the fire's containment, the field data was collected nine years later. We used field data from a later date because that better reflects the long-term seedling and understory recovery and survival (Bright et al. 2019), which would not have been captured by immediate post-fire field sampling, even though this does represent a mismatch of remote-sensing and field data collection dates. The use of satellite imagery also means that the information depended on the spatial resolution of the imagery and therefore the possibility that the imagery is failing to capture ecologically meaningful variation, rather than our assumption that the metrics are failing to quantify ecologically meaningful patterns. Satellite imagery cannot generally detect objects that are smaller than 2-3 times the size of a pixel (Strand et al. 2008).

Our results do not support the idea that gradient metrics, by being based on a continuous surface model of post-fire burn severity, capture any additional information than the traditional patch metrics that are based on a categorical landscape model. However, the strong correlations between multiple metrics and distance to live tree has the potential to allow researchers and managers to use remote sensing imagery to calculate an important variable in many models of post-fire tree regeneration, which may warrant further exploration. Further work is still needed to examine whether and how gradient metrics relate to ecological processes as assessed by in-situ data and whether gradient metrics actually, as

they were proposed to do, perform better than the established paradigm of patch metrics. Using the patch-matrix model would also allow the possibility of focusing on metrics calculated by severity class, rather than on the landscape-level as was used in this analysis, which may provide better context and further improve the relationships between patch metrics and field measures.

Conclusions

This research addresses a new direction in landscape pattern metrics research, namely the utility of describing landscape patterns with the newly emerging gradient model compared to the traditional patch-matrix model (McGarigal and Cushman 2005; Frazier 2019; Costanza et al. 2019). To date, a handful of previously published papers have explored the gradient model in a landscape context (Frazier and Kedron 2017b; Gallardo-Cruz et al. 2018). Other previous research has compared the metrics themselves for a variety of landscapes (McGarigal et al. 2009; Kedron et al. 2018), however no other work to our knowledge has documented how gradient and patch-matrix metrics relate to ecological processes essential for post-fire vegetation recovery in forests.

We conclude that at a pixel resolution of 0.6 m, both gradient metrics and patch metrics capture distance to seed source, which is an important characteristic for predicting tree regeneration in forests according to previous research (Kemp et al. 2016; Malone et al. 2018; Korb et al. 2019). However, both models failed to capture seedling density and understory species richness; we suggest three reasons: 1) understory regeneration processes are potentially occurring at a finer scale than our analysis was able to document, emphasizing the important of scale in exploration of landscape pattern metrics research; 2) larger objects, such as trees, obscure or interfere with the detection of smaller objects when using passive reflectance based sensors such as those mounted on Landsat and QuickBird; 3) there is a temporal mismatch in the date of image collection such that microsites could not be detected immediately post-fire when the image was collected. Understanding effects of spatial, thematic, and temporal scale continues to be central topics in landscape ecology research. Furthermore, pattern metrics can be calculated at both the landscape and class scale (McGarigal and Marks 1995). It is possible that metrics calculated at the class level, which would generally be based on the patch-matrix model, are more informative than those

computed at the landscape level for our application. We therefore suggest that future research explores ways to compare gradient and patch matrix metrics at the class level to provide context for the analysis of relating landscape pattern to ecological processes.

.

Chapter 3: Site and climate influences on height growth and density of natural ponderosa pine regeneration following wildfires

Abstract

Though wildfire is a natural process in much of the western USA, over the past century the characteristics of wildfire and the post-fire recovery processes have been changing due to management policies and changing climate. Seedling establishment and growth are two important processes involved in this post-fire recovery process because they drive overstory tree dynamics. Post-fire tree regeneration density can be highly variable depending on burn severity, pre-fire forest condition, tree regeneration strategies, and climate conditions among other variables, however few studies have examined whether different factors impact seedling density and height growth on the same sites. We measured seedling density and height growth in 2015-2016 on three wildfires that burned in ponderosa pine (*Pinus ponderosa*) forests during the time period 2000-2007 across broad environmental and burn severity gradients. Height growth was impacted mainly by soil productivity, basal area of live trees, and climate, particularly winter evapotranspiration and fall degree-days above 5°C. By contrast, density was most strongly impacted by site-based measures and indicates that that higher surviving seedling density is found in low to moderate burn severity sites with higher fine woody fuel load and lower soil cover.

Introduction

Tree regeneration is a critical aspect of post-wildfire recovery in forested ecosystems, since the growth of trees following a fire is a key factor in the perceived recovery of value both ecologically and economically within a burned area. Trees in the western United States have a variety of regeneration strategies and for many fire plays an important role in their long-term survival and growth, as evidenced in part by increased regeneration in burned areas or in areas that burned at high severity (Larson and Franklin 2005; Crotteau et al. 2013; Kemp et al. 2016). The post-fire environment is generally characterized by an increase in nutrient

and light availability, but can also experience changes in soil properties due to heating that occurs during the fire as well as increased erosion post-fire due to removal of vegetation (DeBano et al. 1998). With many post-fire systems experiencing changing climate there has been evidence of declining conifer regeneration across the western US following fires, highlighting the importance of understanding this dynamic post-fire process (Stevens-Rumann et al. 2017).

In the western U.S. the focus of post-fire conifer regeneration research has generally been seedling establishment and density, with studies showing a wide range of factors that influence the success of regeneration. These factors include burn severity (Larson & Franklin 2005; Crotteau et al. 2013; Kemp et al. 2016) and its impacts on duff depth (Kemball et al. 2006; Hesketh et al. 2009), distance to seed source (Bonnet et al. 2005; Keeton and Franklin 2005; Donato et al. 2009; Kemp et al. 2016), and climate or water availability (Dodson and Root 2013; Feddema et al. 2013; Kemp et al. 2016). For studies that include it as a factor, distance to seed source is generally the most dominant predictor of conifer seedling density post-fire, along with pre-fire tree basal area (Kemp et al. 2016). In burned areas the burn severity and patch size (distance to edge/unburned) are the main drivers of distance to seed source, since burn severity is commonly categorized based on tree canopy mortality in forests. For serotinous species, and to a lesser extent for other conifer species in mast years (Pounden et al. 2014), crown mortality does not necessarily mean a removal of the tree as a seed source. However, microsite environmental conditions (Bonnet et al. 2005; Kemball et al. 2006; Hesketh et al. 2009) and climatic water availability (Dodson and Root 2013; Feddema et al. 2013; Savage et al. 2013; Kemp et al. 2016) also play an important role by creating certain "windows" of conditions where seedling establishment and growth are more likely.

Seedling height growth has been relatively understudied in the context of post-fire environments; most studies that do include height use only total height at time of sampling. Dodson and Root (2013) used height as a categorical variable to determine how well naturally regenerated conifer seedlings were established (≥38cm was considered well-established), finding that there was increased density of "well-established" seedlings at wetter, higher elevation sites. Similarly, in a factorial experiment on planted seedlings,

Bansal et al. (2014) used height to determine the "best performing" seedlings from which they sampled several ecophysiological traits, finding that only moderate or high severity surface burns resulted in positive ecophysiological responses.

Studies that have investigated seedling height growth over time have generally been on planted seedlings that undergo some manipulation in order to investigate how specific drivers affect growth. Wang and Kemball (2010) looked at effects of burn severity on the performance of planted black spruce (*Picea mariana*), white spruce (*Picea glauca*), and jack pine (*Pinus banksiana*) seedlings and found that height and diameter growth three and four years post-fire were highest in severely burned areas and lowest in low severity areas, though for seedlings that were artificially released from competition (via herbicide and mechanical clipping of competing vegetation) there was no longer an effect of burn severity on growth. To look at the potential effects of climate change on seedling growth following disturbance, Rother et al. (2015) manipulated temperature and water availability over two years for planted ponderosa pine (*Pinus ponderosa*) and Douglas-fir (*Pseudotsuga menziesii*), finding that warming treatments slowed height growth rates and percent survival for both species.

Given that tree height growth in the long term is a crucial aspect of site recovery, field-based studies investigating the patterns and drivers of height growth in natural regeneration following wildfire are a fundamental step in understanding the processes of site recovery. To this end, our goal was to examine what climate and site variables influenced height growth and seedling density on sites with established ponderosa pine seedlings approximately 10 years after three large wildfires. Ponderosa pine is a widespread species across the western US and may be particularly at risk of decreased regeneration success post-fire because of changing climate and historic management (Donato et al. 2016; Stevens-Rumann et al. 2017). Sites with higher water availability, more potential microsites (provided by downed woody fuels or potentially shrubs), and lower competition (lower percent cover of understory green plants, lower overstory canopy cover) are hypothesized to have higher average yearly height growth as well as higher seedling density. Few studies have captured yearly height growth data and there has been limited work examining whether predictors for seedling height growth are the same as those for seedling density, which is more widely studied.

Methods and Materials

Sites and field methods

Three fires (Hayman, Jasper, and Egley) in ponderosa pine-dominated forests in the western U.S. were sampled for this study. The Hayman Fire (55,893 ha) burned in the Front Range of central Colorado in 2002, the Jasper Fire (33,794 ha) in the Black Hills of southwest South Dakota in 2000, and the Egley Complex (56,800 ha) in Malheur National Forest of central Oregon in 2007. The three fires have generally similar temperature regimes but differ in the amount and timing of precipitation (**Figure 3-1**). Precipitation at the Egley Fire primarily falls in October-May whereas Jasper and Hayman receive the majority of their precipitation March-August, Egley also receives 80% less overall precipitation than Jasper and 30% less than Hayman.

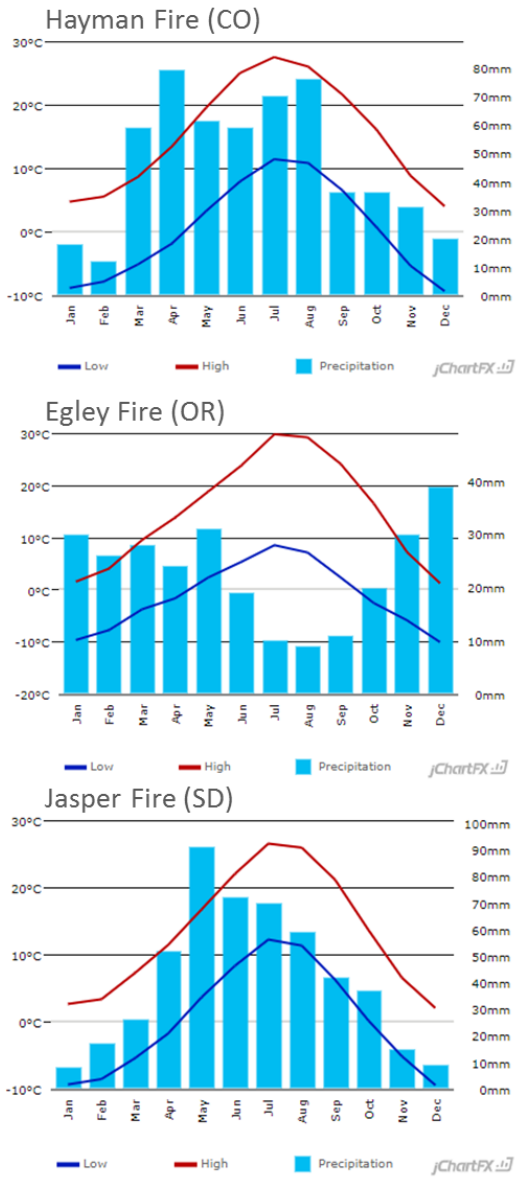

Figure 3-1 Monthly temperature and precipitation climate normals (1981-2010) for the Hayman (Colorado), Egley (Oregon), and Jasper (South Dakota) fires.

Field sites were stratified on burn severity from the Monitoring Trends in Burn Severity (MTBS; www.mtbs.gov) one-year post-fire delta Normalized Burn Ratio (dNBR) classified burn severity product (unburned, low, moderate, high), transformed aspect (Roberts and Cooper 1989), and elevation (high or low, based on the elevation spread of each fire). Transformed aspect reflects sites that are cool-wet or warm-dry based on the topographic solar-radiation index (TRASP) transformation (Roberts and Cooper 1989) that varies from 0 (cool, moist) to 1 (warm, dry) [0 = 30º and 1= 210º]. The total number of sites and year of

sampling varied between fires: 19 sites were sampled at Hayman in 2015 (13 years post-fire), 16 sites at Jasper in 2015 (15 years post-fire), and 41 sites at Egley in 2016 (9 years post-fire).

The MTBS product was used to stratify sites because it is a free, validated source of burn severity maps for all large fires and therefore is commonly used by both researchers and managers for post-fire ecological studies, impact assessments, and to guide potential restoration. To create this product, continuous dNBR values are calculated as the pre-fire NBR (Normalized Burn Ratio) minus post-fire NBR, where NBR is a normalized ratio calculated from 30m resolution Landsat near infrared band (NIR) and short wave infrared band (SWIR); i.e., (NIR-SWIR)/(NIR+SWIR). Continuous dNBR is then categorized as unburned, low, moderate, or high severity, or increased green based on thresholds determined by the MTBS analyst (Eidenshink et al. 2007). The dNBR index is sensitive to changes in green vegetation, bare soil, and char, where areas with higher char and bare soil will have higher NBR values (Key and Benson 2006; Hudak et al. 2007).

Within each site, five plots were established 30 m apart in a cross formation with the first outer plot established upslope of the site center according to the dominant slope. Seedlings and saplings (seedling is defined as taller than 15 cm but shorter than 1.37 m; sapling is taller than 1.37 m with a diameter at breast height (DBH) less than 10 cm) were tallied by full quarters in 5.6 m radius plots until a minimum of six seedlings had been encountered. Up to six representative seedlings or, if they were determined to represent post-fire regeneration based on estimated age, saplings were measured for the length between terminal bud scars to obtain approximate age and yearly growth increments (Urza and Sibold 2013). This analysis focused on the most recent seven complete years of growth (2009-2015 for Egley and 2008-2014 for Hayman and Jasper) because field observations and previous work (e.g., Urza and Sibold 2013) indicate that recent bud scars of recent years are more reliably identified.

The distance from each plot to the nearest live ponderosa seed tree was recorded. Fractional cover of green vegetation, nonphotosynthetic vegetation, mineral soil, and percent char of soil and nonphotosynthetic vegetation was visually estimated in five-1 m^2 plots. Nonphotosynthetic vegetation included woody debris, senesced grass or forbs, tree bark, or

leaf and needle litter. Additionally, we measured litter and duff depth, fine woody fuels (1-, 10-, 100-hour timelag classes; <1 cm, 1-2.5 cm, and 2.5-7 cm diameter, respectively) were estimated using a photoload guide (Keane and Dickinson 2007), and canopy cover of the overstory (trees and shrubs exceeding breast height [1.37 m]) was estimated using a convex densiometer.

At each of the four peripheral plots, standing trees were recorded using a 2 m^2/ha basal area factor prism; for each tree the species, vigor (dead, healthy, unhealthy), and DBH was recorded. At only the center plot, all trees were tallied and measured in a 0.02 ha plot (8 m radius). Percent cover of tall shrubs (> 1.37 m height) was ocularly estimated, and large downed woody fuels (1000-hr timelag class, >7.62 cm diameter) were measured using the photoload guide (Keane and Dickinson 2007) within a 0.01 ha plot (5.6 m radius) at the center plot only.

Derived variable sources

In addition to field-collected variables, burn severity, climate, and soil variables were derived from public data sources. Continuous dNBR, indicative of burn severity, for each site was obtained from the MTBS database. Climate data was generated using the ClimateNA v.6.21 software package (http://climatena.ca/; accessed November 2019), which calculates and derives scale-free point estimates of climate data (Wang et al. 2016). Climate data were generated for 2008-2015 to represent the growth timeframe for seedlings used in this analysis, and then averaged by season within a year: winter (December-February), spring (March-May), summer (June-August), and fall (September-November). Soil variation among sites within a fire and between fires was accounted for with the soil Productivity Index (PI), which ranks soil productivity from 0 (least productive) to 19 (most productive) at 240 m resolution (Schaetzl et al. 2012).

Statistical methods

We used 52 sites (Hayman = 12, Jasper = 11, and Egley= 29) that had ponderosa pine seedlings present and were not planted following the fire to capture natural tree regeneration. Each year's growth was standardized on total seedling height in that year (Littlefield 2019), and a site-level average yearly growth was determined by averaging the growth of all

seedlings at a site. The response variable "seedling height growth" therefore represents the average yearly height growth for a seedling at a given site for the past seven years of growth prior to sampling, standardized to account for the height of the seedling in a given year of growth. Seedling density was calculated as seedlings per hectare based on the number of seedlings counted divided by the area sampled on a site.

Non-parametric multiplicative regression (NPMR) in HyperNiche v.2 (McCune and Mefford 2009) was used to determine the influence of, and potential interactions between, predictor variables on both seedling height growth and density. NPMR allows for predictor variables to interact in non-linear, multiplicative ways to influence the response variables (McCune 2006). Each NPMR free search run was done with local mean model and Gaussian weighting, with default medium controls for overfitting, automatic minimum average neighborhood size (number of sites * 0.05), step size of 5, 10% maximum allowable missing estimates, and minimal backtracking search. HyperNiche automatically runs the free search as an iterative process over various combinations of predictor variables, producing thousands of models in the process. To reduce collinearity and duplication among predictor variables, predictor variables with pairwise correlations greater than 0.9 to another predictor variable were dropped in a step-wise approach based on strength of Spearman's rank correlation to average seedling height growth. This resulted in a final set of 39 variables (**Table 3-1**) that were included in the NPMR free search to examine their influence on seedling growth; 36 predictor variables were included in the seedling density free search, which excluded seedling density variables (total live seedling density, total dead seedling density, and total live sapling density) that were included as predictor variables for the growth free search.

The lists of models generated by the NPMR process were sorted by the cross-validated R^2 (xR^2) to determine what predictor variables appeared in the majority of the top 100 models. This process was used to select the best model for seedling height growth and for seedling density, individually, at which point the models were evaluated for tolerances and sensitivity. Tolerances in NPRM are the standard deviations used in the Gaussian smoothing and must be interpreted based on the range of each predictor, higher tolerance indicates that a variable is less important to the model. Sensitivity values range from 1 to 0, with higher sensitivity

indicating that a percent change in that predictor will result in a similar percent change to the estimate of the response variable.

Table 3-1 Potential predictor variables for NPMR models of ponderosa pine seedling height growth and density. Seasonal climate variables (averaged for 2008-2015 to represent post-fire growing conditions) were obtained from ClimateNA (Wang et al. 2016, v. 6.21). Summer was defined as June-August; Fall as September-November; Winter as December-February; Spring as March-May. Burn severity was obtained from MTBS (www.mtbs.gov) and field data were gathered in the summers of 2015 (Hayman and Jasper) and 2016 (Egley). Variables with an asterisk were excluded from the NPRM for seedling density.

Variable	Minimum – Maximum value
Climate variables	
Summer mean maximum temperature	22.1 – 28.2 °C
Fall mean maximum temperature	11.4 – 18.6 °C
Winter precipitation	54.9 – 210.6 mm
Summer precipitation	47.5 – 292.1 mm
Fall precipitation	92.4 – 164.3 mm
Fall degree-days above 5°C	258.1 – 520.0 degree-days
Fall number of frost-free days	33.0 – 51.4 days
Winter precipitation as snow	23.3 – 113.3 mm
Spring precipitation as snow	8.6 – 112.6 mm
Summer precipitation as snow	0.0 – 2.1 mm
Fall precipitation as snow	2.9 – 40.3 mm
Winter Hargreaves Reference Evapotranspiration	0.0 – 25.5 mm
Fall Hargreaves Reference Evapotranspiration	129.0 – 222.9 mm
Spring Hargreaves Climatic Moisture Deficit	19.4 – 148.0 mm
Winter relative humidity	43.3 – 60.8 %
Spring relative humidity	48.3 – 58.5 %
Summer relative humidity	44.0 – 59.3 %
Derived variables	
Elevation	1507.1 – 2858.7 m
Transformed aspect (Roberts and Cooper 1989)	0.0097 – 0.9960
Slope	0.79 – 32.15 %
Differenced Normalized Burn Ratio	-24.0 – 717.6

Soil Productivity Index	6.0 – 15.0
Field variables	
Distance to nearest cone-bearing tree	2.1 – 200.0 m
Understory species richness	4.2 – 17.6
Understory live vegetation cover	5.2 – 81.0 %
Understory non-photosynthetic vegetation cover	14.0 – 94.4 %
Rock cover	0.0 – 21.4 %
Soil cover	0.0 – 60.0 %
Total cover of charred surface components	0.0 – 141.0 %
Tall shrub cover	0.0 – 2.0 %
1000hr woody fuel load	0.0 – 8.8 kg ha^{-1}
Fine (1-, 10-, and 100hr) woody fuel load	0.024 – 1.582 kg ha^{-1}
Litter depth	5.4 – 39.0 mm
Duff depth	0.0 – 24.4 mm
Total basal area of live trees	0.0 – 30.6 m^2 ha^{-1}
Total basal area of dead trees	0.0 – 23.0 m^2 ha^{-1}
Live sapling density*	0.0 – 1913.3 stems ha^{-1}
Dead seedling density*	0.0 – 240.0 stems ha^{-1}
Live seedling density*	20.0 – 13360.0 stems ha^{-1}

Results

The best model for predicting ponderosa pine seedling height growth included the soil Productivity Index (soil PI), live tree basal area, fall degree-days above 5°C, and winter reference evapotranspiration (**Table 3-2**). Height growth peaked at lower soil PI when winter evapotranspiration was high (**Figure 3-2A**) and when live tree basal area was low (**Figure 3-2B**), however height growth was lowest when live tree basal area was high. Soil PI had a less pronounced effect on height growth at lower fall degree-days above 5°C (fall degree-days) but height growth peaked at about 500-450 fall-degree days and lower soil PI (**Figure 3-2C**).

Table 3-2 Selected best models from NPMR free search for ponderosa pine seedling height growth and for seedling density following large wildfires. Average size is the average neighborhood size; i.e., the average number of sample units that contribute to each point's estimated value on the modeled surface. See **Table 3-1** for full variable names and ranges.

Response variable	Model xR^2	Average Size	Predictor variable	Sensitivity	Tolerance
Growth	0.57	4.49	Soil Productivity Index	0.03	1.35 (15%)
			Live basal area	0.16	4.58 (15%)
			Fall degree-days	0.25	26.19 (10%)
			Winter evapotranspiration	0.04	8.93 (35%)
Density	0.27	4.18	dNBR	0.06	148.32 (20%)
			Soil cover	0.09	9.00 (15%)
			Fine fuel load	0.08	0.23 (15%)
			Dead basal area	0.16	2.30 (10%)

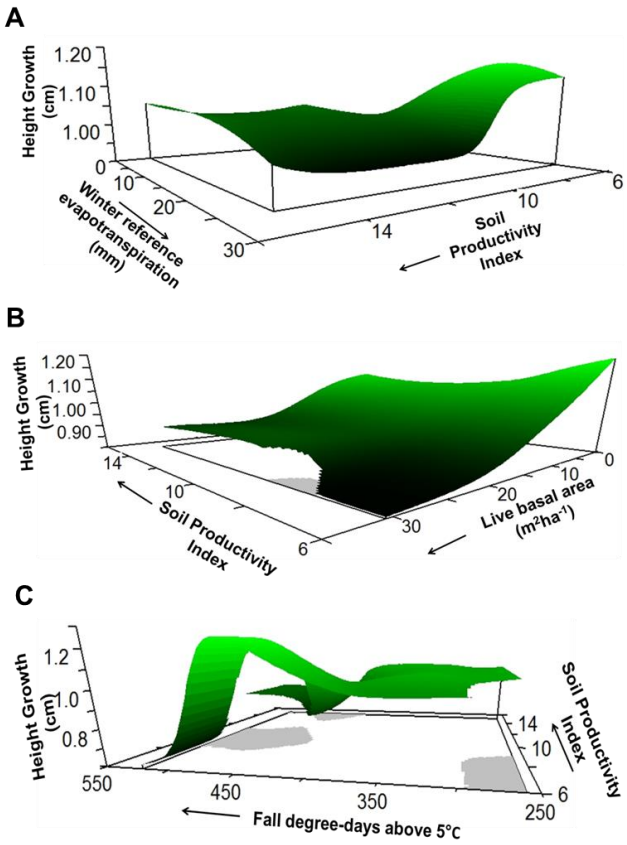

Figure 3-2 Average standardized height growth of ponderosa pine seedlings is affected by Soil Productivity Index in interaction with (**A**) winter reference evapotranspiration, (**B**) basal area of live trees, and (**C**) fall degree-days above 5°C. Grey areas indicate where the model lacked enough information to reliably predict the response.

Height growth also peaked at about 450-500 fall degree-days at low live tree basal area, but height growth was also relatively high at lower fall degree-days when live tree basal area was high (**Figure 3-3A**). Winter evapotranspiration had no effect on height growth at high live tree basal area, but had a positive effect at low live tree basal area and height growth peaked at high winter evapotranspiration and low live tree basal area (**Figure 3-3B**). Height growth was not strongly affected by winter evapotranspiration with fall degree-days, with the highest height growth again being between 450-500 degree-days (**Figure 3-3C**).

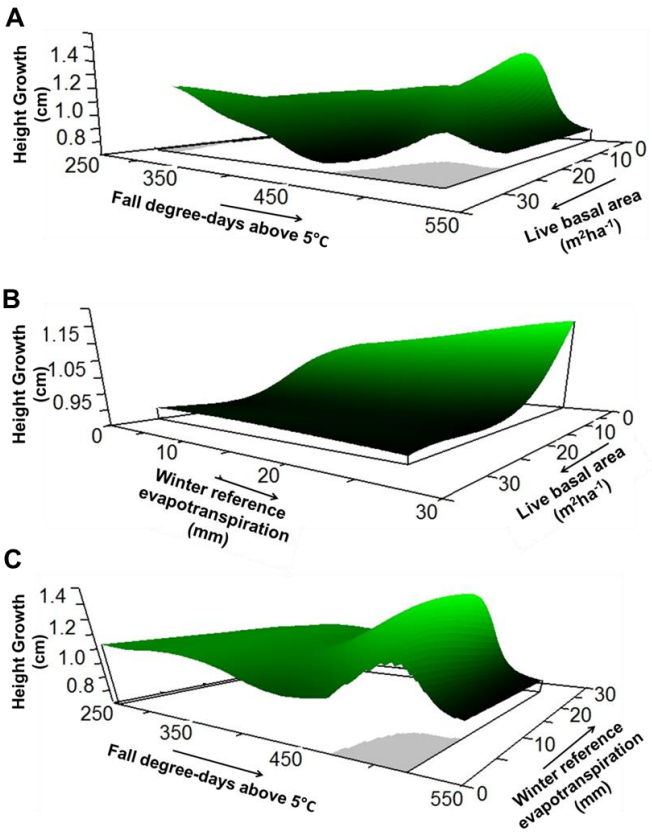

Figure 3-3 Average standardized height growth of ponderosa pine seedlings is affected by interactive effects of (**A**) fall degree-days above 5°C and basal area of live trees, (**B**) basal area of live trees and winter reference evapotranspiration, and (**C**) fall degree-days above 5°C and winter reference evapotranspiration. Grey areas indicate where the model lacked enough information to reliably predict the response.

The best model for ponderosa pine seedling density included dNBR, soil percent cover, fine woody fuel load, and basal area of dead trees (**Table 3-2**). Seedling density was relatively unaffected by dNBR until soil cover was low, at which point density peaked at moderate levels of dNBR, and density was consistently negatively affected by soil cover regardless of dNBR level (**Figure 3-4A**). Similarly, seedling density was positively impacted by fine woody fuel load regardless of dNBR level and density was highest at moderate dNBR and high woody fuel load (**Figure 3-4B**). dNBR had a slight negative effect on seedling density regardless of dead tree basal area, while seedling density peaked at a dead tree basal area of about 10 m^2ha^{-1} regardless of dNBR level (**Figure 3-4C**). Seedling density showed a sharp peak at low soil cover with fine woody fuel load above approximately 1 kg ha^{-1} (**Figure**

3-5A). Soil cover had a small negative effect on seedling density regardless of basal area of dead trees, with the highest seedling densities found at about 10 m^2 ha^{-1} of dead trees regardless of soil cover (**Figure 3-5B**). Similarly, seedling density peaked sharply at high fine woody fuel load and approximately 10 m^2 ha^{-1} dead tree basal area (**Figure 3-5C**).

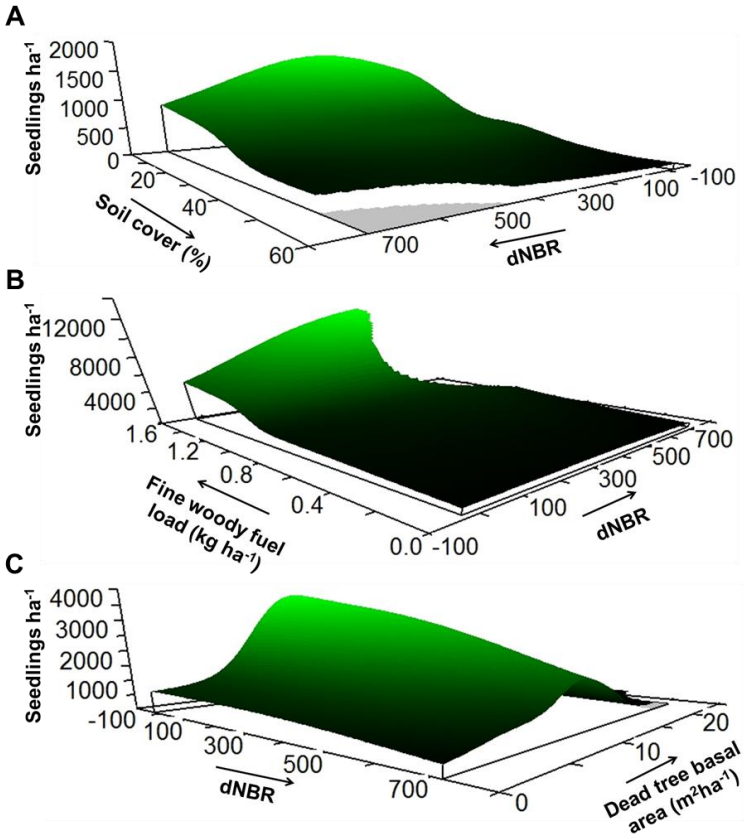

Figure 3-4 Ponderosa pine seedling density is affected by interactive effects of dNBR and (**A**) percent soil cover, (**B**) fine woody fuel load, and (**C**) basal area of dead trees. Grey areas indicate where the model lacked enough information to reliably predict the response.

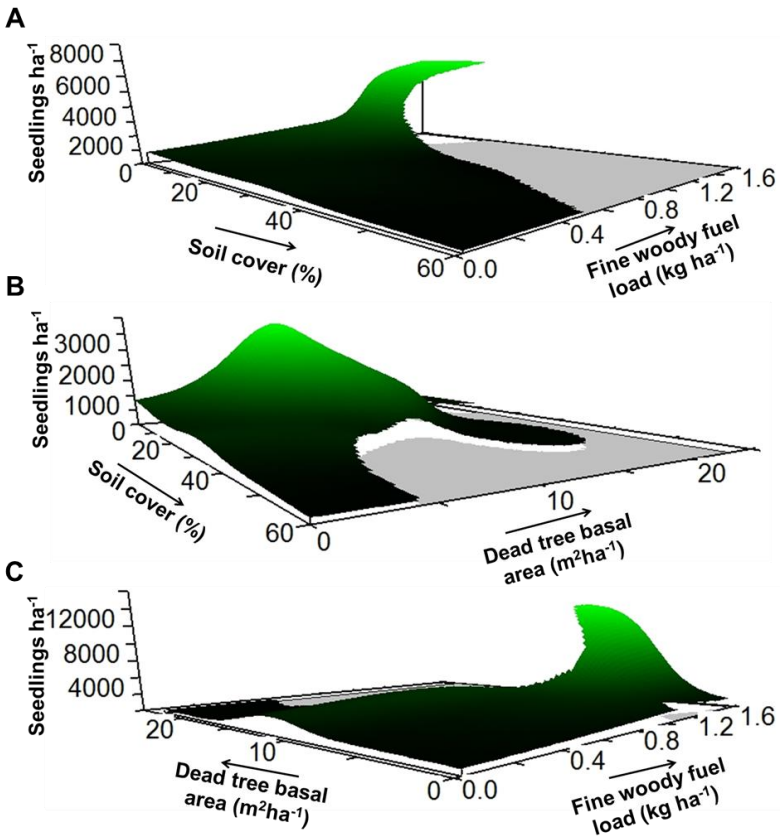

Figure 3-5 Ponderosa pine seedling density is affected by interactive effects of (**A**) soil cover and fine woody fuel load, (**B**) soil cover and basal area of dead trees, and (**C**) basal area of dead trees and fine woody fuel load. Grey areas indicate where the model lacked enough information to reliably predict the response.

Discussion

The results of our research point to the potential for ponderosa pine seedling height growth to be driven by different factors than seedling density on the same sites; this has important implications for long-term site recovery because the majority of post-fire research to date has focused only on seedling density. Height growth on these sites was driven by climate, soil productivity, and live tree basal area. Both of the climate variables are related to warmer fall and winter temperatures. Reference evapotranspiration or reference atmospheric evaporative demand (Eref) represents the evaporation possible for a standardized grass surface with no soil moisture restriction, while degree days above 5°C (DD5) represents the amount of time and number of degrees above 5°C a site experienced. Previous research showed lower

ponderosa seedling growth and survival in experimentally warmed plots than in controls, regardless of whether the warmed plots also received additional water (Rother et al. 2015). However, Rother et al. (2015) did not manipulate the seasonality of warming, instead raising mean midday temperature by approximately 3-4°C across the two-year study period.

Our results indicate that higher winter evapotranspiration generally benefited seedling growth up to a point but could have mixed effects on seedling growth depending on the soil productivity or basal area of live trees on the site. Increasing fall degree days above 5°C had a more consistent relationship; i.e. less interaction with other predictors, with a marked peak in height growth around 500 degree days followed by a sharp decrease in predicted height growth. Similarly, previous work examining seedling radial growth found that ponderosa pine seedlings were more sensitive to growing season temperature whereas adults were more sensitive to moisture (Hankin et al. 2019). Basal area of live trees generally negatively affected seedling growth; likely because more and larger live trees and associated increased canopy shading decreases light availability and potentially water availability. Increased light availability can positively affect conifer seedling height (Burns and Honkala 1990; York et al. 2007; Goodrich and Waring 2017) and may be more important than water availability for planted seedlings (York et al. 2003).

Ponderosa pine seedling density in our study, however, was driven by burn severity (dNBR and basal area of dead trees) and surface cover (percent exposed soil and fine woody fuel load) rather than broader climate conditions. Microenvironment understory conditions created by needle litter have been shown to improve ponderosa seedling germination and success post-fire, likely by impacting factors such as soil temperature variation and improving available soil moisture conditions (Bonnet et al. 2005; Foster et al. 2020). Similar impacts are likely why fine down woody fuel load had a generally positive impact on seedling density in our study. Previous work has also shown that plots burned with high severity (higher dead basal area) had higher seedling density while grass cover had a negative impact on ponderosa pine density (Rodman et al. 2020).

Our results suggest that at climate is more important for seedling growth than it is for seedling density approximately a decade following wildfire. However, it is important to note

that the climate variables are only for the most recent seven years of growth relative to our sampling date (to ensure the best estimates of height growth), which does not necessarily reflect the immediate 1-2 year post-fire climate that might be expected to more strongly impact seedling establishment. The seedling density modeling differs from many previous studies in that it excluded sites with no seedlings, in order to compare the factors influencing growth and density on the same sites. This is likely why distance to seed source is not identified as an important predictor of density in our study, in contrast with previous work on seedling establishment (Kemp et al. 2016; Davis et al. 2019).

Conclusions

Understanding long term post-fire conifer recovery requires understanding the factors influencing short-term seedling germination and establishment as well as longer-term growth and survival. We found that 9-15 years post-fire, ponderosa pine seedling height growth and density were generally impacted by different factors. Soil productivity and climate factors were consistently important influences on height growth but not density, while understory factors (soil cover and fine woody fuel load) were consistently important for density but not height growth. Live tree basal area was important for height growth models whereas dead tree basal area was important for density.

While our results highlight the long-term importance of burn severity for seedling density, our height growth results reiterate concerns related to climate change; driest sites have been previously shown to have lower density of seedlings and continued changes in climate are pushing more sites past established climate envelopes for successful regeneration based on density measures (Stevens-Rumann et al. 2017; Davis et al. 2019). Our results highlight that related processes (seedling establishment and seedling height growth) can be influenced by different factors, indicating that future work on post-fire tree recovery may need to include more than seedling establishment and density in order to offer a complete picture of future forest trajectory under changing climate and burn severity conditions.

Chapter 4: Boreal forest vegetation and fuel conditions 12 years after the 2004 Taylor Complex in Alaska, USA

Abstract

Fire has historically been a primary control on succession and vegetation dynamics in boreal systems, though modern changing climate is potentially increasing fire size and frequency. Large, often remote, fires necessitate large-scale estimates of fire effects and consequences, often using Landsat satellite-derived dNBR (differenced Normalized Burn Ratio) to estimate burn severity. However, few studies have examined long-term field measures of ecosystem condition in relation to dNBR severity classes in boreal Alaska. The goals of this study were: 1) assess changes in dominant vegetation at plots resampled one- and 12-years post-fire, 2) use dNBR classes to characterize vegetation and downed woody fuels 12 years post-fire, and 3) characterize the relationship between biophysical, topographic, and remotely sensed characteristics (e.g., moss/duff depth, canopy cover, elevation, aspect, dNBR) and understory species assemblages 12 years post-fire. Understory species richness doubled (39 to 73) between 2005 and 2016; some common species increased in cover over time (e.g., *Ledum groenlandicum*) while others decreased (e.g., *Hylocomium splendens*). In 2016, live and dead tree densities, tall shrub cover, and 1- and 100Hr woody fuels were significantly different among dNBR classes; moss and duff depth, canopy cover, and spruce seedling density were not. Elevation and aspect significantly influenced tall shrub cover, hardwood sapling density, and downed woody fuel loads. Understory plant community differed between unburned and all burn classes, as well as between low and high dNBR severity. Ordination analysis showed that overstory (e.g., live tree density), understory (e.g., moss depth, woody fuel loading), and site (elevation, aspect, dNBR) significantly influences understory species assemblages. Remeasured sites (sampled one and 12 years post-fire) show recruitment of new understory species and differing, diverse responses to burning by several common plant species. In 2016, low severity sites had generally the highest woody fuel loading, which may increase risk of repeated surface burning, although the reduction in live tree density would still result in decreased fire risk and behavior. Understory community composition correlated with

multiple biotic and abiotic factors, including moss depth, canopy cover, elevation, aspect, and dNBR. Overall, these results can improve landscape-level predictions of ecosystem condition following fire based on dNBR.

Introduction

Wildfire has been a historically prevalent disturbance in the North American boreal forest (Viereck 1983; Ryan 2015), though in recent decades there has been an increase in annual area burned and frequency of large fires (Kasischke and Turetsky 2006; Kasischke et al. 2010; Calef et al. 2015). North American boreal forests characteristically burn in a stand-replacing fire regime (Duchesne and Hawkes 2000), where crown fires are common and there is high tree mortality even in surface fires (Viereck and Schandelmeier 1980; Viereck 1983). Surface fires generally move easily into the crowns of spruce-dominated forests due to the distribution of fine branches and flammable lichen along the entire tree stem (Viereck 1983). Unless fires burn into late summer under dry and hot conditions, fire generally reduces the forest floor organic layer without removing it down to bare mineral soil (Viereck 1983; Duchesne and Hawkes 2000). Thus, overstory consumption typical of high burn severity is not necessarily coupled to severe effects on understory vegetation (Fryer 2014). In this context, fires can produce highly variable effects on boreal forest overstory and understory as an agent of ecosystem change (Simard 1991; Lentile et al. 2006).

Picea mariana (Mill.) Britton Sterns & Poggenb. (black spruce) is a shade-tolerant species that is a dominant component of fire-prone Alaskan forests. Historically, *P. mariana* is generally successful in replacing itself after fire on moister sites and sites burned at low to moderate burn severity level where some organic layer is left unconsumed (Johnstone et al. 2010). Germination success is variable but consistently higher soon after a fire, with establishment from semi-serotinous cones beginning the first year after fire and continuing for up to ten years (Viereck 1983; Duchesne and Hawkes 2000). The other dominant conifer in Alaska boreal forests, *Picea glauca* (Moench) Voss (white spruce), often decreases in dominance following fire except when fire coincides with a masting event (Peters et al.

2005). Hardwood trees in this region of the Alaskan boreal forest generally increase in density following fire and may dominate for years to decades before being replaced by spruce (Viereck 1983), though fires in young (<25 years old) stands or areas where organic layer consumption is high may reduce spruce regeneration to the point that hardwoods are never replaced as the domianant tree (Johnstone and Chapin III 2006b; Johnstone et al. 2010). Although aboveground structures are easily killed even by low severity surface fires, *Populus tremuloides* Michx. (quaking aspen), *Populus balsamifera* L. (balsam poplar), and *Betula papyrifera* Marshall (paper birch) all resprout vigorously after high severity burns. *Betula papyrifera* in particular can also seed in aggressively following fire, particularly in areas where the organic layer is consumed (Johnstone and Chapin III 2006a).

Post-fire understory species succession in boreal forests generally proceeds from dominance of rapidly-growing, vascular plants within the first few years following fire to increasing dominance of bryophytes (mosses and liverworts) and lichens as time since fire increases (Hart and Chen 2006). This succession can be measured by either resampling the same sites through time in successive years or by sampling different sites along a known chronosequence of post-fire stand ages. Chronosequence sampling can alleviate some issues related to resampling sites and generally provides a longer view of time-since-fire, since it is often difficult to maintain resampling on the order of 100+ years necessary to capture the full range of succession in these slow-growing forests (e.g. Black and Bliss 1978; Morneau and Payette 1989; Chipman and Johnson 2002). However, resampling the same site has the benefit of tracking changes through time without the compounding factors associated with sampling different locations (e.g. differences in soil or microclimate). While generally sampling a shorter timescale, these remeasurement studies allow the explicit relation of immediate post-fire plant communities to longer-term trends. Remeasurement studies have, however, shown generally similar trends in species composition through time as the chronosequence-based studies, while also highlighting the fact that time since disturbance is generally not enough to fully explain differences in observed understory species communities (Rydgren et al. 2004; Day et al. 2017).

Because live and decaying mosses and lichen create a deep organic layer that dominates the forest floor, particularly in later successional stages, fire effects on understory species

assemblages in boreal forests are considered to be mostly driven by the depth of organic layer consumption (Wang and Kemball 2005; Gibson et al. 2016). Depth of this organic layer is a strong control on soil temperature and resulting permafrost layer melting or formation, which in turn affects site soil drainage and related factors (Viereck 1983; Yoshikawa et al. 2002; Kasischke and Johnstone 2005). Lower organic consumption by fire means that mosses [e.g., *Pleurozium scherberi* (Brid.) Mitt. (red-stemmed feathermoss), *Hylocomium splendens* (Hedw.) Schimp. (splendid feathermoss)] generally continue to dominate, whereas increased depth of burn results in a shift to higher forb cover, often *Chamerion angustifolium* L. Holub (fireweed) or grasses such as *Calamagrostis canadensis* (Michx.) P. Beauv. (bluejoint). Shrubs, including *Salix* (willow) spp., *Vaccinium uliginosum* L. (blueberry), *Alnus* (alder) spp., and *Ledum groenlandicum* Oeder (synonym *Rhododendron groenlandicum*, bog Labrador tea) frequently gain significant cover following fire and may dominate for up to 25 years post-fire before succeeding to *P. mariana* or *P. glauca* (Duchesne and Hawkes 2000).

These varied ecological effects following fire are dependent in part on "burn severity", which is the degree of ecological change following fire (Lentile et al. 2006; Keeley 2009). In many forested systems, percent of overstory tree mortality is successfully used as a proxy for ecosystem burn severity, i.e. both overstory and understory ecological effects (Lentile et al. 2006; Keeley 2009). Various indices have been developed to assess burn severity based on both surface and overstory effects, e.g. Composite Burn Index (Key and Benson 2006; Morgan et al. 2014). While field-based assessments of burn severity (e.g. CBI) are considered the preferred method for determining burn severity, these indices may not accurately capture ecosystem change due to collapsing of complex post-fire changes into simplified measures (Morgan et al. 2014).

Burn severity across larger scales or remote areas is commonly assessed using remote sensing (Lentile et al. 2006) with the most common method being the differenced Normalized Burn Ratio (dNBR; Eidenshink et al. 2007). However, in boreal systems particularly, some studies have found mixed success in the ability of remotely-sensed indices to predict ground measures of burn severity and particularly that these indices fail to capture depth of organic layer burning (Murphy et al. 2008; Verbyla and Lord 2008; Alonzo et al.

2017). Other work, however, has found that dNBR is broadly effective at mapping burn severity in boreal systems as compared to field measures of CBI (Allen and Sorbel 2008; Boucher et al. 2017). Field-based methods for burn severity assessment (such as percent canopy mortality and CBI) have also been criticized as not characterizing ecologically-significant burn severity in boreal systems, which further complicates validation of dNBR in this ecosystem (French et al. 2008; Kasischke et al. 2008). While more ecosystem-specific methods for determining burn severity have been developed, such as estimation of organic layer consumption by looking at adventitious roots on *P. mariana* (Kasischke et al. 2008; Boby et al. 2010), there is still a need for remotely-sensed burn severity estimation in order to characterize large-scale severity (Burton et al. 2008; Parks et al. 2018).

Given the significant body of research focused on post-fire effects in boreal forests, some gaps in knowledge still remain. While successional phases following wildfire have been well characterized in boreal ecosystems, studies explicitly considering differences in burn severity have usually defined severity using depth of organic layer consumption or similar (e.g. Mallik et al. 2010; Gibson et al. 2016), rather than directly using dNBR or a similar index as a measure of severity. Multiple studies have also focused on the relationship of remotely sensed indices to short-term, field-based measures of burn severity in boreal systems (e.g. French et al. 2008; Murphy et al. 2008; Hoy et al. 2008; Whitman et al. 2018), but few have focused on relating dNBR to field-based measures of long-term overstory and understory condition following wildfire. In addition, long-term measures of vegetation recovery should provide the more telling assessment of the ecological impact (i.e., severity) of the fire.

While acknowledging its shortcomings in boreal ecosystems, I proceeded to consider dNBR as our remotely sensed burn severity index for this study, for practicality and for lack of a clearly preferable alternative (Hudak et al. 2007). Since dNBR is the most commonly used burn severity index by researchers and managers, assessing how dNBR corresponds to post-fire ecological change is still warranted (French et al. 2008). I sampled 32 sites across four burn severity classes (unburned, low, moderate, and high severity) 12 years after the Taylor Complex, while also capitalizing on previously collected one-year post-fire data at a subset of our sites. The Taylor Complex (528,400 ha) was the largest fire complex in Alaska's record-breaking 2004 fire season, when 2.7 million ha burned state-wide. The goal of this

study was to survey long-term ecosystem condition following the Taylor Complex fires with three main objectives: 1) assessing changes in vegetation from one to 12 years post-fire at resampled plots, 2) characterizing vegetation and downed woody fuels conditions 12 years post-fire in relation to dNBR, elevation, and aspect, and 3) characterizing the influence of site biotic and abiotic characteristics (e.g., woody fuel loading, shrub cover, moss/duff depth, elevation, dNBR) on understory species assemblages.

Methods and Materials

Study area

I conducted this study in *P. mariana*-dominated boreal forests along the Taylor Highway, primarily between the communities of Tok and Chicken in Interior Alaska. The climate is subarctic dry continental. Based on 30-year climate normals (1981-2010), the average daily January high temperature is -24°C with an average low of -34°C; in July the average daily high is 22°C with an average low of 5°C. Average annual precipitation is 315 mm; the driest month is April with 6 mm of precipitation (generally snow), and the wettest month is July with 70 mm of rain (ACRC 2018). In this region, *P. mariana* often co-dominates with *P. glauca*. Other common tree species are *P. tremuloides, P. balsamifera,* and *B. papyrifera*. This area is in the discontinuous permafrost zone, where the frozen permafrost layer is patchily distributed and may vary from being absent to several hundred meters thick (Jorgenson et al. 2008).

Landscape stratification and sampling design

Burn severity was indicated by the Monitoring Trends in Burn Severity (MTBS) (Eidenshink et al. 2007) dNBR (differenced Normalized Burn Radio) product (MTBS http://www.mtbs.gov, accessed May 2018). The MTBS product was used because it is a free, validated source of burn severity maps for all large fires in the U.S. and is commonly used by both researchers and managers for post-fire ecological studies, impact assessments, and to guide potential restoration. To create this product, continuous dNBR values are calculated as the pre-fire NBR (Normalized Burn Ratio) minus post-fire NBR, where NBR is a normalized

ratio calculated from 30m resolution Landsat bands 4 (near infrared band, NIR) and 7 (short wave infrared band, SWIR); i.e., (NIR-SWIR)/(NIR+SWIR). Continuous dNBR is then categorized as unburned, low, moderate, or high severity, or increased green based on thresholds determined by the MTBS analyst (Eidenshink et al. 2007). The NBR index is sensitive to changes in green vegetation, bare soil, and char, where areas with higher char and bare soil cover fractions will have higher NBR values (Key and Benson 2006; Hudak et al. 2007). For image dates and proportion of burn severity in each severity class for each fire, see **Appendix A, Table A-1**.

Burned sites were chosen from the Taylor Complex (528,400 ha; centroid 63^{o} 43’ 28”N, 142^{o} 50’ 36”W), comprised of six lightning-ignited wildfires that burned in the summer and fall of 2004. I sampled the three Taylor Complex fires accessible from the Taylor Highway (**Figure 4-1**): Porcupine (108,345 ha; start date June 26, 2004), Chicken (130,626 ha; start date June 15, 2004), and Wall Street (36,123 ha; start date June 22, 2004) (MTBS http://www.mtbs.gov, accessed May 2018). Because these fires were part of the same complex, burned over the same time period, and all burned within the same vegetation types, they were treated as a single burn event when stratifying the sampling sites. Twelve sites were established in 2004 within low (n=4), moderate (n=5), and high (n=3) burn severity conditions based on the full range of burn severity observed in the field (Hudak et al. 2007; Lentile et al. 2007), with some sites overlapping established pre-fire sites (Lewis et al. 2011). These 12 monumented sites were sampled in 2005 to collect one-year post-fire understory species composition and cover data (Lentile et al. 2007), with each site consisting of five plots systematically placed within a 60 m diameter area (i.e., sampling 4-5 Landsat 30 m pixels, see Figure 2). The 12 sites ended up falling within either low (n=4), moderate (n=5), and high (n=3) burn severity classes, based on post-fire dNBR classified by MTBS (**Appendix A, Table A-1** for MTBS details).

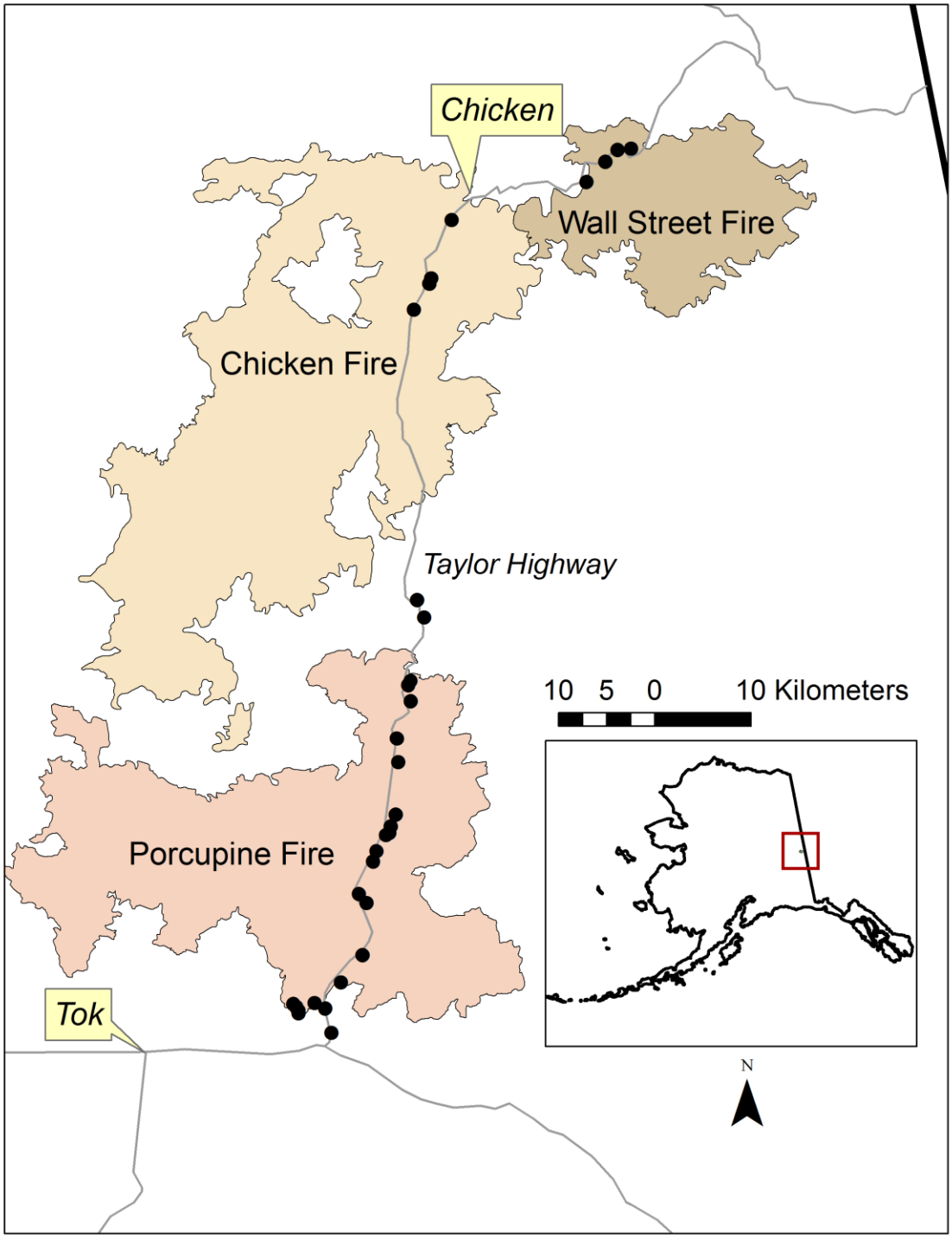

Figure 4-1 Study area location in Interior Alaska, U.S.A., and fire perimeters of the three Taylor Complex fires sampled in this study, with site locations. The communities of Tok and Chicken are highlighted in callout boxes as reference points.

In 2016, in addition to remeasuring the 12 established sites, 20 new sites were added to achieve a balanced sampling design with regard to dNBR severity class (i.e. 32 total sites, with eight sites per unburned, low, moderate, and high severity classes). Because the original 12 sites did not include any unburned areas, all unburned sites in this study were established and sampled in 2016. Site selection followed a stratified random sampling design, with the strata being: the four MTBS dNBR classes (unburned, low, moderate, high); high or low elevation (range 424-1529 m); and cool-wet or warm-dry aspect based on the topographic solar-radiation index (TRASP) transformation (Roberts and Cooper 1989) that varies from 0 (cool, moist) to 1 (warm, dry) [0= 30º north-northeast and 1= 210º south-southwest]. Elevation and TRASP were obtained from a 30 m resolution digital elevation model (USGS https://viewer.nationalmap.gov/basic/). For accessibility, and to mitigate potential edge effects, sites were located within 0.8 km of, but at least 60 m from, the Taylor Highway.

Each site in 2005 and in 2016 consisted of five plots (**Figure 4-2**); field methods are generally described at the plot level, but measurements were summed or averaged to the site level for statistical analysis. The center of every plot was geolocated in 2005 and re-geolocated in 2016 with a Trimble GeoXT Global Positioning System with differential correction to 1-2 m precision. At all five plots per site, understory vegetation was identified to species (when possible) and the percent cover of each species was estimated within a 1 m^2 frame. Canopy closure (all trees and tall shrubs above 1.37 m) was estimated using a convex spherical densiometer. At the center plot all standing trees were recorded if their base was located within a fixed 8-m radius. For each tree the species, status (dead, live), and diameter at breast height (DBH) were recorded.

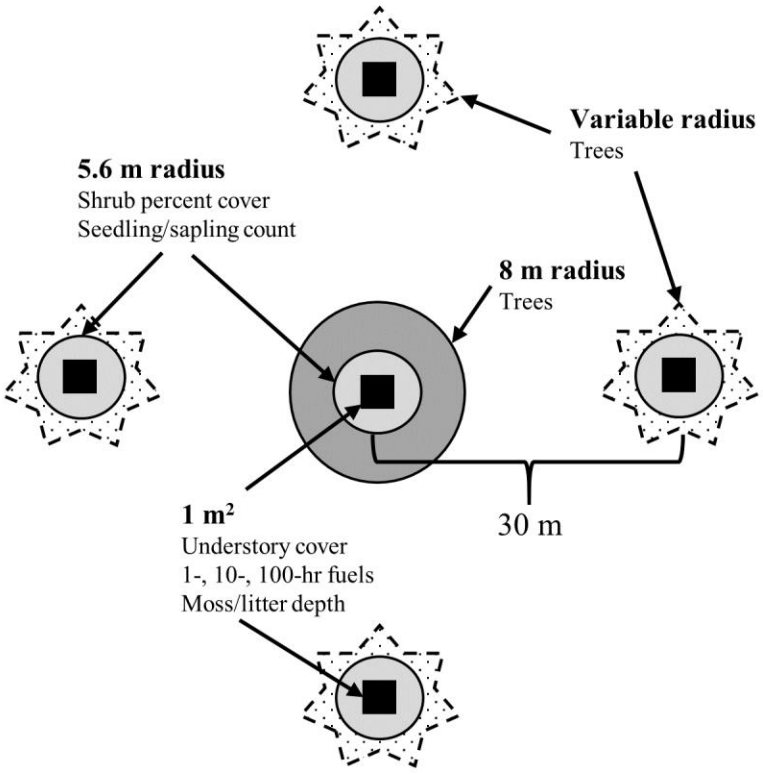

Figure 4-2 Site layout (not to scale) showing central plot and four peripheral plots, along with the attributes measured within each plot. Note that shrub percent cover was measured only at the center plot, and that the variable radius plot was based on a 2 m^2/ha Basal Area Factor prism.

In 2016 additional variables were measured at all 32 sites (**Figure 4-1**). Moss/litter and duff depth in millimeters was determined by cutting down through all organic layers until mineral soil was exposed and fine downed woody fuel loading (1-, 10-, 100 Hr timelag classes; <1 cm, 1-2.5 cm, and 2.5-7 cm diameter, respectively) was estimated using a photoload guide (Keane and Dickinson 2007). Woody fuels were categorized by timelag classes, as is standard for many fire behavior and effects applications, which reflect estimated drying time of fuels of different sizes (Keane and Dickinson 2007). Spruce seedlings (<1.37 m height) and spruce and hardwood saplings [>1.37 m height and <10 cm diameter at breast height (DBH = 1.37 m)] were tallied within a 5.6-m radius of each plot center. Standing trees (>1.37 m height and >10 cm DBH) were recorded at each peripheral plot (four per site) within a variable radius using a 2 m^2/ha basal area factor prism. Percent cover of tall shrubs and large

downed woody fuel loading (1000Hr timelag class, >7.62 cm diameter per Keane and Dickinson 2007) were ocularly estimated within a 5.6-m radius of the center plot at each site.

Data analysis

All analyses were run at the site level (n=12 in 2005, n=32 in 2016); where plot-level (n=60 in 2005, n=160 in 2016) measurement data was aggregated to provide site-level measures and to preclude pseudo-replication due to spatial autocorrelation between plots within sites. The analysis for each objective, including any data transformation or subsetting, was done separately as outlined below.

a. Vegetation change 2005-2016

These analyses were run primarily on the 12 sites sampled in both 2005 and 2016, though the unburned sites (sampled only in 2016) were used as well for some tests. Density of live trees, dead trees, and canopy cover in 2005 and 2016 was compared using a Wilcoxon signed-rank test in R (R Core Team 2017). To examine differences in understory species cover over time I calculated total richness based on all species found on the sites. I then focused on changes in percent cover of only common species, defined as any species that occurred in at least six of the 12 sites in both years. Narrowing our statistical testing to common species was done because it simultaneously highlights species that are both ecologically and socially significant, and it gave sufficient statistical power to run appropriate tests. For these common species, I tested for differences in cover between years using the Wilcoxon signed-rank test. I also tested for differences in cover among unburned sites, burned sites in 2005, and burned sites in 2016 using a Kruskal-Wallis non-parametric analysis of variance with post-hoc Dunn's test for pairwise comparisons. Test significance was defined when $\alpha<0.10$ for all tests. The Kruskal-Wallis was run on all severity levels combined because of the high variation inherent in plant cover data and because of the small number of sites (three) in high severity.

b. 2016 vegetation and fuels condition

I examined the relationship of field variables (tree and seedling density, canopy and shrub cover, downed woody fuel loading, moss and duff depth) to dNBR using Kruskal-Wallis analysis of variance to test for differences among categorical burn severity levels (unburned, low severity, moderate severity, high severity), with post-hoc Dunn's test, for all 32 sites sampled in 2016. All tests were run with significance defined at $\alpha<0.10$ with three degrees of freedom. To test the relationship between field variables and elevation and transformed aspect I used Spearman's *rho* (ρ) rank correlations. Spearman's ρ was also used to examine relationships between elevation and transformed aspect and understory plant community species evenness, species richness, and Shannon and Simpson indices of diversity [calculated in PC-ORD (McCune and Mefford 2011)]. Correlations and *P* values were calculated using *cor.test()* in the R base package with significance defined at $\alpha<0.10$.

c. 2016 understory species community

Differences in understory species composition among burn severity levels were tested using a permutation multivariate analysis of variance (perMANOVA) (Anderson 2001) in PC-ORD. The distance measure selected was Sorensen (Bray-Curtis) and the number of randomizations was 4999. To test for differences in beta-diversity between severity levels, the homogeneity of group dispersions (or the difference in amount of within-group variance) was tested using the default methods with *betadisper()* (*vegan* package [(Oksanen et al. 2018)]) to implement the multivariate test for homogeneity of dispersion described by Anderson (2006). This test can also serve as a proxy measure of beta-diversity; i.e., the dissimilarity in species composition among sampling units for a given area (Anderson et al. 2006). The *betadisper()* test was run with three degrees of freedom and 999 permutations. An indicator species analysis (Dufrêne and Legendre 1997) in PC-ORD determined the degree to which different species served as an indicator of a particular severity level based on both a species' consistent occurrence in, and relative abundance at, a given severity level.

The understory vegetation composition, and its association with various biotic and abiotic site characteristics (e.g., moss/duff depth, canopy cover, dNBR) were visualized using non-metric multidimensional scaling (NMDS) implemented with the *metaMDS()* wrapper from the *vegan* package (Oksanen et al. 2018), which by default implements the recommendations

of Minchin (1987) in R. NMDS was chosen because it does not rely on an assumption of linear relationships among variables and allows examination of the trends in understory species in relation to multiple factors while reducing noise inherent in species diversity data (McCune and Grace 2002). The number of zeros in the data was reduced by excluding rare species that occurred at only a single site, resulting in a reduction from 118 to 74 species. A three axis solution with Bray-Curtis distance measure was chosen, with the default *metaMSD()* Wisconsin square-root transformation of the data to correct for the large range in cover values. The starting configuration was random and dimensionality was determined based on a scree plot of stress and dimensions (run in PC-ORD), where using four dimensions did not measurably improve the stress of the model (McCune and Grace 2002). Site characteristic vectors (e.g., dNBR, fuel loading) were then fit to the final ordination solution using the *envfit()* function (*vegan* package).

Results

Vegetation change 2005-2016

There were no significant differences (all $P \geq 0.181$, $V=0$, 18, 41.5, respectively) at the sites between 2005 and 2016 live tree density [60±39 (mean±S.E) and 37±25], dead tree density (280±84 and 173±36), or canopy cover (23±3 and 20±4). The overall or global understory species richness of the sites increased, from 39 species identified in 2005 to 73 species in 2016. Six understory species were common at the sites in both 2005 and 2016 (**Appendix A, Table A-2**). When tested pairwise for differences in cover between years only *L. groenlandicum* ($V=9$, $P=0.037$), *Salix* spp. ($V=1$, $P=0.003$), and *Vaccinium uliginosum* ($V=2$, $P=0.012$) had significant changes, all increasing in cover over time. When tested for differences in cover among unburned sites, 2005 burned sites, and 2016 burned sites (**Figure 4-3**), *Chamerion angustifolium* had significantly higher cover at burned sites in both years than in unburned sites; *Hylocomium splendens* had significantly lower cover in 2016 than in 2005 or in unburned sites; *Ledum groenlandicum* had significantly lower cover in 2005 than in 2016 or in unburned sites; *Salix* spp. had significantly higher cover in 2016 than in unburned sites or in 2005; *Vaccinium uliginosum* had significantly higher cover in 2016 than in 2005 or in

unburned; and *Vaccinium vitis-idaea* L. (lingonberry) had significantly lower cover in 2005 than in unburned sites.

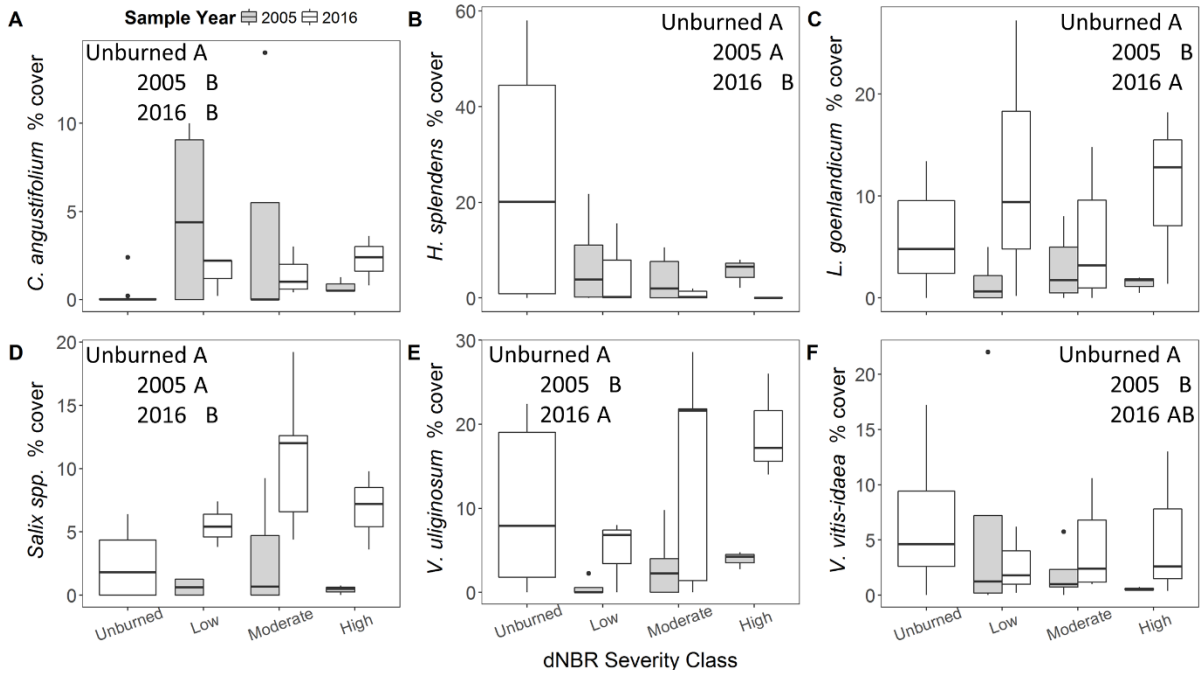

Figure 4-3 Percent cover of common species at sites measured in 2005 (dark grey) and 2016 (white). Note that unburned sites were not measured in 2005. Species shown are (A to F): *Chamerion angustifolium, Hylocomium splendens, Ledum groenlandicum, Salix* spp., *Vaccinium uliginosum, Vaccinium vitis-idaea*. Boxplots show median, hinges (25th and 75th percentiles), and whiskers that extend to values no more than 1.5*IQR (inter-quartile range) from upper or lower hinge, respectively. Points outside this range are considered outliers and plotted separately. All Kruskal-Wallis tests were significant among unburned, all burned sites in 2005, and all burned sites in 2016 (df=2, $\chi^2 \geq 5.29$, $P \leq 0.07$); Dunn's pairwise test for differences are shown with letters to indicate significant pairwise differences ($\alpha < 0.1$).

2016 vegetation and fuels condition

Density of live trees was significantly higher in unburned sites [2302±2048 stems per ha (mean ± standard deviation)] than in low (782±1584, P=0.022), moderate (105±297, P<0.001) or high severity areas (0±0, P<0.001) and was higher in low severity than in high (P=0.077), with no other significant differences ($P \geq 0.187$) (**Figure 4-4**A). Density of dead trees was significantly lower in unburned areas (578±926) than low (1533±679, P=0.043), moderate (1189±894, P=0.103), and high severity (3204±2126, P<0.001) severity areas (**Figure 4-4**B). Moderate

severity also had significantly lower dead tree density than high severity (P=0.078). Moss and duff depth were not significantly different among burn severity levels (**Figure 4-4**C and D). Canopy cover showed no difference between severity levels (**Figure 4-5**A) but tall shrub cover (**Figure 4-5**B) was significantly higher in high severity areas (14±10%) than in low severity (3±3%) areas (P=0.023), with the most common shrubs being *Salix* spp., *Alnus* spp., and *Betula* spp.

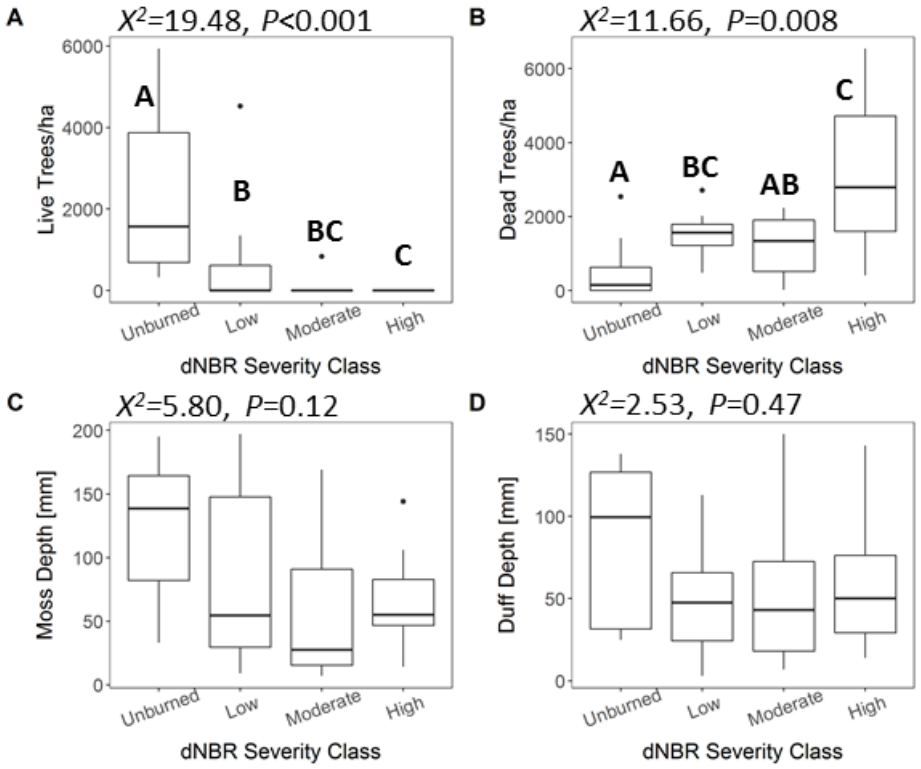

Figure 4-4 Density of live (A) and dead (B) trees, moss (C) and duff (D) depth by dNBR class. Kruskal-Wallis chi-square and P-value shown above each plot. Boxplots show median, hinges (25th and 75th percentiles), and whiskers that extend to values that are no more than 1.5*IQR (inter-quartile range) from upper or lower hinge, respectively. Points outside this range are outliers and plotted separately. Dunn's pairwise test significance are indicated by letters (α=0.1).

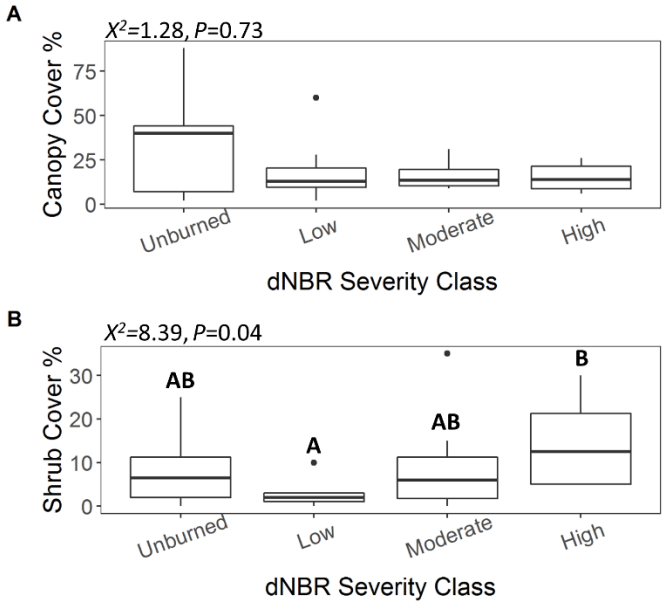

Figure 4-5 Percent canopy cover (all cover >1.37m high) measured by densiometer and percent tall shrub cover (visually estimated within 5.6m radius) by dNBR class. Kruskal-Wallis chi-square and *P*-value shown above each plot. Boxplots show median, hinges (25^{th} and 75^{th} percentiles), and whiskers that extend to values that are no more than 1.5*IQR (inter-quartile range) from upper or lower hinge, respectively. Points outside this range are outliers and plotted separately. Dunn's pairwise tests are indicated by letters (α=0.1).

Comparison of seedling and sapling density showed no significant difference among severity classes for separate spruce or hardwood species (data not shown) or for lumped total spruce or total hardwood seedling/sapling density by severity class (**Figure 4-6**). Downed woody fuel loading in the 1Hr fuels class (**Figure 4-7**A) was significantly (*P*=0.006) higher in low severity (0.052±0.030 kg/m^2) than in high severity (0.023±0.011 kg/m^2) or in unburned (0.026±0.009 kg/m^2) areas (*P*=0.05), and higher in moderate (0.052±0.046 kg/m^2) than in high severity (*P*=0.06). Similarly, 100Hr fuels (**Figure 4-7**C) were significantly (*P*=0.038) higher in low severity areas (0.234±0.218 kg/m^2) than in unburned areas (0.033±0.0478 kg/m^2). There were no significant differences among severity classes for 10Hr and 1000Hr fuels (**Figure 4-7**B and D). Elevation (**Figure 4-8**) was negatively correlated with canopy cover, hardwood sapling density, and 1000Hr and 100Hr fuel load, while positively correlated with tall shrub cover and duff depth. Transformed aspect (**Figure 4-9**) was positively correlated with 1-, 10-, and 100Hr fuel loads as well as with duff depth.

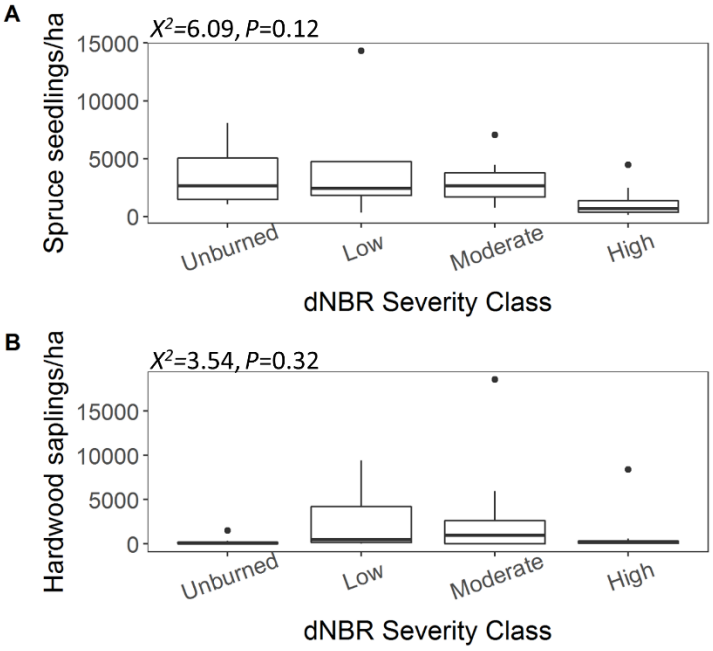

Figure 4-6 Spruce seedling density (A) and hardwood sapling density (B) by dNBR class. Kruskal-Wallis chi-square and *P*-value shown above each plot. Boxplots show median, hinges (25th and 75th percentiles), and whiskers that extend to values that are no more than 1.5*IQR (inter-quartile range) from upper or lower hinge, respectively. Points outside this range are outliers and plotted separately.

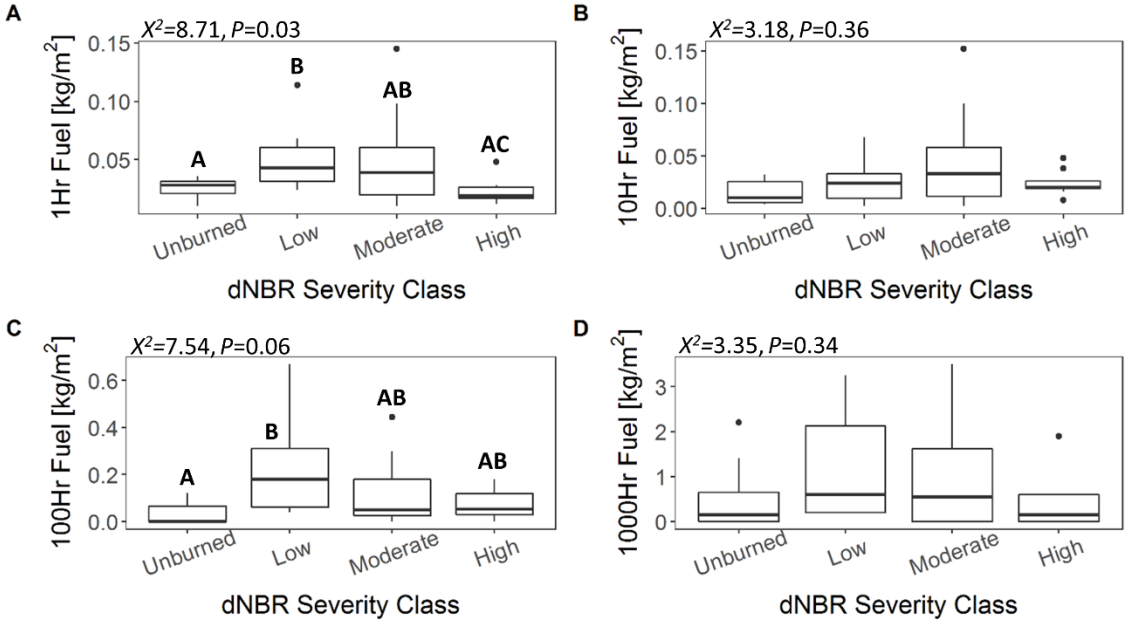

Figure 4-7 Size classes of downed woody fuel loading by dNBR class. Kruskal-Wallis chi-square and P-value shown above each plot. Boxplots show median, hinges (25th and 75th percentiles), and whiskers that extend to values that are no more than 1.5*IQR (inter-quartile range) from upper or lower hinge, respectively. Points outside this range are outliers and plotted separately. Dunn's pairwise tests are indicated by letters (α=0.1).

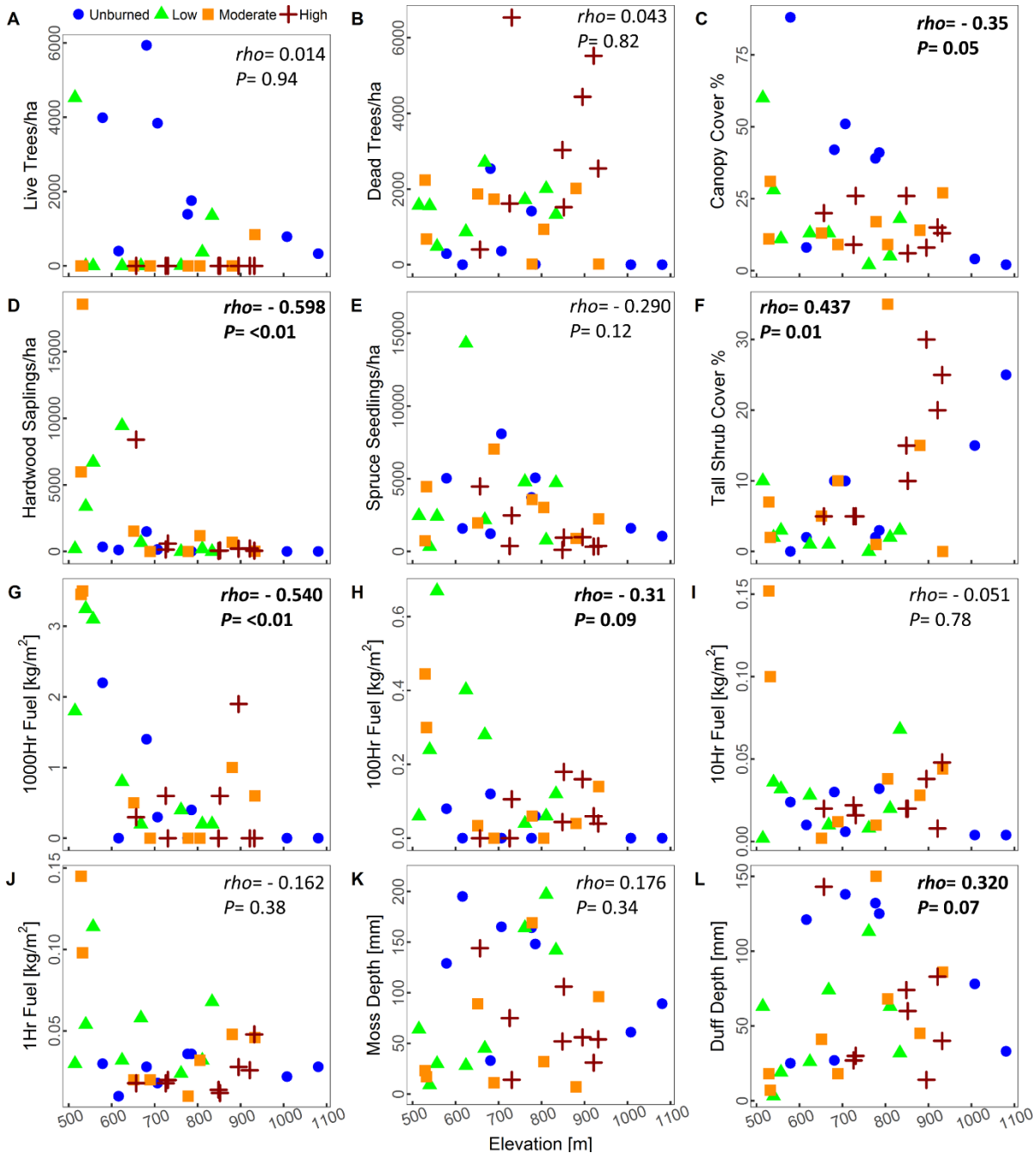

Figure 4-8 Results for Spearman's rank correlation between elevation and field measures. Results significant at $\alpha<0.1$ are bolded.

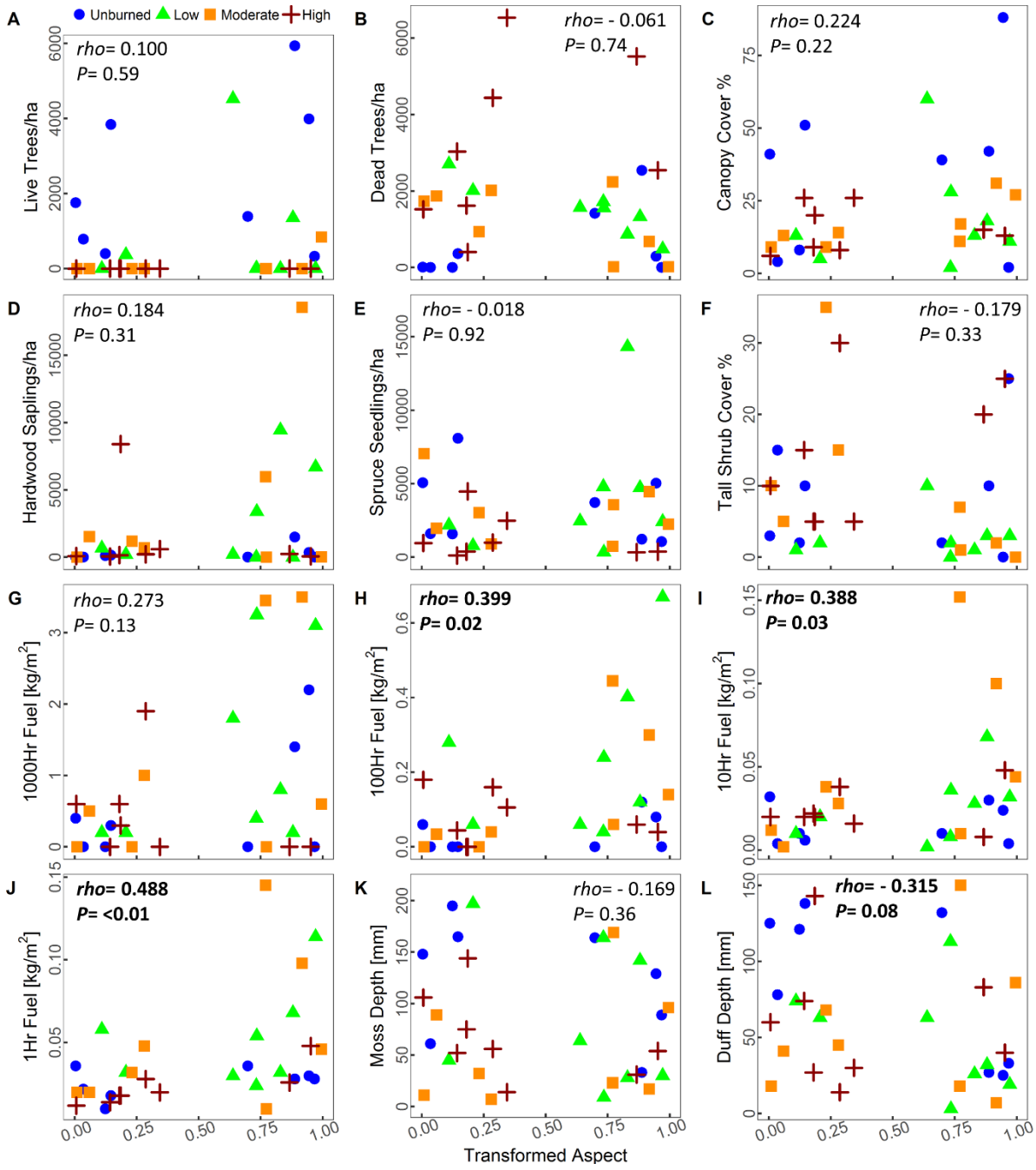

Figure 4-9 Results for Spearman's rank correlation between transformed aspect (where 0=north-northeast and 1=south-southwest) and field measures. Results significant at $\alpha<0.1$ are bolded.

2016 understory species community

Species richness, evenness, and diversity (Shannon's and Simpson's) were not significantly correlated with elevation, transformed aspect, or any of the field measurements (Appendix A Table A.3), except 100Hr fuel load. Species richness and both Shannon and Simpson indices were negatively associated with 100-hr fuel loading (all $\rho \geq |0.321|$, $P \leq 0.07$). The beta-dispersion analysis showed that while low burn severity had the highest average distance to median (0.53), indicating higher beta-diversity, and high severity the lowest (0.39); these differences were not significant based on a permutation test (data not shown; df=3, F=1.71, P=0.18). Species richness of unburned areas (i.e., the total number of species found at all eight unburned sites) was 68, low severity richness was 84, moderate severity richness was 64, and high severity richness was 58. There were 38 understory species (representing 32% of total species sampled) that were found on plots of all severity levels including unburned, and 17 species were found at over 50% of the sites (Appendix B). *Polytrichum* moss and *Vaccinium vitis-idaea* were the most common, occurring at 97% of sites, and unidentified fungi of multiple species occurred at 94% of sites. In contrast, 13 species were found exclusively in unburned areas, 18 species exclusively in low severity, nine species in moderate severity, and seven in high severity sites. Many of these severity-specific species were found only at a single site, which may indicate they simply represent rare species rather than species with strong severity-specific preferences.

Understory plant communities differed significantly with burn severity (perMANOVA, df=3, F=2.06, P=0.002), where unburned had significantly different communities than low (P=0.10), moderate (P=0.001), and high severity (P<0.001) sites. Low and high severity areas were also significantly different (P=0.05). There were also several species of vascular plants, lichen, and moss that were significant indicators of unburned and high severity sites (**Table 4-1**).

Table 4-1 Indicator species analysis Monte Carlo test (4999 permutations) results, where the observed indicator value (IV) is the percent of perfect indication based on relative abundance and relative frequency, the randomized IV is calculated from randomized groups, and *P* is the proportion of randomized trials with indicator value equal to or exceeding the observed indicator value. Only species significant at the $\alpha<0.05$ level are shown.

Species	**Severity level**	**Average cover %**	**Growth form**	**Observed IV**	**Randomized IV [mean (SD)]**	***P-value***
Empetrum nigrum L.	Unburned	5	Shrub/Subshrub	51.5	24.1 [9.24]	0.015
Flavocetraria cucullata (Bellardi) Karnefelt & A. Thell	Unburned	3	Lichenous	83.7	24.6 [10]	<0.001
Geocaulon lividum (Richardson) Fernald	Unburned	1	Forb/Herb	37.5	12.9 [7.88]	0.042
Hylocomium splendens (Hedw.) Schimp.	Unburned	24	Nonvascular	65.5	28.4 [10.1]	0.005
Peltigera aphthosa (L.) Willd.	Unburned	2	Lichenous	58.3	33.6 [11.41]	0.044
Pleurozium schreberi (Brid.) Mitt.	Unburned	9	Nonvascular	47.5	26.4 [8.73]	0.029
Chamerion angustifolium (L.) Holub	High	3	Forb/Herb	48.6	34.3 [7.44]	0.044
Unknown lichen	High	3	Lichenous	51.7	29.0 [9.19]	0.027
Vulpicida pinastri (Scop.) J.-E. Mattsson & M.J. Lai	High	1	Lichenous	71.6	22.7 [8.18]	<0.001

These differences in understory community composition can be partially visualized in an NMDS ordination [k=3, type 1 stress (weak ties) equal to 0.134, 20 tries for two convergent solutions] (**Figure 4-10**). The first two axes contain the majority of variation (axis 1 $R^2 \sim 0.53$, axis 2 $R^2 \sim 0.20$) and are therefore the axes displayed. Elevation, dNBR, aspect, fuel loading (all size classes), moss and duff depth, and live tree density all influenced the distribution of understory species (**Table 4-2**). Certain variables, including 1-, 10-, and 100Hr fuel loading and moss depth, were strongly associated with the first axis, while the remaining variables were not directly correlated with a single axis. The location of specific species in ordination space offers some insights on influences for species presence (Appendix A Figure A.1), for example shrub and hardwood species *Betula neoalaskana* Sarg., *Populus tremuloides*, and *Populus balsamifera* are all grouped to the far right along Axis 1, indicating a correlation with high fuel loading and low moss/duff depth. However, the precise location of any individual species should be interpreted with caution given the high type I stress error in the final solution.

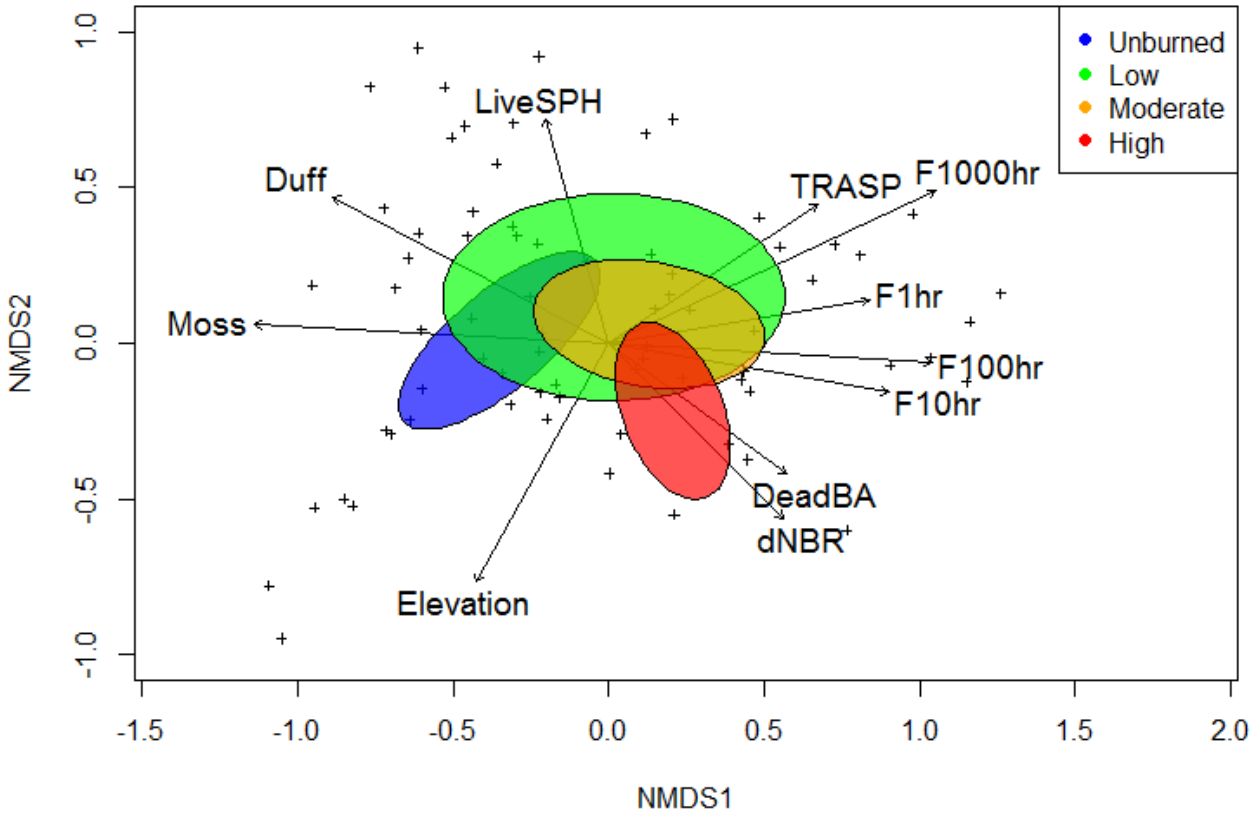

Figure 4-10 Non-metric multi-dimensional scaling (cumulative R^2 for all three axes~0.81, first two axes shown here represent R^2~0.73) results showing individual species plotted in the background with a joint bi-plot of environmental covariables, where arrows indicate direction of correlation and the length of the arrow indicates strength of the correlation. Ovals represent standard error around the location of the sites as plotted in ordination space. The final number of dimensions was three, with stress = 0.013. See **Table 4-2** for correlations with environmental covariates and **Appendix A Figure A.-1** for individual species.

Table 4-2 Correlations of environmental factors with non-metric dimensional scaling axes (**Figure 4-10**). Values in NMDS1 (non-metric multidimensional scaling axis 1) and NMDS2 (axis 2) are the direction cosines (i.e., the coordinates in ordination space for the head of the plotted vector arrow). R^2 correlations and *P*-values calculated based on permutation test. Significance of *P*-value indicated as: ***< 0.001, **< 0.01, *< 0.05, .<0.1

Variable	Description	NMDS1	NMDS2	r^2	*P*-value
dNBR	Continuous burn severity index	0.70571	-0.70850	0.2274	0.030 *
Elevation	Meters	-0.48782	-0.87294	0.2772	0.007 **
TRASP	Aspect (transformed)	0.83260	0.55388	0.2341	0.033 *
ForestType	Spruce, hardwood, or mixed dominant trees	0.97347	0.22881	0.1033	0.217
TotalSPH	Total tree stems/ha	0.75575	0.65486	0.0326	0.633
LiveSPH	Live tree stems/ha	-0.27365	0.96183	0.2014	0.032 *
DeadBA	Basal area of standing dead trees (m^2/ha)	0.80759	-0.58974	0.1813	0.051 .
Canopy	Canopy cover (%)	0.04618	0.99893	0.1370	0.123
Shrub	Tall shrub cover (%)	0.00888	-0.99996	0.0276	0.679
F1000hr	1000hr fuel load (kg/m^2)	0.90617	0.42291	0.4832	0.001 ***
F100hr	100hr fuel load (kg/m^2)	0.99832	-0.05795	0.3884	0.002 **
F10hr	10hr fuel load (kg/m^2)	0.98490	-0.17311	0.2996	0.006 **
F1hr	1hr fuel load (kg/m^2)	0.98683	0.16173	0.2589	0.014 *
Moss	Depth to duff (mm)	-0.99860	0.05298	0.4701	0.001 ***
Duff	Depth to mineral soil (mm)	-0.88372	0.46801	0.3624	0.004 **

Discussion

Overstory and understory 2005-2016

Neither density of live nor of dead trees changed significantly from one to 12 years post-fire, indicating that the one -year post-fire sampling likely captured the majority of fire-related tree mortality. However, substantial but expected changes in cover of understory species occurred over time and a large number of species recruited between one and 12 years post-fire: the total species richness found on the 12 sites doubled. Bernhardt et al. (2011) also documented a sharp initial decline in the number of species post-fire in this ecosystem, likely reflected in the low richness of our 2005 sampling, while our 2016 results highlight an influx of species into the burned sites over 11 years. This also reflects previous work showing that differing recruitment strategies (e.g. re-seeding from off-site, from seedbank, resprouting from underground structures) interacted with burn severity to result in both spatial and temporal changes in species richness with time since fire (Viereck 1983; Wang and Kemball 2005; Hollingsworth et al. 2013).

Individual species comparisons show a spectrum of responses. The increased cover of *V. uliginosum*, *L. groenlandicum*, and *Salix* spp. reflects trends found in other work, as does the decreased cover of *H. splendens* (Lecomte et al. 2005; Bernhardt et al. 2011). Bernhardt et al. (2011) found, in sites measured pre- and post-2004 wildfires in Interior Alaska, that *L. groenlandicum, V. uliginosum,* and *V. vitis-idaea* abundance significantly decreased one and two years post-fire, which is reflected in the differences our study found between unburned and one-year results. However, our 12-year post-fire results show that, despite the initial decrease, *L. groenlandicum, V. uliginosum,* and *Salix* spp. have already recovered to or exceeded unburned average cover, likely due to their ability to resprout from underground rhizomes (Viereck 1983). On the other hand, cover of *H. splendens* at these sites continued to decrease from 2005 to 2016, reflecting continuing mortality of this climax stage, shade-loving species (Tesky 1992). The cover of *Chamerion angustifolium*, an important off-site seeding species that may also resprout from rhizomes, generally decreased but remained above unburned levels. This is an unsurprising trend given that *C. angustifolium* is considered a diagnostic species for the first stage (1-20 years) of post-fire recovery (Black and Bliss 1978).

Twelve year post-fire forest condition reflects dNBR class and site characteristics

Density of live and of dead trees varied predictably with dNBR burn severity class, tracking with previous research that showed relatively strong relationships between overstory and remotely-sensed indices (Murphy et al. 2008; Hudak et al. 2007). Spruce seedling density on the other hand was not significantly different among dNBR severity classes. Previous studies relating spruce regeneration to burn severity have alternately shown that *P. mariana* is most successful on sites with some organic layer remaining (Johnstone and Chapin III 2006b; Shenoy et al. 2011), that there is no relationship of seedling density to depth of organic layer burning (Gibson et al. 2016), or that regeneration success was highest in areas with exposed mineral soil and minimal organic cover (Mallik et al. 2010). The lack of trend in seedling density could reflect the lack of difference in moss and duff depth among dNBR classes at our sites, which may be traced back to the insensitivity of dNBR to organic layer consumption (French et al. 2008).

Given previous work relating field measures of surface burn severity to dNBR, I did not necessarily expect to see a strong trend in moss and duff depth with dNBR severity class (e.g. Hoy et al. 2008) and in fact there was no significant difference in organic layer depth among dNBR classes at our sites. Likely issues are the insensitivity of Landsat to height variation, and that the 30 m pixel resolution of Landsat is too coarse to capture the highly heterogeneous patterns of organic layer consumption (Alonzo et al. 2017). In addition, issues of topographic and canopy shadowing due to low solar elevation angles that affect dNBR and similar indices, even at lower latitudes, are compounded in high latitude areas such as Alaska (French et al. 2008). Overall our results support the established understanding that Landsat-based dNBR reflects differences in overstory, but not necessarily understory, burn severity in this ecosystem.

On the other hand, downed woody fuel load did vary significantly among dNBR classes, with higher fuel loads in areas classified as low severity. In general fire is expected to affect downed woody fuels by first consuming them during the active fire event (thus lowering fuel loading) but then by contributing fuels from mortality of trees and woody shrubs that become part of the surface fuel layer as they fall, as was evident upon revisiting the sites 11 years later. Higher

fuel loads may raise the risk of more severe reburn effects but only at times when conditions are sufficiently dry to allow for fire to carry in the relatively high-moisture moss and duff layers ground layer (Johnstone et al. 2010). However, I did not explicitly test the probability of reburn, and the canopy fuel load would still be much lower in these areas than in unburned stands (based on live tree density). Other studies of post-fire downed woody fuel loading in North American boreal forests have generally focused on quantifying accumulation of woody fuels over time (e.g. Johnston et al. 2015) without differentiating between burn severity levels while others have focused only on finer fuel available for flaming consumption (e.g. Thompson et al. 2017) or on stands at least 30 years post-fire (e.g. Hély et al. 2000), making comparison with our results difficult. Our fuel load estimates were similar to those measured in at least some similar stands of a study focused on time-since-fire (Johnston et al. 2015). However, our estimates of coarse woody debris (1000Hr) were higher, likely because our sampling was concentrated in a timeframe where more dead trees had recently fallen to become surface fuel.

Species richness responded to both dNBR and woody fuel loading. Fuel load in the 100Hr timelag class was negatively correlated with understory species richness and diversity indices, which contrasts with the findings of Day et al. (2017) in a *Pinus banksiana*/*Picea mariana* ecosystem, though Day et al. (2017) used only the presence/absence of woody debris rather than any measure of loading. Closer examination of the species composition at our low severity sites that may be driving this trend showed a higher understory cover of *B. neoalaskana* and *P. tremuloides*, which potentially increased fuel loading while shading out other understory species. This is also reflected in our NMDS results, where those particular hardwood species were associated with higher woody fuel load. Total species richness was lowest for sites classified as high severity and highest for those classed as low severity, which mirrors previous work by Hollingsworth et al. (2013) in the area as well as that of Lentile et al. (2007) who measured our same sites one year post-fire, suggesting that the effects of burn severity on overall species richness lingers for at least a decade.

Sites classified as moderate and high severity had different plant community composition than unburned areas 12 years after fire, with low and high severity areas also still differing from each other. The understory species community was influenced in part by surface factors, such as depth of moss and duff, as well as downed woody fuel loadings, which

mirrors previous findings that bare ground and woody debris affect species composition (Day et al. 2017). Overstory variables like live tree density and basal area of dead trees, as well as factors like burn severity (dNBR), elevation, and aspect, were also significant drivers of understory vegetation composition. Whitman et al. (2018) found that similar factors, including overstory and understory tree density and basal area as well as soil moisture and heat-moisture index, were the dominant drivers of understory community dissimilarity with burn severity having significant but secondary effects. Others have found that pre-fire forest type (Day et al. 2017) and burn severity (Hollingsworth et al. 2013) were primary drivers of species composition.

Several vascular and non-vascular plants were indicative of unburned areas. *Empetrum nigrum*, *H. splendens*, and *P. schreberi* are known climax/late seral understory species that are maladapted to fire and may take decades to regain their pre-fire cover, making them unsurprising indicator species for unburned sites (Lutz 1956; Johnson 1981; Tesky 1992). There is more limited information about post-fire response of *Geocaulon lividum*, but it has been shown to colonize early post fire and to increase in cover over time (Matthews 1994). I found no published information about the response of *Flavocetraria cucullata* to fire; however, *Peltigera aphthosa* is generally killed by fire, is not a rapid recolonizer, and is often found in mature forests (Matthews 1993).

Chamerion angustifolium, a classic post-fire colonizer that often dominates high severity burns in interior Alaskan boreal forests (Cormack 1953; Lutz 1956), was a significant indicator of high severity. I found no published data on the response of *Vulpicida pinastri* to fire specifically, though previous studies have theorized that certain lichens could serve as site pioneers (Ahti and Hepburn 1967), which could be why this species was a significant indicator of high severity sites. The soil crust lichen (unknown species) was unsurprisingly only found in high severity sites in this ecosystem, since these forests are characterized by a moss understory that often has no exposed soil. Morneau and Payette (1989) noted that a crustaceous lichen (*Trapeliopsis granulosa*), which was not specifically identified at our sites, was present and at maximum cover 14 years after fire in black spruce-dominated northern Quebec.

Abiotic site factors, elevation and aspect, were significantly related to of density of hardwoods, tall shrub cover, and downed woody fuels. Likely because the upper limit of elevation sampled (1081 m) was nearing treeline, there were negative correlations of elevation and hardwood sapling density, canopy cover, and 100 and 1000Hr woody fuels. There was, however, a positive correlation between elevation and tall shrub cover with the dominant shrubs being *Salix, Alnus,* and *Betula* species, reflecting the transition to a shrub-dominated landscape near treeline. Fine woody fuel loads (i.e. 1-, 10-, and 100Hr classes) were higher on the warmer, south-southwest facing aspects than on the cooler north-northeast aspects. The warmer and dryer aspects may have had higher fine fuel loading because these areas are more likely to be dominated by *Picea glauca* or a mix of hardwood species, which have significantly higher average woody fuel loading than *P. mariana* stands that dominate cooler aspects (Pattison et al. 2018).

Conclusions

Species richness at remeasured sites increased by almost double the number of understory species over the 11 years between measurements. Cover of late-successional moss species (*Hylocomium splendens*) decreased over time while cover of resprouting and early-successional shrub species (*Salix* spp., *Vaccinium uliginosum, Ledum groenlandicum*) increased. Twelve years post-fire, remotely-sensed burn severity classes (Landsat-derived dNBR) were related to long-term ecological condition in many of the ways I expected based on previous research using ground-based severity estimates (e.g. Hollingsworth et al. 2013; Gibson et al. 2016; Day et al. 2017). Density of live trees decreased and shrub cover increased at higher severity classes, while downed woody fuel loading tended to peak in low and moderate classes. Understory plant community composition was still significantly different at all burn severity levels as compared to unburned, and at low severity as compared to high severity. As expected based on previous studies, plant composition was influenced by a variety of factors in addition to burn severity; including downed woody fuel loading and moss depth. Elevation and aspect also influenced understory species composition, in addition to influencing other factors such as hardwood sapling density, woody fuel loading, and shrub cover.

As wildfires increase in both size and number in boreal ecosystems, the need to estimate burn severity and its effects on a large scale will only increase in importance (Kasischke and Turetsky 2006; Mann et al. 2012; Calef et al. 2015; Young et al. 2017). While dNBR and the MTBS product have significant flaws, particularly in their ability to estimate depth of surface burning in boreal systems, these methods remain one of the primary sources for managers and others seeking to estimate burn severity. Efforts to improve upon the calculation of dNBR (Parks et al. 2018), and, for boreal systems specifically, to use lidar (Alonzo et al. 2017) or hyperspectral imagery (Lewis et al. 2011) to estimate organic layer consumption post-fire offer promising avenues for applications of burn severity estimation that require more accurate data on surface burning (e.g., estimates of ecosystem carbon). However, the results of this study can help inform broad-scale estimates of post-fire ecosystem condition such as those created by LANDFIRE (Landscape Fire and Resource Management Planning Tools Project, www.landfire.cr.usgs.gov).

Chapter 5: Conclusion

The goal of this dissertation was to improve our understanding of how burn severity and pattern impact long-term vegetation recovery processes. The research presented in this dissertation shows that burn severity, particularly as measured by the dNBR index, has both immediate and long-term effects on post-fire vegetation and woody fuels. These vegetation effects subsequently impact the density and height growth of tree regeneration, factors that will influence future forest composition and structure that plays a driving roll in future fires. Spatial patterns of burn severity immediately following fire can be captured by both continuous and categorical landscape models and these patterns relate strongly to important post-fire measures such as distance to live tree, which is important in predicting where natural tree regeneration will occur post-fire. Understanding long-term burn severity effects and the spatial patterns these effects create on a landscape helps to inform theoretical and management-oriented understandings of how landscapes will recover following fires.

Our analysis found that metrics from both a novel gradient surface model and the established patch-matrix categorical landscape model correlated strongly to distance to nearest live seed tree on the Egley Fire Complex, which burned in ponderosa pine forest as a mosaic of low to stand-replacing high severity fire. High resolution imagery captured shortly following a large wildfire in ponderosa pine was used to develop the landscape models, while field data collected nine years post-fire gave seedling density and understory species richness data. Distance to live seed tree is an important predictor of post-fire seedling density and the strength of these correlations consistently peaked when the metrics were calculated within a 120m or 240m window around the site, reflecting a known seed dispersal distance of approximately 60m for ponderosa pine. However, none of the metrics correlated strongly (rho>0.5) to seedling density itself, nor did we observe any strong correlations to understory species richness. Our results suggest that landscape metrics calculated on high resolution imagery could be explored in future research as a surrogate for field or manually measured distance to live tree, however we did not find support for the hypothesis that landscape metrics would capture additional ecologically-important information and thus correlate more strongly to density or richness.

After examining the impact of spatial patterns and landscape models on seedling density, the next chapter examined what further factors influenced ponderosa pine seedling density and height growth. Seedling density on sites across three large fires was influenced by several predictor variables related to burn severity, while seedling height growth was impacted mainly by climate variables and soil productivity. For this analysis we used non-parametric multiplicative regression modeling, which allows for non-linear interactions among predictor variables, based on a suite of potential predictor variables; including derived climate variables, soil productivity, elevation, aspect, and a variety of field-measured vegetation and cover variables. Field sites were established across a burn severity gradient on three large fires that had burned 9-15 years prior to sampling in ponderosa pine-dominated forests. While we know from previous research that climate in the first few years post-fire is important for seedling establishment and survival, and changing climate has pushed many burned areas outside of the estimated climate envelopes for successful regeneration based on seedling density (Stevens-Rumann et al. 2017). Our results highlight that long-term recovery involves more than just the factors impacting seedling density, though warming climate without increased precipitation is likely to negatively impact seedling height growth as well as establishment. Height growth of seedling can indicate the vigor and health of the seedling and seedling density will not result in long-term ecosystem recovery unless the seedlings successfully grow under expected future climate conditions (Rother et al. 2015).

While the previous chapters focused mainly on seedlings as a measure of recovery, the third chapter of this dissertation focused on how remotely-sensed burn severity impacted a range of post-fire ecological responses. Over the 11 years between remeasurements the species richness doubled, cover of late-successional moss species decreased, and cover of select early-successional species increased on sites across the Taylor Complex boreal spruce fires. Burn severity class still significantly influenced various factors, including tree basal area, downed woody fuel, and understory species composition. Thirty-two field sites were sampled in 2016 across the burn severity gradient, with a subset of sites being remeasurements of previously established sites that allowed us to examine changes in understory species thorough time on the same site. While the size and remote nature of many boreal fires necessitates the use of remote sensing to aid in recovery planning, there has been limited research investigating long-term ecological trends in this ecosystem in relation to dNBR burn

severity. Understanding the lingering ecological effects of dNBR burn severity class can help inform large-scale modeling that is often based on dNBR products.

One potential limitation of this research is that the use of remotely sensed imagery and indices to indicate burn severity is central to all three chapters of this dissertation. Remote sensing allows larger-scale and often more rapid response assessment of burn severity than field-based assessments, however it is ultimately only an approximation of burn severity and may not always reflect in-situ burn severity, particularly on finer scales. While remotely sensed burn severity is not a perfect reflection of in-situ burn severity, we chose to use these indices specifically because our results will add to the body of research showing how burn severity indices can reflect long-term ecological trends and their subsequent ability to allow managers and researchers to estimate burn severity on large scales (Lentile et al. 2006, 2007; French et al. 2008).

The goal of this dissertation was to examine different ways in which remotely-sensed measures of burn severity, documented immediately post-fire, can capture ecologically meaningful characteristics that relate to long-term recovery in forests. The results of our third chapter indicates that microsite conditions resulting in part from differing burn severity could be important for seedling establishment and success, while results from the fourth chapter show that burn severity leaves lingering effects and differences in things like surface cover and woody fuels. Our hypotheses that differing landscape metrics could capture these microsite differences driven by burn severity were the basis for the second chapter. Our results show that effects of burn severity linger in the ecosystems we studied for 10+ years post-fire and that those differences continue to influence processes such as seedling density, in addition landscape metrics successfully reflected processes related to seed dispersal, i.e. presence of seed trees, but did not capture microsite differences in an ecologically meaningful way.

Our results show that not only does burn severity having long-last effects on vegetation and fuels, but that severity-driven effect and immediate post-fire spatial patterns of severity all impact ecological processes such as seedling density and height growth. The ability of remotely sensed burn severity to indicate long-term effects supports the use of burn severity indices by managers for strategic planning post-fire. Furthermore, the ability of landscape

metrics to capture important measures such as distance to live tree opens up the possibility of using these metrics for larger-scale models of post-fire tree regeneration potential. Further work is still needed to examine whether the proposed gradient model successfully captures more ecologically meaningful landscape variation, though our results indicate that, in a ponderosa pine ecosystem and at the spatial resolution of our imagery, the established patch-matrix model performs just as well. Changing climate conditions and the resulting effects on burn severity proportion and patterns means that large-scale assessment of burn severity and management at the landscape scale will become increasingly important in the western U.S., highlighting the importance of continued research on long-term effects of burn severity patterns on ecological processes.

Works Cited

Allen JL, Sorbel B (2008) Assessing the differenced Normalized Burn Ratio's ability to map burn severity in the boreal forest and tundra ecosystems of Alaska's national parks. Int J Wildl Fire 17:463. doi: 10.1071/WF08034

Alonzo M, Morton DC, Cook BD, et al (2017) Patterns of canopy and surface layer consumption in a boreal forest fire from repeat airborne lidar. Environ Res Lett 12:065004. doi: 10.1088/1748-9326/aa6ade

Anderson MJ (2001) A new method for non-parametric multivariate analysis of variance. Austral Ecol 26:32–46. doi: 10.1111/j.1442-9993.2001.01070.pp.x

Anderson MJ, Ellingsen KE, McArdle BH (2006) Multivariate dispersion as a measure of beta diversity. Ecol Lett 9:683–693. doi: 10.1111/j.1461-0248.2006.00926.x

Bansal S, Jochum T, Wardle DA, Nilsson MC (2014) The interactive effects of surface-burn severity and canopy cover on conifer and broadleaf tree seedling ecophysiology. Can J For Res Can Rech For 44:1032–1041. doi: 10.1139/cjfr-2014-0112

Bernhardt EL, Hollingsworth TN, Chapin III FS (2011) Fire severity mediates climate-driven shifts in understorey community composition of black spruce stands of interior Alaska. J Veg Sci 22:32–44. doi: 10.1111/j.1654-1103.2010.01231.x

Black RA, Bliss LC (1978) Recovery sequence of Picea mariana - Vaccinium uliginosum forests after burning near Inuvik, Northwest Territories, Canada. Can J Bot 56:2020–2030

Boby LA, Schuur EAG, Mack MC, et al (2010) Quantify ing fire severity, carbon, and nitrogen emissions in Alaska's boreal forest

Bonnet VH, Schoettle AW, Shepperd WD (2005) Postfire environmental conditions influence the spatial pattern of regeneration for Pinus ponderosa. Can J For Res Can Rech For 35:37–47. doi: 10.1139/x04-157

Boucher J, Beaudoin A, Hébert C, et al (2017) Assessing the potential of the differenced Normalized Burn Ratio (dNBR) for estimating burn severity in eastern Canadian boreal

forests. Int J Wildl Fire 26:32. doi: 10.1071/WF15122

Bright BC, Hudak AT, Kennedy RE, et al (2019) Examining post-fire vegetation recovery with Landsat time series analysis in three western North American forest types. Fire Ecol 15:1–14. doi: 10.1186/s42408-018-0021-9

Burns RM, Honkala BH (1990) Silvics of North America. Agric Handb 654 2:877

Burton PJ, Parisien M-A, Hicke JA, et al (2008) Large fires as agents of ecological diversity in the North American boreal forest. Int J Wildl Fire 17:754. doi: 10.1071/WF07149

Buyantuyev A, Wu J (2007) Effects of thematic resolution on landscape pattern analysis. Landsc Ecol 22:7–13. doi: 10.1007/s10980-006-9010-5

Calef MP, Varvak A, Mcguire AD, et al (2015) Recent changes in annual area burned in Interior Alaska: The impact of fire management. Earth Interact 19:Paper No. 5. doi: 10.1175/EI-D-14-0025.1

Chipman SJ, Johnson EA (2002) Understory vascular plant species diversity in the mixedwood boreal forest of western Canada. Ecol Appl 12:588–601. doi: 10.2307/3060965

Collins BM, Stephens SL (2010) Stand-replacing patches within a ‘mixed severity’ fire regime: quantitative characterization using recent fires in a long-established natural fire area. Landsc Ecol 25:927–939. doi: 10.1007/s10980-010-9470-5

Collins BM, Stevens JT, Miller JD, et al (2017) Alternative characterization of forest fire regimes: incorporating spatial patterns. Landsc Ecol 32:1543–1552. doi: 10.1007/s10980-017-0528-5

Costanza JK, Riitters K, Vogt P, Wickham J (2019) Describing and analyzing landscape patterns: where are we now, and where are we going? Landsc Ecol 34:2049–2055. doi: 10.1007/s10980-019-00889-6

Crotteau JS, Morgan Varner J, Ritchie MW (2013) Post-fire regeneration across a fire severity gradient in the southern Cascades. For Ecol Manage 287:103–112. doi: 10.1016/j.foreco.2012.09.022

Cushman SA, Evans JS, McGarigal K (2010) Landscape ecology: past, present, and future.

In: Cushman SA, Huettmann F (eds) Spatial complexity, informatics, and wildlife conservation. Springer US, New York, NY, pp 65–82

Davis KT, Dobrowski SZ, Higuera PE, et al (2019) Wildfires and climate change push low-elevation forests across a critical climate threshold for tree regeneration. Proc Natl Acad Sci U S A 116:6193–6198. doi: 10.1073/pnas.1815107116

Day NJ, Carrière S, Baltzer JL (2017) Annual dynamics and resilience in post-fire boreal understory vascular plant communities. For Ecol Manage 401:264–272. doi: 10.1016/J.FORECO.2017.06.062

DeBano LF, Neary DG, Ffolliott PF (1998) Fire's effects on ecosystems. J. Wiley

Diedenhofen B, Musch J (2015) Cocor: A comprehensive solution for the statistical comparison of correlations. PLoS One 10:. doi: 10.1371/journal.pone.0121945

Dodge JM, Strand EK, Hudak AT, et al (2019) Short- and long-term effects of ponderosa pine fuel treatments intersected by the Egley Fire Complex, Oregon, USA. Fire Ecol 15:. doi: 10.1186/s42408-019-0055-7

Dodson EK, Root HT (2013) Conifer regeneration following stand-replacing wildfire varies along an elevation gradient in a ponderosa pine forest, Oregon, USA. For Ecol Manage 302:163–170. doi: 10.1016/j.foreco.2013.03.050

Donato DC, Fontaine JB, Campbell JL, et al (2009) Conifer regeneration in stand-replacement portions of a large mixed-severity wildfire in the Klamath-Siskiyou Mountains. Can J For Res Can Rech For 39:823–838. doi: 10.1139/x09-016

Donato DC, Harvey BJ, Turner MG (2016) Regeneration of montane forests 24 years after the 1988 Yellowstone fires: A fire-catalyzed shift in lower treelines? Ecosphere 7:e01410

Duchesne LC, Hawkes BC (2000) Fire in northern ecosystems. Rocky Mountain Research Station, Ogden, UT

Dufrêne M, Legendre P (1997) Species assemblages and indicator species: The need for a flexible asymmetrical approach. Ecol Monogr 67:345–366. doi: 10.1890/0012-9615(1997)067[0345:SAAIST]2.0.CO;2

Eidenshink J, Schwind B, Brewer K, et al (2007) A project for monitoring trends in burn severity. Fire Ecol Spec Issue 3:3–21

Feddema JJ, Mast JN, Savage M (2013) Modeling high-severity fire, drought and climate change impacts on ponderosa pine regeneration. Ecol Modell 253:56–69. doi: 10.1016/j.ecolmodel.2012.12.029

Foster AC, Martin PH, Redmond MD (2020) Soil moisture strongly limits Douglas-fir seedling establishment near its upper altitudinal limit in the southern Rocky Mountains. Can J For Res. doi: 10.1139/CJFR-2019-0296

Frazier AE (2019) Emerging trajectories for spatial pattern analysis in landscape ecology. Landsc Ecol 34:2073–2082. doi: 10.1007/s10980-019-00880-1

Frazier AE, Kedron P (2017a) Landscape Metrics: Past Progress and Future Directions. Curr Landsc Ecol Reports 2:63–72. doi: 10.1007/s40823-017-0026-0

Frazier AE, Kedron P (2017b) Comparing forest fragmentation in Eastern U.S. forests using patch-mosaic and gradient surface models. Ecol Inform 41:108–115. doi: 10.1016/J.ECOINF.2017.08.002

French NHF, Kasischke ES, Hall RJ, et al (2008) Using Landsat data to assess fire and burn severity in the North American boreal forest region: an overview and summary of results. Int J Wildl Fire 17:443–462. doi: 10.1071/wf08007

Fryer JL (2014) Fire regimes of Alaskan black spruce communities. In: Fire Eff. Inf. Syst. U.S. Dep. Agric. For. Serv. Rocky Mt. Res. Station. Fire Sci. Lab. https://www.fs.fed.us/database/feis/fire_regimes/AK_black_spruce/all.html. Accessed 3 May 2018

Gallardo-Cruz JA, Hernández-Stefanoni JL, Moser D, et al (2018) Relating species richness to the structure of continuous landscapes: alternative methodological approaches. Ecosphere 9:e02189. doi: 10.1002/ecs2.2189

Gibson CM, Turetsky MR, Cottenie K, et al (2016) Variation in plant community composition and vegetation carbon pools a decade following a severe fire season in interior Alaska. J Veg Sci 27:1187–1197. doi: 10.1111/jvs.12443

Goodrich BA, Waring KM (2017) Pinus strobiformis seedling growth in southwestern US

mixed conifer forests in managed and non-managed stands. For An Int J For Res 90:393–403. doi: 10.1093/forestry/cpw057

Gustafson EJ (1998) Quantifying landscape spatial pattern: What is the state of the art? Ecosystems 1:143–156. doi: 10.1007/s100219900011

Hankin LE, Higuera PE, Davis KT, Dobrowski SZ (2019) Impacts of growing-season climate on tree growth and post-fire regeneration in ponderosa pine and Douglas-fir forests. Ecosphere 10:e02679. doi: 10.1002/ecs2.2679

Harrell FE (2020) Hmisc: Harrell Miscellaneous. R package version 4.4-0. https://CRAN.R-project.org/package=Hmisc

Hart SA, Chen HYH (2006) Understory vegetation dynamics of North American boreal forests. CRC Crit Rev Plant Sci 25:381–397. doi: 10.1080/07352680600819286

Hély C, Bergeron Y, Flannigan MD (2000) Coarse woody debris in the southeastern Canadian boreal forest: composition and load variations in relation to stand replacement. Can J For Res 30:674–687. doi: 10.1139/x99-256

Hesketh M, Greene DF, Pounden E (2009) Early establishment of conifer recruits in the northern Rocky Mountains as a function of postfire duff depth. Can J For Res Can Rech For 39:2059–2064. doi: 10.1139/x09-120

Hollingsworth TN, Johnstone JF, Bernhardt EL, Chapin III FS (2013) Fire Severity Filters Regeneration Traits to Shape Community Assembly in Alaska's Boreal Forest. PLoS One 8:. doi: 10.1371/journal.pone.0056033

Hoy EE, French NHF, Turetsky MR, et al (2008) Evaluating the potential of Landsat TM/ETM+ imagery for assessing fire severity in Alaskan black spruce forests. Int J Wildl Fire 17:500. doi: 10.1071/WF08107

Hudak AT, Morgan P, Bobbitt MJ, et al (2007) The relationship of satellite imagery to immediate fire effects. Fire Ecol Spec Issue 3:64–90

Johnston DC, Turetsky MR, Benscoter BW, Wotton BM (2015) Fuel load, structure, and potential fire behaviour in black spruce bogs. Can J For Res 45:888–899. doi: 10.1139/cjfr-2014-0334

Johnstone JF, Chapin III FS (2006a) Fire interval effects on successional trajectory in boreal forests of northwest Canada. Ecosystems 9:268–277. doi: 10.1007/s10021-005-0061-2

Johnstone JF, Chapin III FS (2006b) Effects of soil burn severity on post-fire tree recruitment in boreal forest. Ecosystems 9:14–31. doi: 10.1007/s10021-004-0042-x

Johnstone JF, Hollingsworth TN, Chapin III FS, Mack MC (2010) Changes in fire regime break the legacy lock on successional trajectories in Alaskan boreal forest. Glob Chang Biol 16:1281–1295. doi: 10.1111/j.1365-2486.2009.02051.x

Jorgenson T, Yoshikawa K, Kanevskiy M, et al (2008) Map: Permafrost Characteristics of Alaksa

Kasischke ES, Johnstone JF (2005) Variation in postfire organic layer thickness in a black spruce forest complex in interior Alaska and its effects on soil temperature and moisture 1. doi: 10.1139/X05-159

Kasischke ES, Turetsky MR (2006) Recent changes in the fire regime across the North American boreal region - Spatial and temporal patterns of burning across Canada and Alaska. Geophys Res Lett 33:. doi: 10.1029/2006GL025677

Kasischke ES, Turetsky MR, Ottmar RD, et al (2008) Evaluation of the composite burn index for assessing fire severity in Alaskan black spruce forests. Int J Wildl Fire 17:515–526. doi: 10.1071/wf08002

Kasischke ES, Verbyla DL, Rupp TS, et al (2010) Alaska's changing fire regime — implications for the vulnerability of its boreal forests. Can J For Res 40:1313–1324. doi: 10.1139/X10-098

Keane RE, Dickinson LJ (2007) The photoload sampling technique: estimating surface fuel loadings from downward-looking photographs of synthetic fuelbeds. Fort Collins, CO

Kedron PJ, Frazier AE, Ovando-Montejo GA, Wang J (2018) Surface metrics for landscape ecology: a comparison of landscape models across ecoregions and scales. Landsc Ecol 33:1489–1504. doi: 10.1007/s10980-018-0685-1

Keeley JE (2009) Fire intensity, fire severity and burn severity: a brief review and suggested usage. Int J Wildl Fire 18:116–126. doi: 10.1071/wf07049

Keeton WS, Franklin JF (2005) Do remnant old-growth trees accelerate rates of succession in mature Douglas-fir forests? Ecol Monogr 75:103–118. doi: 10.1890/03-0626

Kemball KJ, Wang GG, Westwood AR (2006) Are mineral soils exposed by severe wildfire better seedbeds for conifer regeneration? Can J For Res Can Rech For 36:1943–1950. doi: 10.1139/x06-073

Kemp KB, Higuera PE, Morgan P (2016) Fire legacies impact conifer regeneration across environmental gradients in the U.S. northern Rockies. Landsc Ecol 31:619–636. doi: 10.1007/s10980-015-0268-3

Key CH, Benson NC (2006) Landscape assessment: Sampling and analysis methods. USDA For Serv Gen Tech Rep RMRS-GTR-164-CD 1–55. doi: 10.1002/app.1994.070541203

Korb JE, Fornwalt PJ, Stevens-Rumann CS (2019) What drives ponderosa pine regeneration following wildfire in the western United States? For Ecol Manage 454:. doi: 10.1016/j.foreco.2019.117663

Kupfer JA (2012) Landscape ecology and biogeography: Rethinking landscape metrics in a post-FRAGSTATS landscape. Prog Phys Geogr 36:400–420. doi: 10.1177/0309133312439594

Larson AJ, Franklin JF (2005) Patterns of conifer tree regeneration following an autumn wildfire event in the western Oregon Cascade Range, USA. For Ecol Manage 218:25–36. doi: 10.1016/j.foreco.2005.07.015

Lausch A, Blaschke T, Haase D, et al (2015) Understanding and quantifying landscape structure – A review on relevant process characteristics, data models and landscape metrics. Ecol Modell 295:31–41. doi: 10.1016/J.ECOLMODEL.2014.08.018

Lecomte N, Simard M, Bergeron Y, et al (2005) Effects of fire severity and initial tree composition on understorey vegetation dynamics in a boreal landscape inferred from chronosequence and paleoecological data. J Veg Sci 16:665–674. doi: 10.1658/1100-9233(2005)016

Lentile LB, Holden ZA, Smith AMS, et al (2006) Remote sensing techniques to assess active fire characteristics and post-fire effects. Int J Wildl Fire 15:319–345. doi: 10.1071/wf05097

Lentile LB, Morgan P, Hudak AT, et al (2007) Post-Fire Burn Severity and Vegetaion Response Following Eight Large Wildfires Across the Western United States. Fire Ecol 3:91–108. doi: 10.4996/fireecology.0301091

Lewis SA, Hudak AT, Ottmar RD, et al (2011) Using hyperspectral imagery to estimate forest floor consumption from wildfire in boreal forests of Alaska, USA. Int J Wildl Fire 20:255–271. doi: 10.1071/wf09081

Littlefield CE (2019) Topography and post-fire climatic conditions shape spatio-temporal patterns of conifer establishment and growth. Fire Ecol 15:34. doi: 10.1186/s42408-019-0047-7

Lustig A, Stouffer DB, Roigé M, Worner SP (2015) Towards more predictable and consistent landscape metrics across spatial scales. Ecol Indic 57:11–21. doi: 10.1016/J.ECOLIND.2015.03.042

Mallik AU, Bloom RG, Whisenant SG (2010) Seedbed filter controls post-fire succession. Basic Appl Ecol 11:170–181. doi: 10.1016/J.BAAE.2009.11.005

Malone S, Fornwalt P, Battaglia MA, et al (2018) Mixed-Severity Fire Fosters Heterogeneous Spatial Patterns of Conifer Regeneration in a Dry Conifer Forest. Forests 9:45. doi: 10.3390/f9010045

Mann DH, Rupp TS, Olson MA, Duffy PA (2012) Is Alaska's Boreal Forest Now Crossing a Major Ecological Threshold? Arctic, Antarct Alp Res 44:319–331. doi: 10.1657/1938-4246-44.3.319

McCune B (2006) Non-parametric habitat models with automatic interactions. J Veg Sci 17:819–830

McCune B, Grace JB (2002) Analysis of Ecological Communities, 3rd edn. MJM Software, Gleneden Beach, Oregon

McCune B, Mefford J (2009) HyperNiche: multiplicative habitat modeling. Version 2.22. MjM Software, Gleneden Beach, Oregon, USA.

McCune B, Mefford J (2011) PC-ORD. Multivariate Analysis of Ecological Data

McGarigal K, Cushman SA (2005) The gradient concept of landscape structure. In: Wiens

JA, Moss MR (eds) Issues and perspectives in landscape ecology. Cambridge University Press, Cambridge, UK, pp 112–119

McGarigal K, Marks BJ (1995) FRAGSTATS: Spatial Pattern Analysis Program for Quantifying Landscape Structure. Portland, OR

McGarigal K, Tagil S, Cushman SA (2009) Surface metrics: an alternative to patch metrics for the quantification of landscape structure. Landsc Ecol 24:433–450. doi: 10.1007/s10980-009-9327-y

Morgan P, Keane RE, Dillon GK, et al (2014) Challenges of assessing fire and burn severity using field measures, remote sensing and modelling. Int J Wildl Fire 23:1045. doi: 10.1071/WF13058

Morneau C, Payette S (1989) Postfire Lichen Spruce Woodland Recovery At the Limit of the Boreal Forest in Northern Quebec. Can J Bot Can Bot 67:2770–2782. doi: Article

Murphy KA, Reynolds JH, Koltun JM (2008) Evaluating the ability of the differenced Normalized Burn Ratio (dNBR) to predict ecologically significant burn severity in Alaskan boreal forests. Int J Wildl Fire 17:490. doi: 10.1071/WF08050

O'Neill R V., Hunsaker CT, Timmins SP, et al (1996) Scale problems in reporting landscape pattern at the regional scale. Landsc Ecol 11:169–180. doi: 10.1007/BF02447515

Oksanen J, Blanchet FG, Friendly M, et al (2018) "vegan": Community Ecology Package

Parks SA, Holsinger L, Voss M, et al (2018) Mean Composite Fire Severity Metrics Computed with Google Earth Engine Offer Improved Accuracy and Expanded Mapping Potential. Remote Sens 10:879. doi: 10.3390/rs10060879

Peters VS, Macdonald SE, Dale MRT (2005) The interaction between masting and fire is key to white spruce regeneration. Ecology 86:1744–1750. doi: 10.1890/03-0656

Pickett ST, Cadenasso ML (1995) Landscape ecology: spatial heterogeneity in ecological systems. Science 269:331–4. doi: 10.1126/science.269.5222.331

Pounden E, Greene DF, Michaletz ST (2014) Non-serotinous woody plants behave as aerial seed bank species when a late-summer wildfire coincides with a mast year. Ecol Evol 4:3830–3840. doi: 10.1002/ece3.1247

Roberts DW, Cooper SV (1989) Concepts and techniques of vegetation mapping. Ogden, UT

Rodman KC, Veblen TT, Chapman TB, et al (2020) Limitations to recovery following wildfire in dry forests of southern Colorado and northern New Mexico, USA. Ecol Appl 30:. doi: 10.1002/eap.2001

Rother MT, Veblen TT, Furman LG (2015) A field experiment informs expected patterns of conifer regeneration after disturbance under changing climate conditions. Can J For Res 45:1607–1616. doi: 10.1139/cjfr-2015-0033

Ryan KC (2015) Dynamic interactions between forest structure and fire behavior in boreal ecosystems. Silvia Fenn 36:13–39. doi: 10.14214/sf.548

Rydgren K, Økland RH, Hestmark G (2004) Disturbance severity and community resilience in a boreal forest. Ecology 85:1906–1915. doi: 10.1890/03-0276

Savage M, Mast JN, Feddema JJ (2013) Double whammy: high-severity fire and drought in ponderosa pine forests of the Southwest. Can J For Res 43:570–583. doi: 10.1139/cjfr-2012-0404

Schaetzl RJ, Krist FJ, Miller BA (2012) A taxonomically based ordinal estimate of soil productivity for landscape-scale analyses. Soil Sci 177:288–299. doi: 10.1097/SS.0b013e3182446c88

Shen W, Darrel Jenerette G, Wu J, H. Gardner R (2004) Evaluating empirical scaling relations of pattern metrics with simulated landscapes. Ecography (Cop) 27:459–469. doi: 10.1111/j.0906-7590.2004.03799.x

Shenoy A, Johnstone JF, Kasischke ES, Kielland K (2011) Persistent effects of fire severity on early successional forests in interior Alaska. For Ecol Manage 261:381–390. doi: 10.1016/j.foreco.2010.10.021

Simard AJ (1991) Fire Severity, Changing Scales, and How Things Hang Together. Int J Wildl Fire 1:23–34

Smith AC, Dahlin KM, Zarnetske PL (2019) geodiv: Methods for Calculating Gradient Surface Metrics

Stevens-Rumann CS, Kemp KB, Higuera PE, et al (2017) Evidence for declining forest

resilience to wildfires under climate change. Ecol Lett. doi: 10.1111/ele.12889

Strand EK, Vierling LA, Smith AMS, Bunting SC (2008) Net changes in aboveground woody carbon stock in western juniper woodlands, 1946–1998. J Geophys Res Biogeosciences 113:G01013. doi: doi:10.1029/2007JG000544

Thompson DK, Parisien M-A, Morin J, et al (2017) Fuel accumulation in a high-frequency boreal wildfire regime: from wetland to upland. Can J For Res 47:957–964. doi: 10.1139/cjfr-2016-0475

Turner MG (2005) Landscape Ecology: What Is the State of the Science? Annu Rev Ecol Evol Syst 36:319–344. doi: 10.1146/annurev.ecolsys.36.102003.152614

Turner MG (1989) Landscape ecology: The effect of pattern on process. Annu Rev Ecol Syst 20:171–97

Turner MG, Gardner RH, O'Neill RV (2001) Landscape Ecology in Theory and Practice. Springer New York, New York, NY

Turner MG, Romme WH, Gardner RH (1999) Prefire heterogeneity, fire severity, and early postfire plant reestablishment in subalpine forests of Yellowstone National Park, Wyoming. Int J Wildl Fire 9:21–36. doi: 10.1071/wf99003

Turner MG, Romme WH, Gardner RH, Hargrove WW (1997) Effects of Fire Size and Pattern on Early Succession in Yellowstone National Park. Ecol Monogr 67:411–433. doi: 10.2307/2963464

Urza AK, Sibold JS (2013) Nondestructive Aging of Postfire Seedlings for Four Conifer Species in Northwestern Montana. West J Appl For 28:22–29. doi: 10.5849/wjaf.11-014

Uuemaa E, Mander Ü, Marja R (2013) Trends in the use of landscape spatial metrics as landscape indicators: A review. Ecol Indic 28:100–106. doi: 10.1016/J.ECOLIND.2012.07.018

Verbyla D, Lord R (2008) Estimating post-fire organic soil depth in the Alaskan boreal forest using the Normalized Burn Ratio. Int J Remote Sens 29:3845–3853. doi: 10.1080/01431160701802497

Viereck L (1983) The effects of fire in black spruce ecosystems of Alaska and northern

Canada. In: Wein RW, MacLean DA (eds) The Role of Fire in Northern Circumpolar Ecosystems. John Wiley & Sons, Ltd, pp 201–220

Viereck L, Schandelmeier L (1980) Effects of fire in Alaska and adjacent Canada: a literature review. BLM-Alaska Tech Rep 6:1–124

Wang GG, Kemball KJ (2010) Effects of fire severity on early survival and growth of planted jack pine, black spruce and white spruce. For Chron 86:193–199. doi: 10.5558/tfc86193-2

Wang GG, Kemball KJ (2005) Effects of fire severity on early development of understory vegetation. Can J For Res 35:254–262. doi: 10.1139/x04-177

Wang T, Hamann A, Spittlehouse D, Carroll C (2016) Locally downscaled and spatially customizable climate data for historical and future periods for North America. PLoS One 11:. doi: 10.1371/journal.pone.0156720

Whitman E, Parisien MA, Thompson DK, Flannigan MD (2018) Topoedaphic and forest controls on post-fire vegetation assemblies are modified by fire history and burn severity in the northwestern Canadian boreal forest. Forests 9:. doi: 10.3390/f9030151

Wiens JA, Stenseth NC, Horne B Van, Ims RA (1993) Ecological Mechanisms and Landscape Ecology. Oikos 66:369. doi: 10.2307/3544931

Wu J (2013) Key concepts and research topics in landscape ecology revisited: 30 years after the Allerton Park workshop. Landsc Ecol 28:1–11. doi: 10.1007/s10980-012-9836-y

Wu J (2004) Effects of changing scale on landscape pattern analysis: scaling relations. Landsc Ecol 19:125–138. doi: 10.1023/B:LAND.0000021711.40074.ae

Wu J, Shen W, Sun W, Tueller PT (2002) Empirical patterns of the effects of changing scale on landscape metrics. Landsc Ecol 17:761–782. doi: 10.1023/A:1022995922992

York RA, Battles JJ, Heald RC (2007) Gap-Based Silviculture in a Sierran Mixed- Conifer Forest : Effects of Gap Size on Early Survival and 7-year Seedling Growth 1. Restoring fire-adapted Ecosyst Proc 2005 Natl Silvic Work 181–191

York RA, Battles JJ, Heald RC (2003) Edge effects in mixed conifer group selection openings: tree height response to resource gradients. For Ecol Manage 179:107–121.

doi: 10.1016/S0378-1127(02)00487-5

Yoshikawa K, Bolton WR, Romanovsky VE, et al (2002) Impacts of wildfire on the permafrost in the boreal forests of Interior Alaska. J Geophys Res 108:8148. doi: 10.1029/2001JD000438

Young AM, Higuera PE, Duffy PA, Hu FS (2017) Climatic thresholds shape northern high-latitude fire regimes and imply vulnerability to future climate change. Ecography (Cop) 40:606–617. doi: 10.1111/ecog.02205

MTBS Data Access: Fire Level Geospatial Data. MTBS Project (USDA Forest Service/U.S. Geological Survey). Available online: http://mtbs.gov/direct-download [2018, May]

R Core Team (2017) R: A language and environment for statistical computing. R Foundation for Statistical Computing, Vienna, Austria. https://www.R-project.org/

ACRC – Alaska Climate Research Center. Climate Normals. Data for Chicken, Alaska, 99732. http://climate.gi.alaska.edu/Climate/Normals [17 June 2018]

Tesky JL (1992) Hylocomium splendens. In: Fire Effects Information System. U.S. Department of Agriculture, Forest Service, Rocky Mountain Research Station, Fire Sciences Laboratory (Producer). Available: https://www.fs.fed.us/database/feis/plants/bryophyte/hylspl/all.html [2018, June 17].

Johnson EA (1981) Vegetation Organization and Dynamics of Lichen Woodland Communities in the Northwest Territories, Canada. Ecology 62:200–215

Lutz HJ (1956) Ecological effects of forest fires in the interior of Alaska. Tech. Bull. No. 1133. Washington, DC: U.S. Department of Agriculture, Forest Service. 121 p.

Matthews RF (1993) Peltigera aphthosa. In: Fire Effects Information System. U.S. Department of Agriculture, Forest Service, Rocky Mountain Research Station, Fire Sciences Laboratory (Producer). Available: www.fs.fed.us/database/feis/lichens/pelaph/all.html [2018, June 17].

Matthews, RF (1994) Geocaulon lividum. In: Fire Effects Information System. U.S. Department of Agriculture, Forest Service, Rocky Mountain Research Station, Fire Sciences Laboratory (Producer). Available: https://www.fs.fed.us/database/feis/plants/forb/geoliv/all.html [2018, June 17].

Ahti T, Hepburn TL (1967) Preliminary studies on woodland caribou range, especially on lichen stands, in Ontario. Res. Rep. (Wildlife) No. 74. Toronto, ON: Ontario Department of Lands and Forests, Research Branch. 134 p.

Pattison R, Andersen H, Gray A, Schulz B, Smith RJ, Jovan S, tech. coords (2018) Forests of the Tanana Valley State Forest and Tetlin National Wildlife Refuge, Alaska: Results of the 2014 pilot inventory. Gen. Tech. Rep. PNW-GTR-967, Portland, OR: U.S. Department of Agriculture, Forest Service, Pacific Northwest Research Station. 80 p.

Appendix A: Chapter 4 – Tables and figures

Table A.-1 Monitoring Trends in Burn Severity (MTBS) metadata information for the burn severity classification of each fire used in this analysis; all information is from the MTBS fire bundle download (www.mtbs.gov, accessed May 2018). Note that percentages of burn severity classes will not sum to 100 due to non-processing mask (scan line error, cloud cover, water, etc) included in the product.

	Chicken Fire	**Porcupine Fire**	**Wall Street Fire**
Pre-fire image (satellite/acquisition date)	Landsat 5/July 20, 2003	Landsat 5/July 20, 2003	Landsat 5/July 20, 2003
Post-fire image (satellite/acquisition date)	Landsat 7/August 31, 2004	Landsat 7/August 31, 2004	Landsat 5/July 27, 2005
Burn severity distribution (% unburn, low, moderate, high, increased green)	11, 16, 27, 12, 0.5	9, 11, 23, 7, 0	10, 18, 20, 2, 0

Table A.-2 Common species (occurring in 50% or more of the 12 remeasured sites) encountered in 2005 and 2016. Species are presented in alphabetical order first as the species common in both years and then those common in just one year (below the line). See Appendix B for common names and growth types.

	2005				2016		
Species	**Percent of plots present**	**Average cover**	**Maximum cover**	**Species**	**Percent of plots present**	**Average cover**	**Maximum cover**
Chamerion angustifolium	58	3.4	14.0	*C. angustifolium*	100	1.7	3.6
Hylocomium splendens	75	5.5	21.8	*H. splendens*	50	1.8	15.6
Ledum groenlandicum	75	2.1	8.0	*L. groenlandicum*	83	8.2	27.2
Salix spp.	58	1.5	9.3	*Salix* spp.	100	8.0	19.2
Vaccinium uliginosum	58	2.5	9.8	*V. uliginosum*	75	12.1	28.6
Vaccinium vitis-idaea	83	3.0	22.0	*V. vitis-idaea*	92	3.9	13.0
Equisetum arvense	75	1.2	4.3	*Betula neoalaskana*	67	1.3	5.8
Unknown lichen	58	0.8	4.3	*Cladonia* spp.	92	1.0	2.6
				Unknown crust lichen	50	0.5	1.8
				Dicranum sp.	58	2.7	19.0
				Equisetum scirpoides	58	0.8	4.8
				Fungi	92	0.6	1.8
				Petasites frigidus	58	1.1	5.6
				Peltigera sp.	92	0.7	1.6
				Picea glauca	50	0.2	1.2

	Picea mariana	67	1.2	6.4
	Polytrichum sp.	100	14.1	35.6
	Populus tremuloides	58	1.5	11.4
	Rosa acicularis	67	3.1	22.2

Table A.-3 Spearman rank correlation rho (ρ) and P-value for relationship between site species richness, evenness, and Shannon and Simpson indices of diversity. Results significant at α<0.1 are bolded.

	Richness		**Evenness**		**Shannon**		**Simpson**	
	ρ	***P*-value**	***ρ***	***P*-value**	***ρ***	***P*-value**	***ρ***	***P*-value**
dNBR	-0.156	0.3949	0.178	0.3308	0.094	0.6101	0.162	0.3756
Elevation	0.019	0.9197	0.180	0.3229	0.152	0.4053	0.233	0.1984
Aspect	0.115	0.532	0.074	0.6847	0.102	0.5782	0.030	0.8687
Live trees/ha	0.192	0.292	-0.010	0.9554	0.045	0.808	0.016	0.9304
Dead trees/ha	-0.255	0.1594	-0.094	0.6093	-0.137	0.4559	-0.131	0.4732
Canopy cover (%)	-0.040	0.8262	-0.218	0.2313	-0.168	0.357	-0.259	0.1519
Tall shrub cover (%)	0.063	0.7302	0.153	0.4018	0.116	0.5279	0.148	0.418
1000Hr fuel (kg/m^2)	-0.096	0.6024	-0.151	0.4102	-0.206	0.2584	-0.235	0.1946
100Hr fuel (kg/m^2)	**-0.388**	**0.0282**	-0.168	0.3572	**-0.321**	**0.0732**	**-0.343**	**0.05495**
10Hr fuel (kg/m^2)	-0.230	0.2046	-0.153	0.4036	-0.256	0.1574	-0.286	0.113
1Hr fuel (kg/m^2)	-0.082	0.6536	0.023	0.9	-0.038	0.8375	-0.084	0.6465
Moss depth (mm)	0.210	0.2488	0.065	0.7242	0.131	0.473	0.195	0.2838
Duff depth (mm)	0.228	0.2095	0.152	0.4051	0.246	0.1746	0.267	0.1394

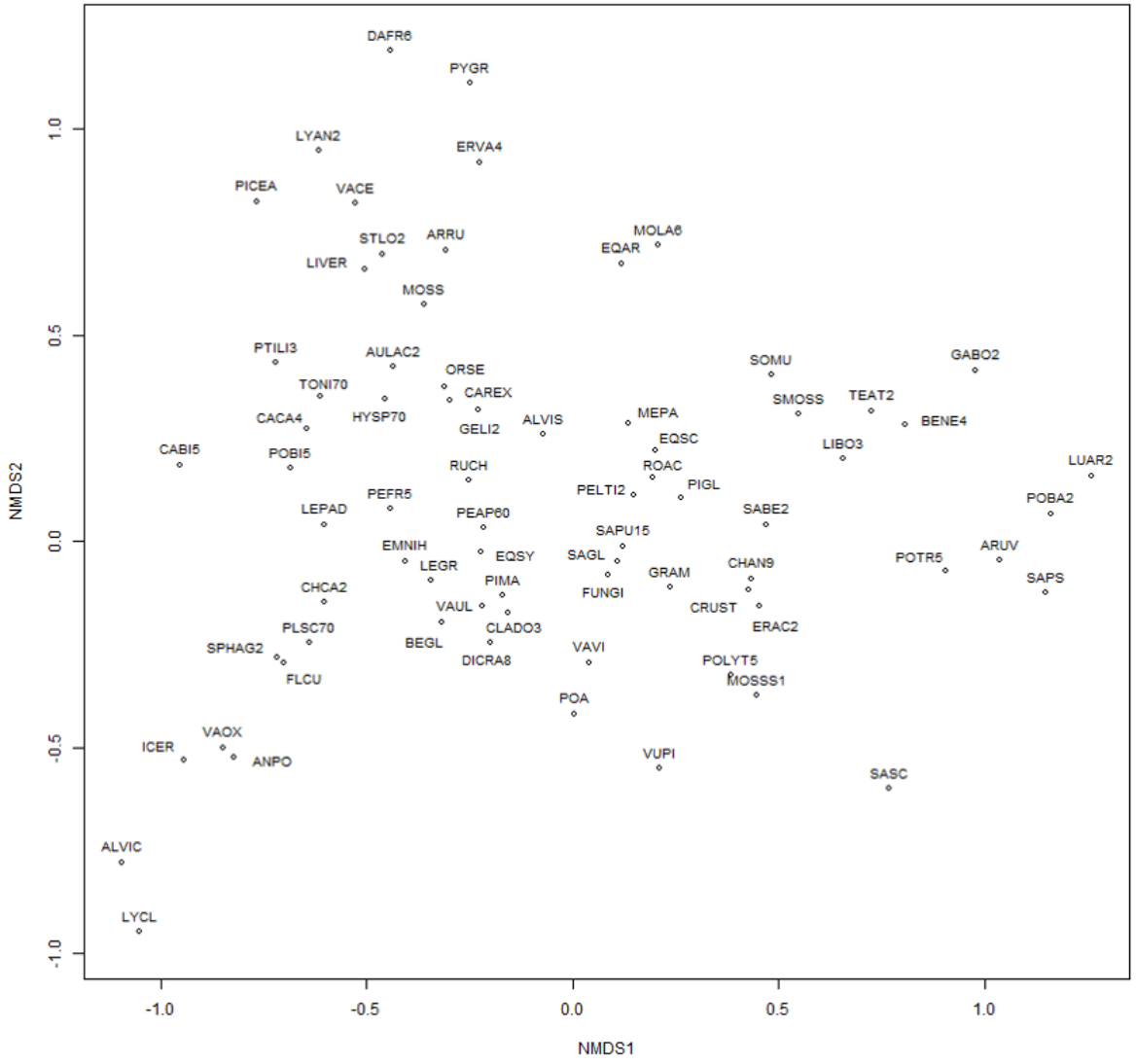

Figure A.-1 Non-metric multidimentional scaling (cumulative R^2~0.81), showing labeled individual understory species in ordination space. Species are identified by USDA plant code, for full species names see Appendix B.

Appendix B: Chapter 4 – Species list

This appendix contains a complete species list of all vegetation species identified on sites sampled across the Taylor Fire Complex in Interior Alaska.

Scientific Name	USDA Code	Common Name	% of sites present	Family	Life Cycle	Functional Type
Achillea millefolium L. var. *borealis* (Bong.) Farw.	ACMIB	boreal yarrow	3	Asteraceae	Perennial	Forb
Achillea sibirica Ledeb.	ACSI	Siberian yarrow	3	Asteraceae	Perennial	Forb
Alnus Mill.	ALNUS	alder	3	Betulaceae	Perennial	Shrub/tree
Alnus viridis (Chaix) DC. ssp. *crispa* (Aiton) Turrill	ALVIC	mountain alder	6	Betulaceae	Perennial	Shrub/tree
Alnus viridis (Chaix) DC. ssp. *sinuata* (Regel) Á. Löve & D. Löve	ALVIS	Sitka alder	13	Betulaceae	Perennial	Shrub/tree
Andromeda polifolia L.	ANPO	bog rosemary	9	Ericaceae	Perennial	Shrub
Anemone multifida Poir.	ANMU	Pacific anemone	3	Ranunculaceae	Perennial	Forb
Arctostaphylos rubra (Rehder & Wilson) Fernald	ARRU	red fruit bearberry	25	Ericaceae	Perennial	Shrub
Arctostaphylos uva-ursi (L.) Spreng.	ARUV	kinnikinnick	19	Ericaceae	Perennial	Shrub
Artemisia tilesii Ledeb.	ARTI	Tilesius' wormwood	3	Asteraceae	Perennial	Forb
Aster L.	ASTER	aster	3	Asteraceae	N/A	Forb
Astragalus L.	ASTRA	milkvetch	3	Fabaceae	N/A	Forb
Aulacomnium Schwägr.	AULAC2	aulacomnium moss	31	Aulacomniaceae	Perennial	Moss

Barbula Hedw.	BARBU2	barbula moss	3	Pottiaceae	Perennial	Moss
Betula glandulosa Michx.	BEGL	resin birch	41	Betulaceae	Perennial	Shrub
Betula neoalaskana Sarg.	BENE4	paper birch	44	Betulaceae	Perennial	Tree
Betula occidentalis Hook.	BEOC2	water birch	3	Betulaceae	Perennial	Tree
Calamagrostis canadensis (Michx.) P. Beauv.	CACA4	bluejoint	34	Poaceae	Perennial	Graminoid
Carex bigelowii Torr. Ex Schewin.	CABI5	Bigelow's sedge	6	Cyperaceae	Perennial	Graminoid
Carex L.	CAREX	sedge	56	Cyperaceae	Perennial	Graminoid
Cerastium beeringianum ssp. *beeringianum* Cham. & Schltdl.	CEBEB4	Bering chickweed	3	Caryophyllaceae	Perennial	Forb
Chamaedaphne calyculata (L.) Moench	CHCA2	leatherleaf	6	Ericaceae	Perennial	Shrub
Chamerion angustifolium (L.) Holub	CHAN9	fireweed	78	Onagraceae	Perennial	Forb
Cladonia P. Browne	CLADO3	reindeer lichen	88	Cladoniaceae	N/A	Lichen
Cnidium cnidiifolium (Turcz.) Schischkin	CNCN	Jakutsk snowparsley	3	Apiaceae	Perennial	Forb
Dasiphora fruticosa (L.) Rydb.	DAFR6	shrubby cinquefoil	13	Rosaceae	Perennial	Shrub
Dicranum Hedw.	DICRA8	dicranum moss	69	Dicranaceae	Perennial	Moss
Drepanocladus (Müll. Hal.) G. Roth	DREPA3	drepanocladus moss	3	Amblystegiaceae	Perennial	Moss
Elymus L.	ELYMU	wildrye	3	Poaceae	Perennial	Graminoid
Empetrum nigrum L. ssp. *hermaphroditum* (Lange ex	EMNIH	black crowberry	38	Empetraceae	Perennial	Shrub

Hagerup) Böcher						
Equisetum arvense L.	EQAR	field horsetail	31	Equisetaceae	Perennial	Forb
Equisetum scirpoides Michx.	EQSC	dwarf scouringrush	69	Equisetaceae	Perennial	Forb
Equisetum sylvaticum L.	EQSY	woodland horsetail	16	Equisetaceae	Perennial	Forb
Erigeron acris L.	ERAC2	bitter fleabane	6	Asteraceae	Annual	Forb
Erigeron L.	ERIGE2	fleabane	3	Asteraceae	N/A	Forb
Eriophorum L.	ERIOP	cottongrass	3	Cyperaceae	Perennial	Graminoid
Eriophorum vaginatum L.	ERVA4	tussock cottongrass	6	Cyperaceae	Perennial	Graminoid
Eritrichium nanum (Vill.) Schrad. ex Gaudin	ERNA	arctic alpine forget-me-not	3	Boraginaceae	Perennial	Forb
Festuca L.	FESTU	fescue	3	Poaceae	Perennial	Graminoid
Flavocetraria cucullata (Bellardi) Karnefelt & A. Thell	FLCU	N/A	34	Parmeliaceae	N/A	Lichen
Foliose lichen	FOLIO1	foliose lichen	3	N/A	N/A	Lichen
Galium boreale L.	GABO2	northern bedstraw	9	Rubiaceae	Perennial	Forb
Geocaulon lividum (Richardson) Fernald	GELI2	false toadflax	9	Santalaceae	Perennial	Forb
Huperzia selago (L.) Bernh. ex Schrank & Mart. var. *selago*	HUSES	fir clubmoss	3	Lycopodiaceae	Perennial	Forb
Hylocomium splendens (Hedw.) Schimp.	HYSP70	splendid feather moss	47	Hylocomiaceae	Perennial	Moss
Icmadophila ericetorum (L.) Zahlbr.	ICER	peppermint drop lichen	6	Baeomycetaceae	N/A	Lichen

Ledum groenlandicum Oeder	LEGR	bog Labrador tea	84	Ericaceae	Perennial	Shrub
Ledum palustre L. ssp. *decumbens* (Aiton) Hultén	LEPAD	marsh Labrador tea	6	Ericaceae	Perennial	Shrub
Leymus innovatus (Beal) Pilg.	LEIN6	downy ryegrass	3	Poaceae	Perennial	Graminoid
Linnaea borealis L.	LIBO3	twinflower	28	Caprifoliaceae	Perennial	Forb
Loiseleuria procumbens (L.) Desv.	LOPR	alpine azalea	3	Ericaceae	Perennial	Shrub
Lupinus arcticus S. Watson	LUAR2	arctic lupine	13	Fabaceae	Perennial	Forb
Luzula parviflora (Ehrh.) Desv.	LUPA4	smallflowered woodrush	3	Juncaceae	Perennial	Graminoid
Lycopodium annotinum L.	LYAN2	stiff clubmoss	6	Lycopodiaceae	Perennial	Forb
Lycopodium clavatum L.	LYCL	running clubmoss	6	Lycopodiaceae	Perennial	Forb
Masonhalea richardsonii (Hook.) Karnefelt	MARI60	Richardson's masonhalea lichen	3	Parmeliaceae	N/A	Lichen
Mertensia paniculata (Aiton) G. Don	MEPA	tall bluebells	31	Boraginaceae	Perennial	Forb
Moehringia lateriflora (L.) Fenzl	MOLA6	bluntleaf sandwort	13	Caryophyllaceae	Perennial	Forb
Myurella julacea (Schwägr.) Schimp.	MYJU70	myurella moss	3	Pterigynandraceae	Perennial	Moss
Orthilia secunda (L.) House	ORSE	sidebells wintergreen	16	Pyrolaceae	Perennial	Shrub
Parnassia palustris L.	PAPA8	marsh grass of Parnassus	3	Saxifragaceae	Perennial	Forb
Pedicularis L.	PEDIC	lousewort	3	Scrophulariaceae	Perennial	Forb
P*edicularis verticillata* (L.)	PEVE	whorled	3	Scrophulariaceae	Perennial	Forb

		lousewort				
Peltigera aphthosa (L.) Willd.	PEAP60	felt lichen	53	Peltigeraceae	N/A	Lichen
Peltigera Willd.	PELTI2	felt lichen	84	Peltigeraceae	N/A	Lichen
Petasites frigidus (L.) Fr.	PEFR5	arctic sweet coltsfoot	53	Asteraceae	Perennial	Forb
Picea A. Dietr.	PICEA	spruce	6	Pinaceae	Perennial	Tree
Picea glauca (Moench) Voss	PIGL	white spruce	38	Pinaceae	Perennial	Tree
Picea mariana (Mill.) Britton Sterns & Poggenb.	PIMA	black spruce	69	Pinaceae	Perennial	Tree
Pleurozium schreberi (Brid.) Mitt.	PLSC70	Schreber's big red stem moss	47	Hylocomiaceae	Perennial	Moss
Poa arctica R. Br.	POAR2	arctic bluegrass	3	Poaceae	Perennial	Graminoid
Poa L.	POA	bluegrass	41	Poaceae	N/A	Graminoid
Polemonium L.	POLEM	Jacob's-ladder	3	Polemoniaceae	Perennial	Forb
Polygonum bistorta L.	POBI5	meadow bistort	16	Polygonaceae	Perennial	Forb
Polytrichum commune Hedw.	POCO38	polytrichum moss	3	Polytrichaceae	Perennial	Moss
Polytrichum Hedw.	POLYT5	polytrichum moss	97	Polytrichaceae	Perennial	Moss
Populus balsamifera L.	POBA2	balsam poplar	9	Salicaceae	Perennial	Tree
Populus tremuloides Michx.	POTR5	quaking aspen	44	Salicaceae	Perennial	Tree
Ptilium De Not.	PTILI3	ptilium moss	6	Hypnaceae	Perennial	Moss
Pulsatilla patens (L.) Mill.	PUPA5	eastern pasqueflower	3	Ranunculaceae	Perennial	Forb
Pyrola grandiflora Radius	PYGR	largeflowered	13	Pyrolaceae	Perennial	Shrub

		wintergreen				
Pyrola minor L.	PYMI	snowline wintergreen	3	Pyrolaceae	Perennial	Shrub
Ranunculus lapponicus L.	RALA	Lapland buttercup	3	Ranunculaceae	Perennial	Forb
Ribes hudsonianum Richardson	RIHU	northern black currant	3	Grossulariaceae	Perennial	Shrub
Rosa acicularis Lindl.	ROAC	prickly rose	50	Rosaceae	Perennial	Shrub
Rubus chamaemorus L.	RUCH	cloudberry	31	Rosaceae	Perennial	Forb
Rubus idaeus L.	RUID	American red raspberry	3	Rosaceae	Perennial	Shrub
Rumex L.	RUMEX	dock	3	Polygonaceae	N/A	Forb
Salix bebbiana Sarg.	SABE2	Bebb willow	41	Salicaceae	Perennial	Tree/shrub
Salix glauca L.	SAGL	grayleaf willow	66	Salicaceae	Perennial	Tree/shrub
Salix niphoclada Rydb.	SANI10	barrenground willow	3	Salicaceae	Perennial	Shrub
Salix pseudomonticola C.R. Ball	SAPS	false mountain willow	6	Salicaceae	Perennial	Shrub
Salix pulchra Cham.	SAPU15	tealeaf willow	72	Salicaceae	Perennial	Shrub
Salix scouleriana Barratt ex Hook.	SASC	Scouler's willow	19	Salicaceae	Perennial	Tree/shrub
Saussurea angustifolia (Willd.) DC.	SAAN3	narrowleaf saw-wort	3	Asteraceae	Perennial	Forb
Solidago multiradiata Aiton	SOMU	Rocky Mountain goldenrod	13	Asteraceae	Perennial	Forb
Sphagnum L.	SPHAG2	sphagnum	44	Sphagnaceae	Perennial	Moss
Spiraea stevenii (C.K.	SPST3	beauverd spirea	3	Rosaceae	Perennial	Shrub

Schneid.) Rydb.						
Stellaria longipes Goldie	STLO2	longstalk starwort	6	Caryophyllaceae	Dicot	Forb
Stereocaulon Hoffm.	STERE2	snow lichen	3	Stereocaulaceae	N/A	Lichen
Tephroseris atropurpurea (Ledeb.) Holub	TEAT2	arctic groundsel	16	Asteraceae	Perennial	Forb
Thuidium Schimp.	THUID	thuidium moss	3	Thuidiaceae	Perennial	Moss
Tomentypnum nitens (Hedw.) Loeske	TONI70	tomentypnum moss	6	Brachytheciaceae	Perennial	Moss
Unknown crust lichen	CRUST	soil crust lichen	53	N/A	N/A	Lichen
Unknown forb	UNKSIL	Silene-like forb	3	Caryophyllaceae	N/A	Forb
Unknown fungi	FUNGI	fungi	94	N/A	N/A	Fungi
Unknown gramminoid	GRAM	grass	47	N/A	N/A	Graminoid
Unknown Marchantiophyta	LIVER	liverwort	13	N/A	N/A	Moss
Unknown moss	MOSSS1	small, short green-yellow carpet	38	N/A	N/A	Moss
Unknown moss	MOSS	N/A	25	N/A	N/A	Moss
Unknown moss	SMOSS	small moss	19	N/A	N/A	Moss
Vaccinium cespitosum Michx.	VACE	dwarf bilberry	9	Ericaceae	Perennial	Shrub
Vaccinium oxycoccos L.	VAOX	small cranberry	19	Ericaceae	Perennial	Shrub
Vaccinium uliginosum L.	VAUL	bog blueberry	75	Ericaceae	Perennial	Shrub
Vaccinium vitis-idaea L.	VAVI	lingonberry	97	Ericaceae	Perennial	Shrub
Vulpicida pinastri (Scop.) J.-E.	VUPI	N/A	38	Parmeliaceae	N/A	Lichen

Mattsson & M.J. Lai						
Zigadenus elegans Pursh	ZIEL2	mountain deathcamas	3	Liliaceae	Perennial	Forb